UNIVERSITI MALAYSIA PAHANG

DECLARATION OF THESIS AND COPYRIGHT

Author's full name	:	**HAZRULRIZAWATI BT ABD HAMID**
Date of birth	:	**23 March 1982**
Title	:	**CHARACTERISATION AND BIOLOGICAL ACTIVITIES OF *TINOSPORA CRISPA* (MENISPERMACEAE) EXTRACT WITH EMPHASIS ON ALKALOIDS**
Academic Session	:	2012/2013

I declare that this thesis is classified as

☐	**CONFIDENTIAL**	(Contains confidential information under the Official Secret Act 1972)*
☐	**RESTRICTED**	(Contains restricted information as specified by the organization where research was done)*
√	**OPEN ACCESS**	I agree my thesis to be published as online open access (Full text)

I acknowledged that University Malaysia Pahang reserves the right as follows:

1. The thesis is the property of University Malaysia Pahang
2. The Library of University Malaysia Pahang has the right to make copies for the purpose of research only
3. The Library has the right to make copies of the thesis for academic exchange

Certified by:

SIGNATURE	**SIGNATURE OF SUPERVISOR**
820323-02-5792 **NEW IC NUMBER**	Prof. Dr. Mashitah Mohd. Yusof **NAME OF SUPERVISOR**
Date:	Date:

Notes: * If thesis is CONFIDENTIAL or RESTRICTED, please attach with the letter from the organization with period and reasons for confidentiality or restriction

CHARACTERISATION AND BIOLOGICAL ACTIVITIES OF *TINOSPORA CRISPA* (MENISPERMACEAE) EXTRACT WITH EMPHASIS ON ALKALOIDS

HAZRULRIZAWATI BT ABD HAMID

Thesis submitted in fulfillment of the requirements
for the award of the degree of
Doctor of Philosophy of Science in Industrial Chemistry

Faculty of Industrial Sciences and Technology
UNIVERSITI MALAYSIA PAHANG

JULY 2013

SUPERVISOR'S DECLARATION

We hereby declare that we have checked this thesis and in our opinion, this thesis is adequate in terms of scope and quality for the award of the degree of Doctor of Philosophy of Science in Industrial Chemistry

Signature
Name of Supervisor: Prof. Dr. Mashitah Mohd. Yusoff
Position: Dean of Faculty of Industrial Sciences and Technology
Date:

Signature
Name of Co-supervisor: Dr Seema Zareen
Position: Lecturer of Faculty of Industrial Sciences and Technology
Date:

STUDENT'S DECLARATION

I hereby declare that the work in this thesis is my own except for quotations and summaries which have been duly acknowledged. The thesis has not been accepted for any degree and is not concurrently submitted for award of other degree.

Signature

Name: Hazrulrizawati bt Abd hamid

ID Number: PKD10001

Date:

ACKNOWLEDGEMENTS

Thanks to Allah the Almighty who give me, His bless in finishing my research. Special thanks is extended to Prof. Dr. Mashitah Mohd Yusoff, who had provided a significant contribution by giving all the advices, guidance, support, ideas and knowledge needed throughout my work and learning process. Again thankful to her for the continuous help that extended beyond the professional level.

I also express my appreciation to my co-supervisor, Dr Seema Zareen for her superb nuclear magnetic resonance experience that allowed the interpretation of NMR spectra of the compounds and for her time and effort to teach me interpreted almost all spectroscopic data contained in this dissertation.

I am thankful to Dr M. Nadeem Akhtar for bringing my samples to H.E.J and and Prof Dr. M. Iqbal Choudhary for his cooperation in determining the mass spectra in this research project at International Center of Chemical and Biologal Sciences (H. E. J. Research Institute of Chemistry), Pakistan.

I wish to thank both science officers at Central Laboratory, Mrs Nor Hafizah bt. Zainal Abidin and Mr Aimi Ilmar b. Ramli for acquisition of 500 MHz NMR spectra. A lot of thanks to lab assistant Mr Muhamad Hussaini b. Sulaiman and Mrs Nordiana bt Hazani for allowing me to use the laboratory and their invaluable assistance. My thanks to Ms Norlaili bt Abd Rahim who provide me all the microbial strains.

I am highly indebted to Universiti Malaysia Pahang for financial support for this work *via* research grant (UMP RDU 100322).

Words cannot adequately express my gratitude towards my beloved husband, En Mohd Adib b Haron, who endured many sacrifices during my graduate study period, inspiration, encouragement, sincere help and always supporting me in resolving various research problems. I am grateful to my children's, Delisha Qasrina bt Mohd Adib and Muhammad Darwisy b Mohd Adib for filling my life with joy and motivation.

My thanks also due to my parent, father Abd Hamid b Salleh and mother Zakiah bt Arifin, parent in law, brothers and sisters who give me all the support, useful advices, the prayer and always be patience with me, thank you so much.

Last but no least to all the person that I am not mentioned above, thank you for helping me and giving me the opportunity to learn and experience a lot of things to make become a better person in the future. May Allah the Almighty bless all of you.

ABSTRACT

A study was carried out on the characterisation and biological activities of *Tinospora crispa* extract with emphasis on alkaloids. Methanolic extraction, crude alkaloid fractionation and separation using different chromatographic techniques (open columns and preparative TLC) were used for isolation of pure compounds. The structure of the isolated compounds were elucidated by spectroscopic methods such as UV, IR, 1D (^{1}H, ^{13}C, DEPTQ), 2D (COSY, HMQC, HMBC) NMR, MS and also by comparison with the literature. Twelve compounds were isolated from these plants comprising eight alkaloids and four nonalkaloid compounds. Six of the alkaloid, viz., *N*-formylannonaine, *N*-formylnornuciferine, lysicamine, magnoflorine, columbamine and dihydrodiscretamine previously isolated from *T.crispa* and other species the genus *Tinospora*. In addition, one known alkaloid, liriodenine was found for the first time in this study. A novel alkaloid, 4,13-dihydroxy-2,8,9-trimethoxydibenzo[a,g]quinolizinium was isolated and its structure was established by modern spectroscopic technique. A biosynthethic route to this alkaloid is proposed. Another new compound isolated was aliphatic amine, *N*,*N*-dimetylhexadecan-1-amine. Three types of bioactivity studies, viz., acetylcholinesterase inhibitory, radical scavenging and antimicrobial studies were carried out on isolated compounds containing nitrogen. The quaternary protoberberine alkaloids; columbamine and dihydrodiscretamine were found to be potent acetylcholinesterase inhibitors. Most of the isolated quaternary alkaloids showed moderately (IC_{50} > 500-800 μg/mL) radical scavenging activity. Oxaporphine alkaloids, lysicamine, liriodenine and aliphatic amine inhibited the growth of the *Gram*-positive bacteria, *Staphylococcus aureus* (+) and *Enterococcus faecalis* (+). Aliphatic amine also exhibited inhibitory activity against *Gram*-negative bacteria, *Proteus vulgaris* (-) and *Psuedomonas aeurogenosa* (-). Results of the present biological activity investigation further points to the potential of this plant species as a good source of new AChE inhibitors. The antioxidant and antimicrobial properties of different compounds support documented traditional use of *T. crispa* in wound healing and treatment of rheumatic, diarrhoea, ulcers, itches and wounds.

ABSTRAK

Satu kajian telah dijalankan terhadap pencirian dan aktiviti biologi ekstrak pokok *Tinospora crispa* dengan tumpuan kepada alkaloid. Ekstrak methanol, pemisahan campuran alkaloid dan kaedah-kaedah kromatografi (kromatografi kolum gravity dan kromatografi lapisan nipis persediaan) telah digunakan dalam proses pengasingan alkaloid. Struktur-struktur alkaloid tersebut dikenalpasti menggunakan kaedah spektroskopi seperti spekroskopi ultra lembayung, spektroskopi inframerah, spekroskopi 1D RMN, spekroskopi korelasi RMN, spektroskopi jisim serta perbandingan data dengan tinjauan kajian. Dua belas sebatian telah diasingkan yang terdiri daripada lapan sebatian alkaloid dan empat sebatian bukan alkaloid. Enam daripada sebatian alkaloid, *N*-formylannonaine, *N*-formylnornuciferine, lysicamine, magnoflorine, columbamine dan dihydrodiscretamine telah dilaporkan pengasingannya daripada *T.crispa* dan spesis lain daripada genus *Tinospora*. Tambahan satu sebatian alkaloid yang telah dikenalpasti iaitu liriodenine telah diasingkan buat pertama kali dalam pokok ini. Satu sebatian alkaloid baru, 4,13-dihydroxy-2,8,9-trimethoxydibenzo[a,g]quinolizinium telah diasingkan dan dibuktikan dengan kaedah spektroskopi moden. Penghasilan alkaloid ini secara biosynthesis turut dicadangkan. Satu lagi sebatian baru adalah sebatian amina rantai lurus, *N*,*N*-dimetylhexadecan-1-amine. Tiga jenis aktiviti biologi telah dijalankan ke atas sebatian yang mengandungi elemen nitrogen iaitu, perencatan enzim acetylcholinesterase, aktiviti perangkap radikal bebas serta aktiviti antimikrobial. Alkaloid kuarterner protoberberine; columbamine and dihidrodiscretamine didapati berpotensi sebagai salah satu perencat enzim acetylcholinesterase. Hampir semua sebatian kuaternar alkaloid menunjukkan aktiviti sederhana (IC50 > 500-800 μg/mL) sebagai perangkap radikal bebas. Alkaloid daripada kumpulan oxoaporphine, lysicamine, liriodenine dan sebatian amina rantai lurus didapati merencatkan pertumbuhan bakteria *Gram*-positif; *Staphylococcus aureus* (+) and *Enterococcus faecalis* (+). Sebatian amina rantai lurus juga menujukkan perencatan aktiviti bagi *Gram*-negatif bakteria; *Proteus vulgaris* (-) dan *Psuedomonas aeurogenosa* (-). Hasil kajian aktiviti biologi memberi petunjuk akan potensi pokok ini sebagai satu sumber baru sebagai perencat enzim acetylcholinesterase. Aktiviti antioksida dan antibakteria yang ditunjukkan oleh sebatian yang berbeza adalah sebagai sokongan kepada penggunaan pokok *T.crispa* secara tradisional dalam merawat sakit sendi tulang, cirit birit, ulser, kegatalan dan luka.

TABLE OF CONTENTS

LIST OF TABLES

LIST OF FIGURES

LIST OF SYMBOLS

β	beta
δ	chemical shift
°C	degree Celsius
cm^{-1}	per centimeter
υ	frequency of the wave
γ	gamma
g	gram
Hz	hertz
k	kilo
L	liter
λ	wavelength
λ_{max}	maximum wavelength
mg	milligram
mL	milliliter
mM	millimolar
M	molar
µ	micro
µL	microliter
%	percentage
ppm	part per million
U	unit
UmL^{-1}	unit per milliliter

LIST OF ABBREVIATIONS

AChE	acetylcholinesterase enzyme
ATCI	acetylthiocholine iodide
^{13}C NMR	carbon nuclear magnetic resonance
CC	column chromatography
$CDCl_3$	deuterated chloroform
CD_3OD	deuterated methanol
$CHCl_3$	chloroform
COSY	correlation spectroscopy
d	doublet
dd	doublet of doublet
ddd	doublet of doublet of doublet
DEPTQ	distortionless enhancement by polarization transfer with retention of quaternaries
DPPH	2,2,-diphenyl-1-picrylhydrazyl
DTNB	5,5'-dithio-bis(2-nitrobenzoic acid)
EIMS	electron impact mass spectrometry
EtOAc	ethyl acetate
EtOH	ethanol
GCMS	Gas Gromathoraphy-Mass Spectroscopy
HCl	hydrochloric acid
^{1}H NMR	proton nuclear magnetic resonance
HMQC	heteronuclear multiple quantum coherence
HSQC	heteronuclear single quantum coherence
IC_{50}	concentration providing 50% inhibition
IR	infrared
J	coupling constant
KBr	potassium bromide
m	multiplet
M^+	molecular ion
MeOH	methanol
$MgCl_2$	magnesium chloride

MHz	megahertz
MIC	minimum inhibitory inhabitation
MS	mass spectrometry
m/z	mass to charge ratio
NaCl	sodium chloride
NH_4OH	ammonium hydroxide
NIST	National Institute of Standards and Technology
NMR	nuclear magnetic resonance
pH	power of hydrogen
PTLC	preparative thin layer chromatography
R_f	retention factor
RP-18	reverse phase silica gel
s	singlet
SiO_2	silica gel
t_R	retention time
t	triplet
TIC	total ion current chromatogram
TLC	thin layer chromatography
UV	ultraviolet

CHAPTER 1

1.1 BACKGROUND

The importance of natural products, particularly those derived from plants as a source of molecular diversity for drug discovery research and development may seem obvious. Historically, a number of recent reports have provided information about the importance of natural products as a source of bioactive compounds. Plants have good reason to produce bioactive substances. This is probably related in large part to the fact that they do not move, and therefore defend themselves by repelling or killing predators, that comprise insects, microorganisms, animals, or even other plants. Plants have evolved a complex chemical defense production system, and this may involve a large number of different chemical compounds. A great advantage of the natural products drug discovery approach is that it is capable of delivering complex molecules that are not accessible by other routes. In addition, it can provide templates leads for future drug design (Ibrahim, 2007).

Traditional plant-based medicines historically used in different parts of the world or different cultural systems are considered as “alternative medicine”. Since these plants, used singly and/or in combination with other botanicals and ingredients, have been a part of which cultural pharmacopeia and primary health care, they may provide new leads for modern medicine and new chemical entities. In many parts of the world such as Africa and Asia, the plants traditionally used for health care and medicine are still as important today as they have been previously as the only health care options affordable (Welch, 2010).

A number of traditional medicines have been scientifically proven efficacious and several have led to new mechanisms of therapeutic action against cancer,

inflammation, autoimmune diseases, Alzheimer's disease, Parkinson's disease, malaria, and cardiovascular disease (Kong et al., 2003). Certain areas of drug therapy depend largely on bioactive compounds derived from natural product and natural product mimics, in particular, antibacterial, anti-infectives and antihypertensive drugs (Cos et al., 2003). Natural product chemistry is an area of chemistry that has successfully delivered a large number of antimicrobial agents, anticancer and antiviral drugs that have been promoted to the commonly prescribed drugs (Kong et al., 2003).

Today, natural product chemists are involved in performing phytochemical studies on plants having biomedical importance in folk medicine history. These studies have yielded several biomedical agents including paclitaxel and emetin. Paclitaxel (Taxol®), which was isolated from bark extract of the Pacific yew tree, (*Taxus brevifolia*) , is an important drug used in the treatment of cancer (Burstein et al., 1992). It is an effective drug of choice for the treatment of lung, ovarian and breast cancer. Similarly, the isoquinoline alkaloid, emetine isolated from *Cephaelis ipecacuanha*, has been used for many years for the treatment of abscesses caused by the spread *of Escherichia histolytica* infections (Chang and But, 1986).

Drug discovery from plants has evolved to include numerous fields of inquiry and various methods of analysis. The process typically begins with a botanist, ethnobotanist, ethnopharmacologist or plant ecologist collecting and identifiying plants of interest. Phytochemists then prepare extracts from the plant material, subject these extracts to biological screening in pharmacologically relevant assays and commence the process of isolation and characterization of the active compounds through bioassay-guide fractionation (Balunas and Kinghorn, 2005).

The investigation of bioactive natural product was mainly concerned with the study of discovering bioactive constituents from plant and living organisms. During the early stages of natural product research, detection, isolation and structural elucidation of natural product were the main focus of researchers. Nowadays, the advent of more efficient methods of isolation, separation, purification and the availability of new bioassay techniques have greatly stimulated the development of research in this field (Vlietinck, 1998).

Tinospora crispa (family: Menispermaceae; Malay: akar seruntun, patawali) is widely used in Malay traditional medicine as well as other indigenous peoples in Malaysia as an ethno-remedy for the treatment of hypertension and diabetes (Dweck and Cavin, 2006). Besides that, *T. crispa* is also used to treat tooth and stomach aches, coughs, asthma and pleurisy (Rahman et al., 1999). Scientifically, *T. crispa* has been demonstrated to possess antibacterial (Zakaria and Matjais, 2006), antiflarial, antimalarial, antipyretic and antihyperglycaemic activities (Kongkathip et al., 2002). Based on this ethanomedical importance of plants, the present study is designed to explore the active phytochemicals from the plants.

The plant family Menispermaceae has long been a rich source of alkaloids, terpenoids and glycosides. *Tinospora* is a genus within Menispermaceae reputed for it medicinal properties (Pathak et al., 1995). The great majority of compounds isolated from *Tinospora* species have been furanoid diterpenes of the clerodane type, and their glycoside derivatives (Hungerford et al., 1998). More than 50 clerodane-based compounds have been isolated from various *Tinospora* species. Quaternary alkaloids are the major alkaloid type isolated from *Tinospora* species, and these are mostly of the protoberberine. Some non-quaternary alkaloids have also been isolated from certain *Tinospora* species and most recently the *N*-acyl aporphine alkaloids (Hungerford et al., 1998). The medicinal value of *Tinospora* species can most probably be attributed to the wide variety and high concentrations of alkaloids.

Alkaloids constitute one of the most important natural products produced in the plant kingdom. Alkaloids are organic nitrogenous bases found mainly in plants, but also to a lesser extent in microorganisms and animals. Several alkaloids in popular use include caffeine; a psychostimulant is largely obtained from the decaffeination of *Coffea* species and codeine as an antitussive. Cocaine is used as a local anesthetic (Roberts and Wink, 1998). Morphine is an indispensable analgesic used for treatment of severe pain. Quinine is noted for its antimalarial activity and remains on the market as an antipyretic (fever suppressant), although its earlier dominance by synthetic drugs such as quinoline derivatives include chloroquine, amodiaquine, quinine, quinidine, mefloquine, primaquine, lumefantrine and halofantrine (Travassos and Laufer, 2009).

1.2 PROBLEM STATEMENT

The chemical constituents of *T. crispa* extracts have been extensively studied since the 1980s. The major active ingredients of *T. crispa* are identified as terpenoids and terpenoid glycosides. The terpenoid glycosides are mainly composed of borapetosides A, B, C, D, E and F (Cavin et al., 1998; Choudhary et al., 2010; Kongkathip et al., 2002; Martin et al., 1996; Pachaly and Schneider. 1992 and Pathak et al., 1995). Recently, Choudhary et al. (2010) reported the isolation of a new aporphine alkaloid, *N*-formylasimilobine 2-O-β D-glucopyranoside, along with nine known alkaloids from stems of *T. crispa*. Although the same species had been studied by researchers from Malaysia, China, Pakistan, India and Thailand, different localities or environment probably give variations of constituents because of geographic distribution, climate, different plant parts and morphology as well as ecological conditions which influence the biosynthesis of secondary metabolites of the plants. There are many more bioactive compounds waiting to be isolated. *T. crispa* is widely used in traditional medicine; however there are only a few reports that indicate which chemical compounds contribute to the medicinal properties of the plant (Ruan et al., 2012). *T. crispa* is often used as tonic plants due to its bitter taste. This can be attributed to the high concentration of alkaloids in these plants. Many alkaloids are pharmacologically active substance (Robert and Wink, 1998).

1.3 RESEARCH OBJECTIVES

This research is directed towards the study of *T. crispa* extract including the isolation, identification and characterisation of the compounds with emphasis on alkaloids as well as the biological activities. The specific objectives of this research are to:

1. To isolate compounds with emphasis on alkaloids in *T. crispa*.
2. To elucidate the structure of compounds by spectroscopic techniques.
3. To evaluate for radical scavenging activity, acetylcholinesterase inhibitory activity and antimicrobial activity.

1.4 SCOPE OF THE STUDY

There are two main approaches in natural product researches including chemical investigations and the bioactivity studies. Specifically, the chemical compounds of the alkaloid extracts were purified by chromatographic techniques and followed by recrystallization. Characterisation of isolated compounds was carried out by spectroscopic methods such as IR, NMR (^{1}H, ^{13}C, DEPTQ, COSY, HMQC, HMBC) and MS.

Evaluation of the biologically activities of the isolated compounds were carried out using more than one technique to cover the bioactivity of interest. The isolated compounds were screened for radical scavenging activity, acetylcholinesterase inhibitory activity and antimicrobial activities.

CHAPTER 2

LITERATURE REVIEW

2.1 BOTANICAL OVERVIEW

Tinospora crispa is classified under family Menispermaceae of the order Ranunculales (Figure 2.1).

Kingdom	: Plantae
Division	: Angiospermae
Class	: Magnoliidae
Order	: Ranunculales
Family	: Menispermaceae
Genus	: Tinospora
Species	: *Tinospora crispa*

Figure 2.1: Specific classification of species *Tinospora crispa*

Source: Wang et al. (2007)

2.1.1 Menispermaceae

The Menispermaceae is composed of 71 genera and about 520 species (Jacques and Zhou, 2010). The family Menispermaceae is highly specialized in that its extraordinarily rich diversification of bisbenzylisoquinoline and aporphine derivatives.

Up to the end of 1996, 1858 alkaloids have been described from 244 species of the family (Barbosa-Fillo et al., 2000). These alkaloids include many important discoveries in the field of medicine and pharmaceutically active compounds (Dewick, 2002). A literature survey revealed that twenty-one genera are used for medicinal purposes in the world. Nine genera in use are *Cissampelos*, *Cocculus*, *Dioscoreophyllum*, *Jateorhiza*, *Sphenocentrum*, *Stephania*, *Tiliacora*, *Tinospora* and *Triclisia* (De Wet, 2006).

Menispermaceae are twinning or rarely erect shrubs or lianas; rarely herbs or trees. Wood in cross-section showing broad, medullary rays. The leaves are alternate, spiral, petiolate. Flowers of Menispermaceae are dioecious. (De Wet, 2006). Seeds often curved and horseshoe-shaped, with uniform or ruminate endosperm or without endosperm. Embryo straight or curved; cotyledons flat or more or less terete, foliaceous or fleshy, divaricate or appressed (Kessler, 1993).

2.1.2 Genus *Tinospora*

Genus *Tinospora* consists of approximately 35 species where 23 are found in Asia, Australia and the Pacific, two in Madagascar, seven in tropical Africa and three in southern Africa (De Wet, 2006). Species of the *Tinospora* genus have prominent roles in the traditional medicinal practices of Australia, Africa and Asia (Hungerford et al., 1998).

Tinospora smilacina Benth. (Menispermaceae), commonly known as `snakevine', is a semideciduous woody climber which inhabits open forests and low, open woodlands across northern Australia and the east coast to northern New South Wales. The stems, leaves and roots of this species have been used in traditional aboriginal medicine for treatment of a remarkably wide range of disorders. In particular, the roots were used to counter animal stings and used in Western Australia spesifically as a snakebite remedy (Hungerford et al., 1998).

Tinospora cordifolia is an official herb in the Indian Pharmacopoeia and also in the Ayurvedic Pharmacopoeia. The stems of *T. cordifolia* (TC) known as Guduchi

vernacular name, is widely used in Ayurveda as Rasayana to enhance general body resistance, promote longevity and as antistress and adaptogen (Patil et al., 2009).

Tinospora rumphii Boerl. (synonyms *T. tuberculata* Buemee and *T. crispa* Miers) is a climbing vine with stems rich in warts. It is widely distributed in the Philippines and in some Southeast Asian countries. This bitter tasting plant, known in the Philippines as Makabuhai, is used for the treatment of stomach troubles, ulcers and fevers, as a tonic and a febrifuge for malaria and smallpox, as a vulnerary for itches and wounds, and many other purposes (Martin et al., 1995).

The Chinese Materia Medica recorded 4 major *Tinospora* species (*Tinospora sagittata*, *Tinospora sinensis*, *Tinospora crispa* and *Tinospora capillipes*). Traditional Chinese Medicines (TCM) products like the famous Fufang Danshen tablets is prepared from the roots of *Tinospora sagittata* (Oliv.) Gagnep and *Tinospora capillipes* Gagnep. (Shi et al., 2007).

Overall the genus *Tinospora* has been cited four times as analgesic, fourteen times for anti-malarial property and sixteen times for diabetes treatment (De Wet, 2006). *Tinospora* is mostly used in the rest of the world as an anthelmintic, treatment of arthritis and rheumatism, diabetes, fever, malaria, wounds, ulcers and as tonic (De Wet, 2006). Their potential in ethnopharmacology and drug discovery should not be underestimated.

2.1.3 *Tinospora crispa*

Tinospora crispa (L.) Miers ex Hook. f. &Thoms, known by different botanical synonyms such as *Tinospora rumphii* or *Tinospora tuberculata*, belongs to the family Menispermaceae (Martin et al, 1995) *T. crispa* is also known as “patawali” or “akar seruntum” in Malay, “boraphet” in Thai, “makabuhay” in Philipines, “day coc” in Vietnamese and Bo Ye Qing Niu Dan in Chinese (Fukuda et al., 1983). It is found in primary rainforests or mixed deciduous forests throughout a large part of Asia and Africa (Pathak et al., 1995).

T. crispa is a climbing, dioeciously vine reaching a height of 4-10 meters. The stem is about 1 centimeter thick, somewhat fleshy, with scattered protuberances. The leaves are thin, ovate, 6-13 centimeters long and 6-13 centimeters wide. The petiole is 5-15 centimeters long. Inflorescences racemose, unbranched or occasionally shortly branched, appearing before leaves, flowers 2- or 3-fascicled. Male inflorescences very slender, 5-10 cm or longer. Male flowers: sepals 6 in 2 whorls, green, glabrous, petals 3-6, yellow, obovate-spatulate. Female inflorescences 2-6 cm, flowers mostly 1 per node. Female flowers: sepals and petals as in male; stigma lobes very short.Fruiting peduncle 15-20 mm; carpophores 2-3 mm (Hooker and Thomson, 1855).The botanical features of *T. crispa* is depicted in Figure 2.2**.**

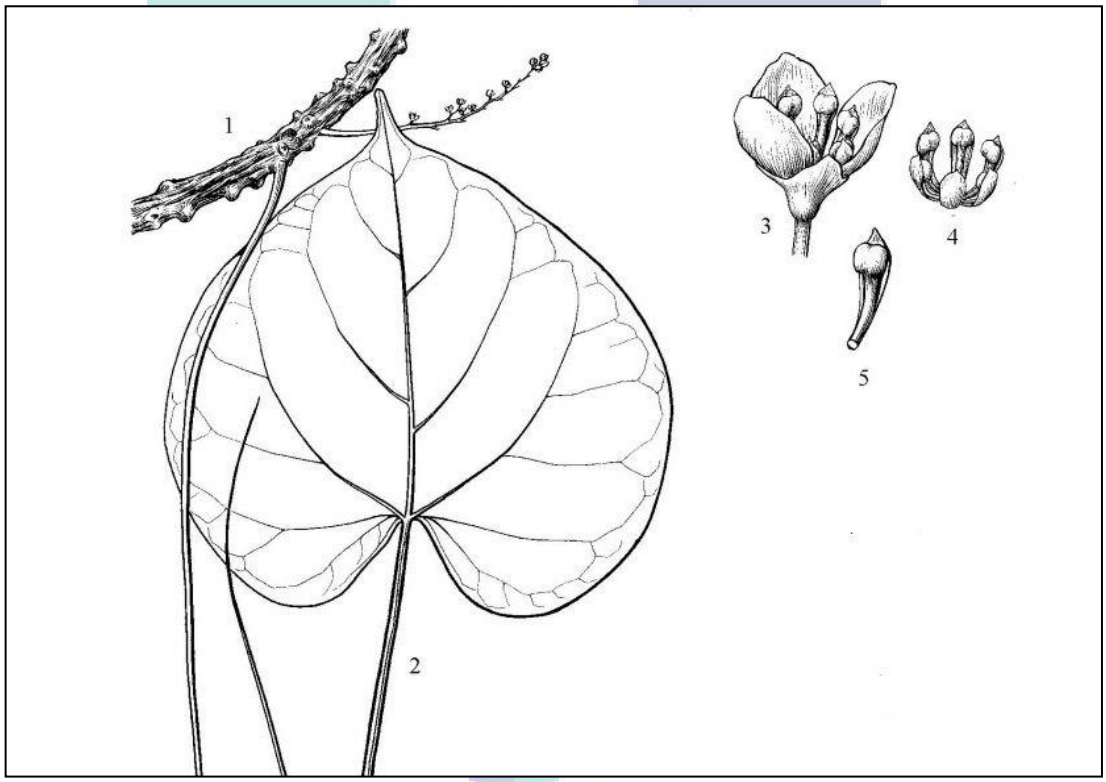

Figure 2.2: *Tinospora crispa*, 1.Flowering branch with aerial root, 2.Leaf, 3.Male flower, 4.Male flower with sepal remove, 5.Stamen

Source: Hooker and Thomson (1855)

2.2 ETHNIC MEDICAL USAGE

In Malaysia, an aqueous extract of *T. crispa* stems is taken orally to treat diabetes mellitus (Noor and Ashcroft, 1989). The young stem of the plant is chewed to relieve hypertension, toothache and abdominal pains (Zaridah et al., 2001). Extracts of *T. crispa* roots pounded with garlic and a pinch of salt is drunk once per day for 3 days for filarial eradication. Poultice made by pounding *T. crispa* root with rice wash and charred coconut husks was used to cure rheumatism (Ahmad and Raji, 1993).

In Thailand, the stem of *T. crispa* is one of the most popular traditional appetizer and for febrifuge for malaria and smallpox. According to the Thai, it makes the blood "bitter and cool" (Fukuda et al., 1983).

T. crispa is known to the Filipinos as "makabuhay" meaning 'that which bring back life' due to their believed that it can cure malarial fever (Salazar et al., 1987). In the Philippines it is also used for the treatment of stomach troubles, ulcers and as a vulnerary for itches and wounds (Martin et al., 1995).

2.3 PHARMACOLOGICAL IMPORTANCE

Various studies have been conducted on the pharmalogical effectiveness of *T. crispa* extracts to support ethnopharmacological claims.

The antihyperglycaemic and insulinotropic effect of *T. crispa* observed in *in vivo* and *in vitro* experimental models supports the anecdotal claims for its antidiabetic activity (Noor and Ashcroft, 1989). This could lead to the formulation of a novel drug for the treatment of noninsulin-dependent diabetes mellitus. However, vigorous characterisation of the extract with respect to its mechanism of action is necessary before a pharmacological role can be assigned. The results clearly showed that the antihyperglycaemic effect is not due to interference with intestinal glucose uptake or uptake of the sugar into the peripheral cells. Rather, the antihyperglycaemic effect of *T. crispa* is probably due to stimulation of insulin release via modulation of intracellular Ca^{2+} concentration in pancreatic β-cells (Noor and Ashcroft, 1998). That the

insulinotropic effect of *T. crispa* is physiological suggests that the extract contains compounds which could be purified for use in the treatment of type II diabetes.

The suggestion by Noor and Ashcroft (1998) had been proven by the study conducted by Ruan et al., (2012). In the study, they proved that borapetoside C can increase glucose utilization, delay the development of insulin resistance and enhanced insulin sensitivity. The activation or the enhancement of insulin stimulation of the insulin receptor (IR) and protein kinase B (Akt) as well as the expression of glucose transporter-2 (GLUT2) pathway may contribute to the plasma glucose-lowering effect of borapetoside C in in diabetic mice.

T. crispa has also been used in folkloric medicine for the control of blood pressure. According to Thai traditional medicine *T. crispa* have therapeutic effects on the cardiovascular system (Praman et al., 2012). It has been confirmed the extract of *T. crispa* stems decreased the mean arterial blood pressure with a transient decrease followed by an increase in the heart rate in rats (Praman et al., 2011). In order to investigate the mechanisms of action on blood pressure and heart rate, five isolated compounds from *T. crispa* extracts; adenosine, uridine, salsolinol, higenamine and tyramine were studied in anesthetized, normal and reserpinized rats *in vivo*. The results demonstrate that these five compounds from *T. crispa* acted in concert on the cardiovascular system of anesthetized rats. Salsolinol, tyramine and higenamine acted via the adrenoreceptors, whereas uridine and adenosine acted via the purinergic adenosine A_2 and P_2 receptors to decrease blood pressure with a transient decrease followed by an increase of heart rate (Praman et al., 2012).

Cardiac contractility of two triterpenes isolated from the stems of *T. crispa* had been studied and the results demonstrated cycloeucalenol slightly increased the right atrial force of contraction whereas it showed an initial reduction followed by sustained reduction of about 10% on the left atria of the rat *in vitro*. Cycloeucalenone showed slight change from the control on the right and left atrial force. These results suggest that cycloeucalenol and cycloeucalenone produced mild cardiotonic effects (Kongkathip et al., 2002).

Ethanol extract of *T. crispa* were reported to exert antinociceptive and anti-inflammatory activity in various animal models. The ability to inhibit chemically and thermally-induced nociception indicates the extracts characteristic as strong analgesics. The results of this study justify the folklore uses the plant in treating pain and anti-inflammation related ailments (Sulaiman et al., 2008).

The antioxidant and anti-proliferative activity of the aqueous crude extract of *T. crispa* stem was investigated. The findings from this study suggest that *T. crispa* has the potential to be a source of natural antioxidants and nutrients, besides having a moderate anti-proliferative effect on selected human cancer cell lines (IC_{50} MCF-7:107 µg/mL, HeLa:165 µg/mL, Caov-3:100 µg/mL and HepG2:165 µg/mL) . The results obtained from this study suggest that *T. crispa* could be used as an easily accessible source of natural antioxidants and possible supplement in the food supplement manufactured. However, the major components responsible for preventing cancer activities need to be further investigated (Zulkhairi et al., 2008). Another study reported that *N*-trans-feruloyltyramine (**31**), *N*-cis feruloyltyramine (**32**) and secoiolariciresinol isolated from the dichloromethane extract of *T. crispa* exhibited antioxidant and strong radical scavenging properties toward β-carotene and 2,2-diphenyl-1-picrylhydrazyl (DPPH) radicals (Cavin et al., 1997).

A methanol extract of *T. crispa* stems showed considerable antimalarial activity against *Plasmodium falciparum* (*in vitro*) and *Plasmodium berghei* (*in vivo*) (Rahman et al., 1999). This suggested the existence of fast-acting antimalarial principal which can be isolated and the effect was probably due the presence of quaternary alkaloids such as berberine whose action was to block protein synthesis in *Plasmodium falciparum.*

2.4 PHYTOCHEMICAL REVIEW OF GENUS *TINOSPORA*

Several studies have been conducted on the constituents of the genus *Tinospora*, and a variety of compounds have been isolated including furanoditerpene lactones, steroids, flavonoids, lignans, alkaloids and phenolics (Maurya et al., 1994). The great majority of compounds isolated from *Tinospora* species have been furanoid diterpenes of the clerodane type, and their glycoside derivatives (Hungerford et al., 1998). More

than 50 clerodane-based compounds have been isolated from various *Tinospora* species, and some representative examples are shown in Figure 2.3.

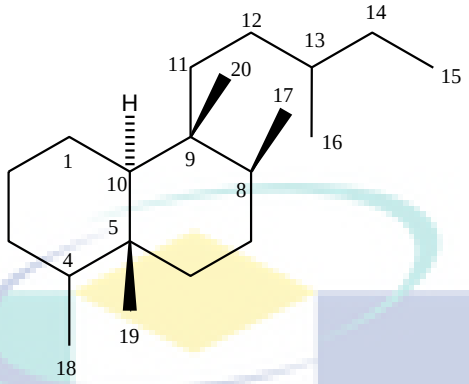

(**1**) The clerodane skeleton

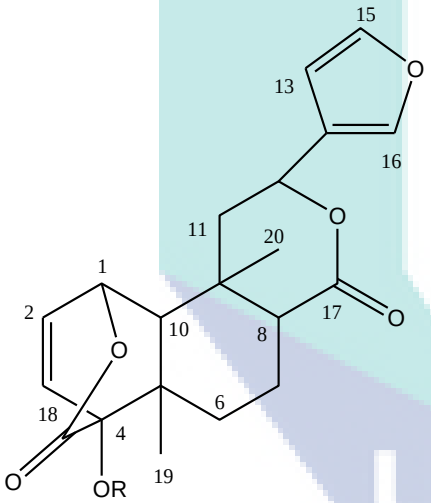

	R	Compound
(**2**)	H	columbin
(**3**)	β-D-glyc	palmatoside C

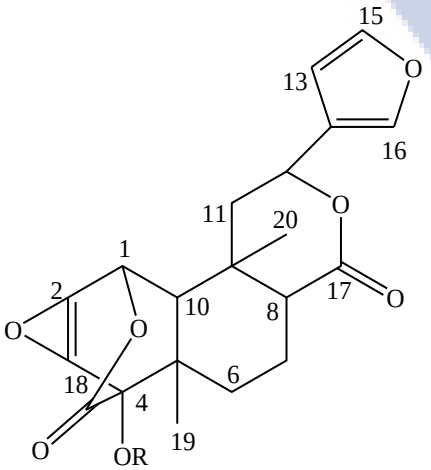

	R	Compound
(**4**)	H	jeteorin
(**5**)	β-D-glyc	palmatoside F

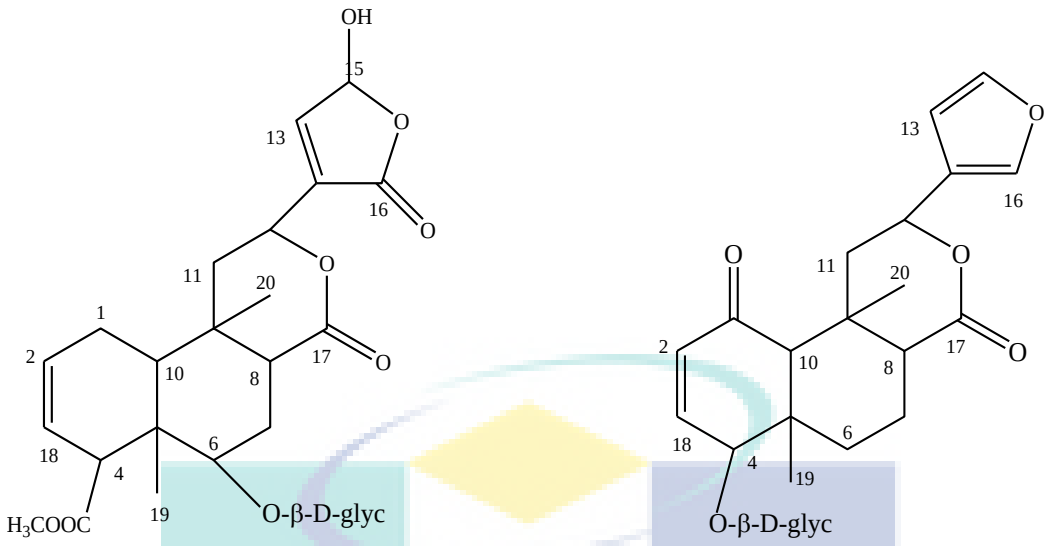

(**6**) rumphioside A (**7**) tinosporaside

Figure 2.3: Clerodane-based furanoid diterpenes and their glycoside derivatives

A new clerodane diterpene, tinoscorside C (**8**), and a new phenylpropanoid, sinapyl 4-O-β-D-apiofuranosyl-(1→6)-O-β-D-glucopyranoside (tinoscorside D) (**9**) had been isolated from *T. cordifolia* (Phan et al., 2010).

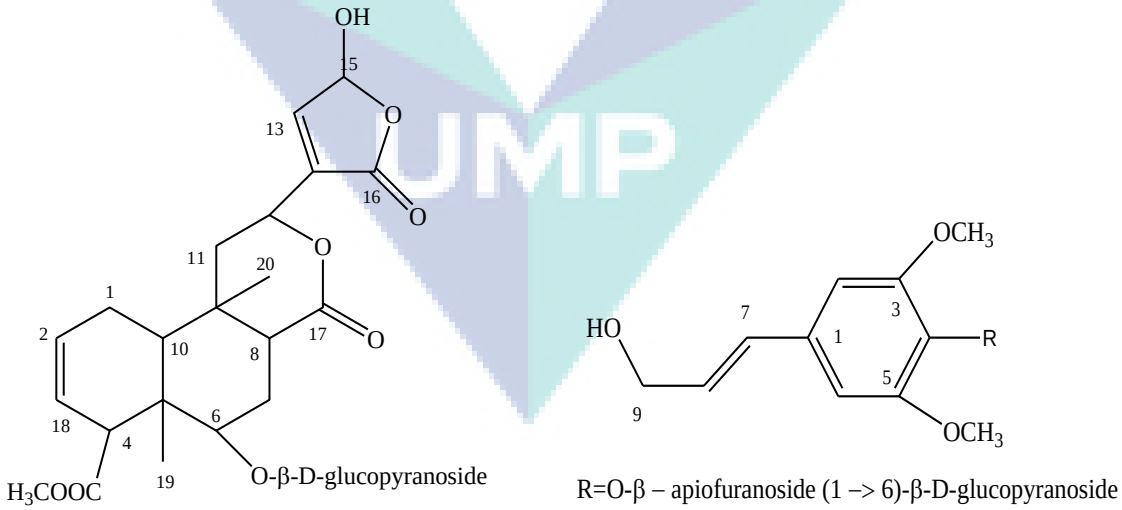

(**8**) (**9**)

A diterpene tinosporan ($C_{20}H_{22}O_8$) was isolated from the stems of *T. crispa*. The chemical constituents of *T. crispa* have been extensively studied since 1983. Compounds isolated from *T. crispa* have been identified as terpenoids and terpenoid

glycosides: borapetol A (**10**), borapetoside A (**11**), borapetol B (**12**), borapetoside B (**13**), and γ-sitosterol (**14**) (Fukuda et al., 1983, 1985, 1986 and Pachaly et al., 1992).

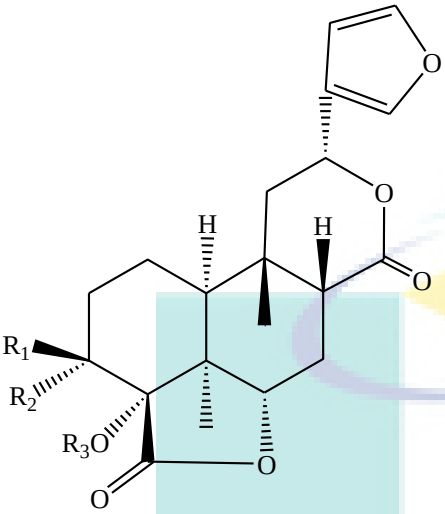

Compound	R_1	R_2	R_3
(**10**)	-O-β-D-gly·pyr.	H	H
(**11**)	OH	H	H

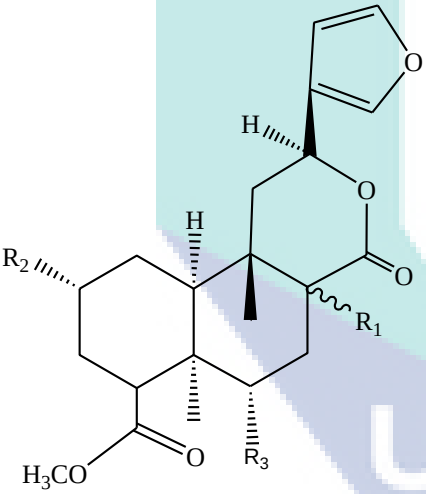

Compound	R_1	R_2	R_3
(**12**)	α-H	OH	-O-β-D-gly·pyr
(**13**)	α-H	OH	OH

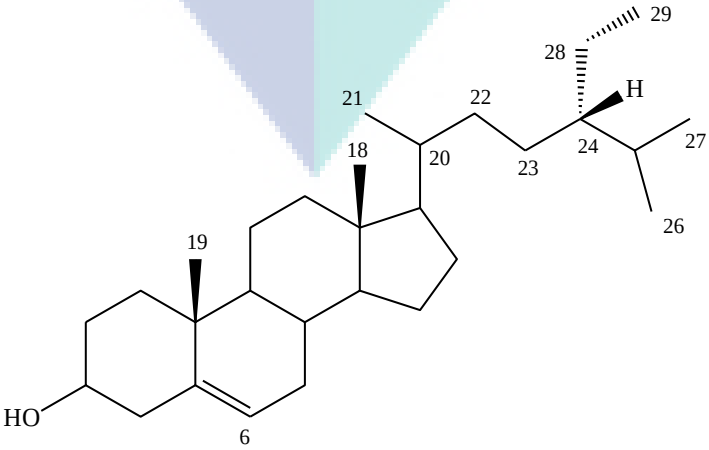

(**14**)

In addition another two phenolic amides were isolated from *T. crispa* and reported are *N*-trans-feruloyltryamine (**15**) and *N*-cis-feruloyltryamine (**16**) (Cavin et al.,1998).

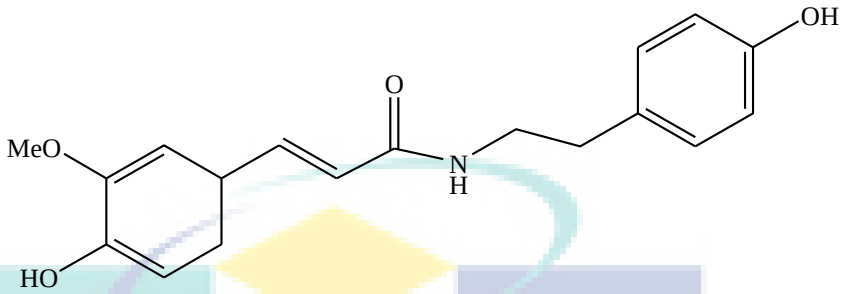

(**15**)

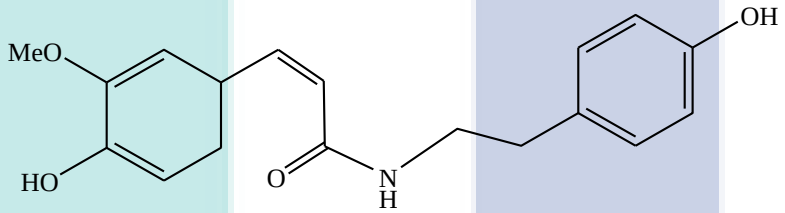

(**16**)

More recently, two triterpenoids have been isolated from the stems of *T. crispa*, namely, cycloeucalenol (**17**) and cycloucalenone (**18**). Both of these triterpenes possess cardiotonic activities (Kongkathip et al., 2002).

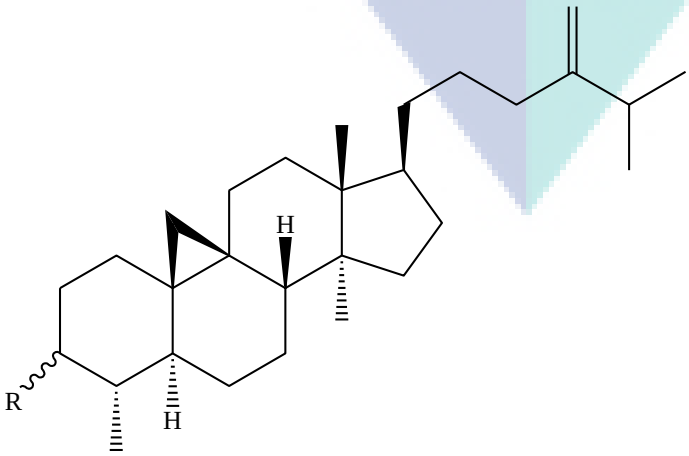

Compound	R
(**17**)	β-OH
(**18**)	=O

Luteolin 4'-methyl ether 7-glucoside (**19**), luteolin 4'-methyl ether 3'-glucoside (**20**), genkwanin 7-glucoside (**21**), genkwanin (**22**) and diosmetin (**23**) were some

flavone glycosides and aglycones isolated from the stems of *T. crispa* (Umi Kalsom and Noor, 1995).

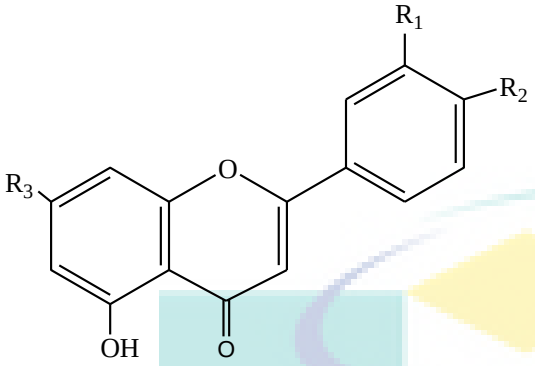

Compound	R_1	R_2	R_3
(**19**)	OH	OCH_3	*O*-Glc
(**20**)	*O*-Glc	OCH_3	OH
(**21**)	H	OH	*O*-Glc
(**22**)	H	OH	OCH_3
(**23**)	OH	OCH_3	OH

Quaternary alkaloids are the major alkaloid type isolated from *Tinospora* species, and these are mostly of the protoberberine, and aporphine classes. A review discussing the quaternary alkaloids of *Tinospora* species has been published. Some non-quaternary alkaloids have also been isolated from certain *Tinospora* species, and recently *N*-acyl aporphine alkaloids were isolated from the *T. crispa* of Indonesia and South-East Asia (Hungerford et al., 1998).

2.5 ALKALOIDS

The definition of an alkaloid as a basic nitrogenous compound occurring in plants and usually having some physiological activity seems to have been discarded (Sangster and Stuart, 1964) . Several alkaloids have been isolated from animals, some are nonbasic and some groups of compounds have also been classified as alkaloids by a numbers of author and not as alkaloids by others. It can be concluded that basic compounds can be considered as genuine alkaloids (Sangster and Stuart, 1964). The alkaloid name is in fact derived from alkali. However, the degree of basicity varies greatly, depending on the structure of the alkaloid molecule, and the presence and location of other functional groups (Ibrahim, 2007).

Alkaloids are nitrogen-containing compounds that occur naturally not only in plants but also in microorganisms, marine organisms, and animals (Kuramoto, et al., 2004). Most alkaloids have p*K*a values of about 6 to 12, with several having narrow

pKa value of 7-9 (Pelleties, 1983). The free base is soluble in organic solvents and not in water. Protonation of the nitrogen in the free base usually results in a water-soluble compound. This behavior is the basis of the selective isolation of alkaloids by liquid/liquid partitioning processes. Quaternary alkaloids are poorly soluble in organic solvents but soluble in water at any pH. Alkaloids are not very stable; in particular, *N*-oxidation is quite common. Stability is influenced by solvents, as well as heat and light. Halogen-containing organic solvents such as chloroform and dichloromethane are widely used in alkaloid research. Chloroform in particular is a very suitable solvent, because of its relatively strong proton donor character. However, this solvent easily causes the formation of artifacts, e.g. *N*-oxidation products. The presence of dichloromethane may result in the formation of quaternary *N*-dichlorometho-compounds. Similar compounds are formed with the minor impurities present in chloroform. Peroxides in ethers may also cause *N*-oxidation (Pelleties, 1983).

Alkaloids are often classified according to the nature of the nitrogen-containing structure, such as pyrrolidine (**24**), pyridine (**25**), piperidine (**26**), imidazole (**27**), quinoline (**28**), isoquinoline (**29**) and indole (**30**) (Figure 2.4).

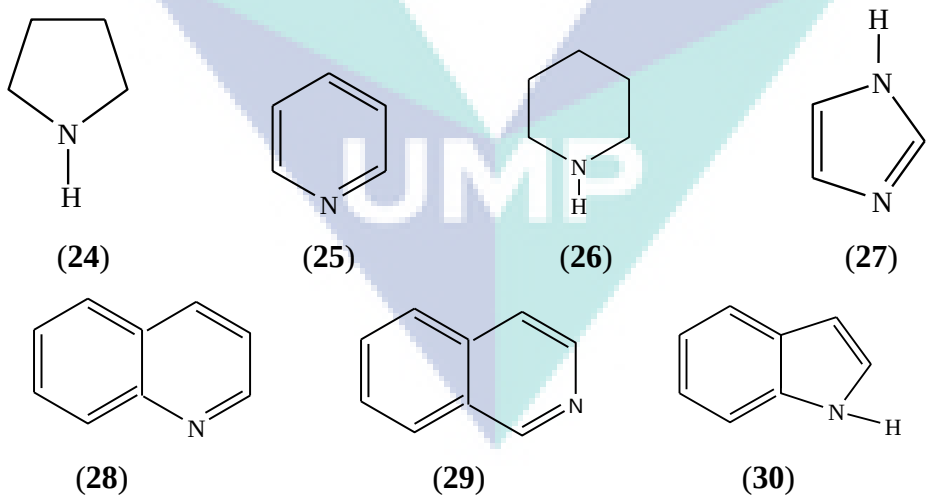

Figure 2.4: Classification of alkaloids

2.5.1 Biosynthesis

Since the genus *Tinospora* rich of alkaloids protoberberine and aporphine types, it is worthwhile to describe the biogenetic pathway of benzylisoquinoline alkaloid in nature. Theoretically these two types of alkaloids derive from such precursors. Although many authors had reported the biosynthesis pathway for both alkaloids (Grycova et al., 2007; Schafer and Winks, 2009 and Thornber, 1970), the general sequences are summarizing in Figure 2.5. It was shown that the benzylisoquioline alkaloids are constructed from two molecules of tyrosine. Along one branch, tyrosine is converted to dopamine and a second molecule of tyrosine is converted to 4- hydroxyl phenylacetaldehyde (4-HPA) along a second branch. The earliest enzyme cloned in this pathway is tyrosine decarboxylase (TYDC) which catalyzes the decarboxylation of tyrosine to tyramine or dihydroxyphenylalanine (L-dopa) to dopamine. The other cloned enzyme in this upstream pathway is norcoclaurine synthase (NCS) which catalyzes the condensation of dopamine and 4-HPA, the first committed step in benzylisoquinoline alkaloid biosynthesis (Chow and Sato, 2013).

The formation of norcoclaurine is catalyzed by an enzyme 6-O-methyltransferase (6OMT). Next, the norcoclaurine is converted into (S)-reticuline and catalyzed by 3'-hydroxy-N-methylcoclaurine 4'-O-methyltransferase (4'OMT) (Hagel and Faccini, 2010). A number of aporphine alkaloids can be conceive of as arising from oxidative phenolic coupling between C-8 and C-2' or between C-8 and C-6' of (S)-reticuline (Hagel and Facchini, 2010).

The formation of (S)-reticuline also had led to biosynthesis of protoberberine alkaloids. Oxidative cyclization of (S)-reticuline through two steps; the formation of a methylene iminium ion followed by nucleophilic attack at the imine carbon by C-2' to yield the C-8 berberine bridge. This reaction is catalyzed by berberine bridge enzyme (BBE). Tetrahydroprotoberberine oxidase is required for the conversion to quaternary form (Hagel and Facchini, 2010).

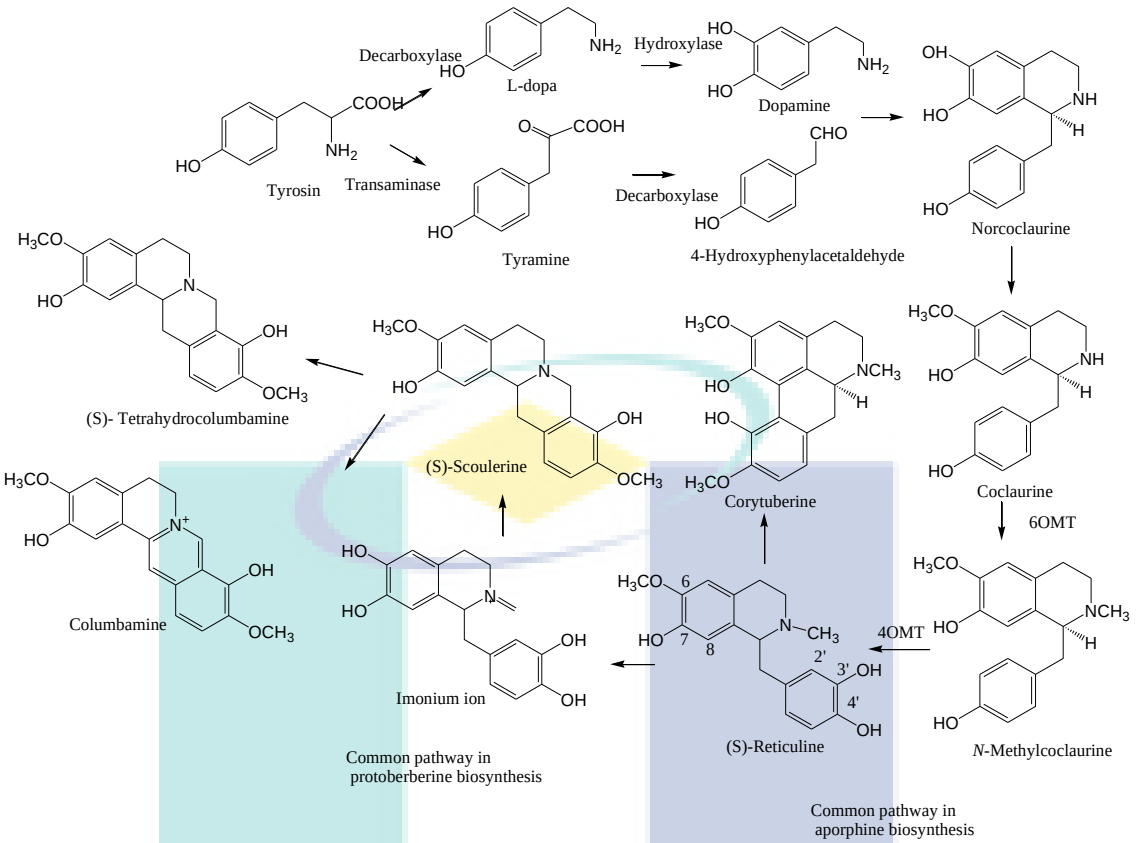

Figure 2.5: Biosynthesis pathway of aporphine and protoberberine alkaloids

2.5.2 Aporphine Alkaloids

Aporphines comprise the largest type of isoquinolines alkaloids. All aporphine alkaloids are based on the skeleton depicted in Figure 2.6 and consisting of di, tri, tetra, penta, and hexasubstituted derivatives with the substituents being hydroxy, methoxy, or methylenedioxy groups. The substitutents in aporphine alkaloids may be located in all four rings, with the exception of the methylenedioxy group, which is found only in rings A and D. In the case of all the disubstituted aporphines which had been isolated, the substituents are present in positions 1 and 2 in ring A. The most widespread in nature are the 1,2,9,10- and 1,2,10,11-tetrasubstituted bases, but pentasubstituted aporphines in which functional groups occupy positions at various carbon atoms are also found. The nitrogen atom in the aporphines may be secondary (R = H), tertiary (R = CH_3, $COCH_3$), or quaternary (Israilov et al., 1980).

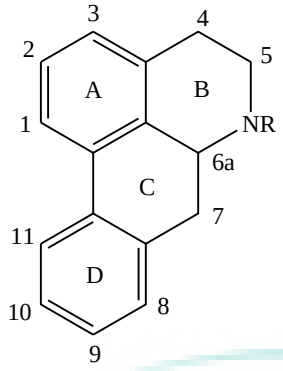

R= -H, -CH_3, -$COCH_3$

(31)

Figure 2.6: Basic sckeleton of aporphine alkaloid

2.5.3 Protoberberine Alkaloids

The protoberberine alkaloids are biogenetically derived from tyrosine. The quaternary protoberberine alkaloids (QPA) represent approximately 25% of all currently known alkaloids with a protoberberine skeleton isolated from natural sources (Grycova et al., 2007). Most protoberberine alkaloids exist in plants either as tetrahydroprotoberberines or as quaternary protoberberine salts. Substituents are usually present at positions 2,3,9,10 or 2,3,10,11 and the prefix pseudo- is often used for the substitution pattern in the latter (Figure 2.7). Additionally, compounds with substituents at carbon atoms C-1, C-4, C-5 and C-13 have been isolated from natural sources. Typical substituents are hydroxy, methoxy and methylenedioxy groups (Grycova et al., 2007).

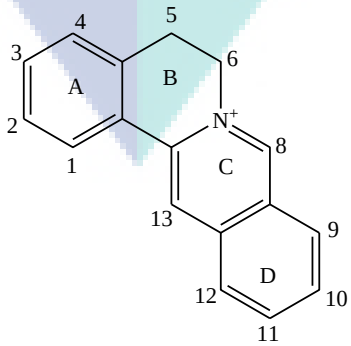

(32)

Figure 2.7: Basic sckeleton of protoberberine alkaloid

2.5.4 Alkaloids in Genus *Tinospora*

Atta-ur-Rahman and Ahmad (1987) had reported the isolation of three alkaloids from *T. crispa*: *N*-formylannonaine (**33**), an aporphine alkaloid, and two *N*-acyl aporphine alkaloids, *N*-formylnornuciferine (**34**) and *N*-acetylnornuciferine (**35**).

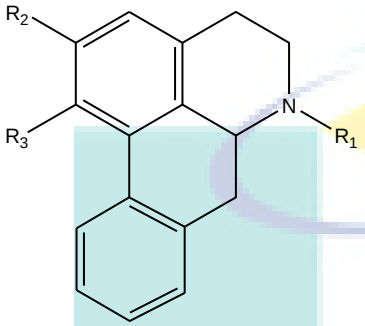

Compound	R_1	R_2	R_3
(**33**)	CHO	O-CH_2-O	
(**34**)	CHO	OCH_3	OCH_3
(**35**)	$COCH_3$	OCH_3	OCH_3

The presence of *N*-formylnornuciferine (**33**) in *T. crispa* had been confirmed by Cavin et al. (1998) through isolation from the dichloromethane fraction through MPLC. They also identified an alkaloid *N*-formylannonain (**34**) via on-line identification LC/MS analysis.

Kokusaginine (**36**), the first furoquinoline alkaloid from Menispermaceae was isolated from *T. malabrica* (Bowen et al., 1985).

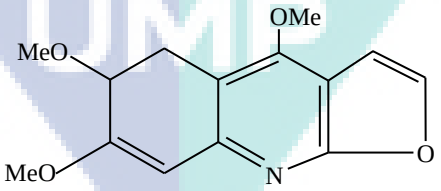

(**36**)

The occurance of quaternary alkaloids in *Tinospora* species was studied and the main compounds were generally protoberberine bases berberine (**37**), palmatine (**38**) and jattrohizine (**39**) and minor constituent, the aporphine bases magnoflorine (**40**) and tembetaratine (**41**) were also present (Pathak et al., 1995). Table 2.1 summarizes the quaternary alkaloids isolated from *Tinospora* species.

Table 2.1: Summary quaternary alkaloids isolated from *Tinospora* species

Alkaloids (Structure No.)	**Name of Plant (Part Used)**	**Reference**
Berberine (**37**)	*T. cordifolia (S)*	Pachaly and Schneider, 1981
Palmatine (**38**)	*T. cordifolia (S)*	Bisset and Nawaiwu, 1983
	T. malabrica (S)	Atta ur-Rahman et al., 1992
Jatrorrhizine (**39**)	*T. cordifolia (S)*	Bisset and Nawaiwu, 1983
	T. cappillipes (R)	Chang et al., 1984
Magnoflorine (**40**)	*T. cordifolia (S)*	Pachaly and Schneider, 1981
	T. malabrica (S)	Prakesh and Zaman, 1982
	T. cappillipes (R)	Chang et al., 1984
Tembetarine (**41**)	*T. cordifolia (S)*	Pachaly and Schneider, 1981
Stepharanine (**42**)	*T. cappillipes (R)*	Chang et al., 1984
Columbamine (**43**)	*T. cappillipes (R)*	Chang et al., 1984
Dihydrodiscertamine (**44**)	*T. cappillipes (R)*	Chang et al., 1984
Menisperine (**45**)	*T. cappillipes (R)*	Chang et al., 1984

S-stem *R*-root

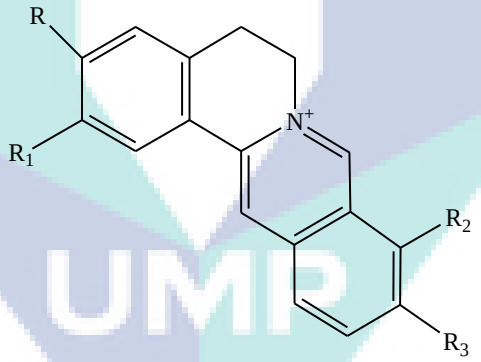

Compound	**R**	**R_1**	**R_2**	**R_3**
(**37**)	O-CH_2-O		OCH_3	
(**38**)	OCH_3		OCH_3	
(**39**)	OH	OCH_3	OCH_3	
(**42**)	OCH_3	OH	OCH_3	OH
(**43**)	OCH_3	OH	OCH_3	
(**44**)	OH	OCH_3	OCH_3	OH

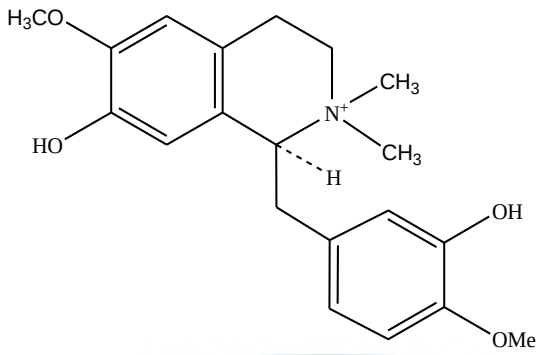

(**41**)

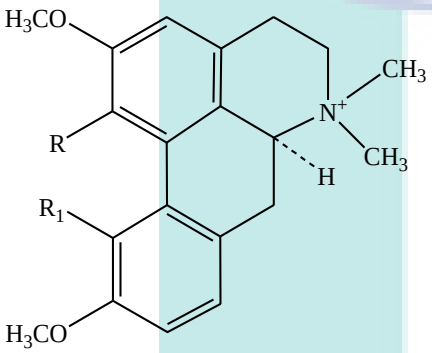

Compound	**R**	**R_1**
(**40**)	OH	
(**45**)	OCH_3	

Two new aporphine alkaloids, *N*-formylasimilobine 2-O-β-D-glucopyranosyl-(1→2)-β-D-glucopyranoside (tinoscorside A) (**46**) and *N*-acetylasimilobine 2-O-β-D-glucopyranosyl- (1→2)-β-D-glucopyranoside (tinoscorside B) (**47**) had been isolated from aerial parts of *T. cordifolia* (Phan et al., 2010).

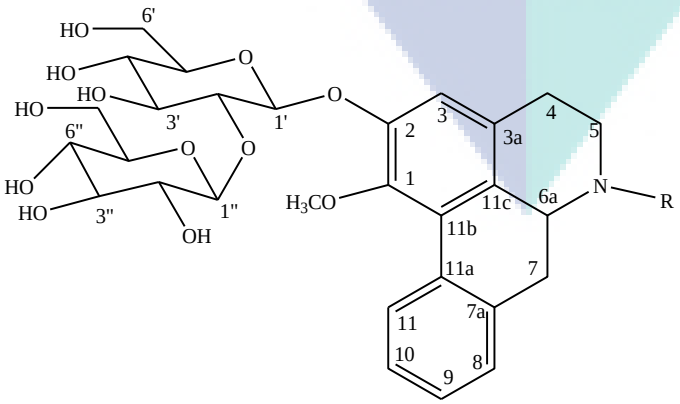

Compound	**R**	**R_1**
(**46**)	CHO	
(**47**)	$COCH_3$	

Phytochemical investigations of the stems of *T. crispa* led to the isolation of one new aporphine alkaloid, *N*-formylasimilobine 2-O-β D-glucopyranoside (**48**), along with nine known alkaloids, *N*-formylasimilobine 2-O-β-D-glucopyranosyl-(1→2)-β-D-glucopyranoside (tinoscorside A) (**46**), *N*-formylanonaine **(33)**, *N*-formylnomuciferine (**34**), *N*-formyldehydroanonaine (**49**), *N*-demethyl-*N*-formyldehydronornuciferine (**50**), magnoflorine (**40**), paprazine (**51**), *N*-trans-feruloyltyramine (**15**), and cytidine (**52**) (Choudhary et al., 2010).

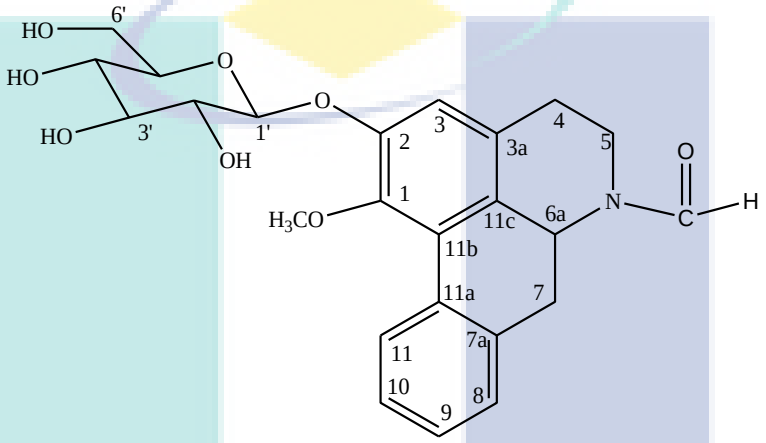

(**48**)

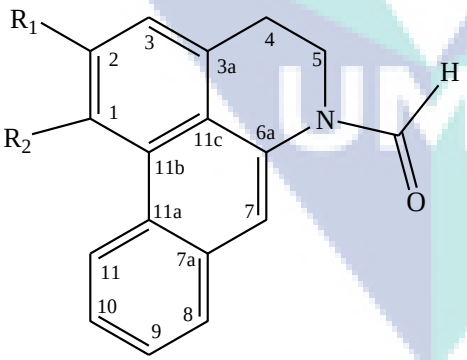

Compound	R_1	R_2
(**49**)	O-CH_2-O	
(**50**)	OCH_3	OCH_3

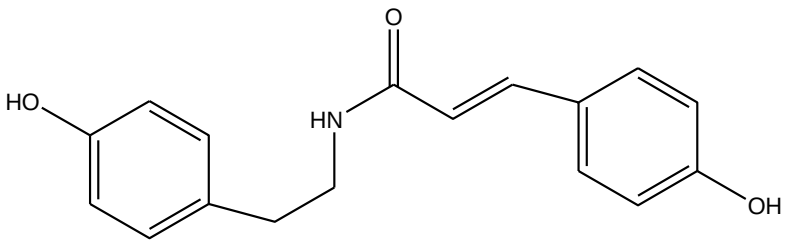

(**51**)

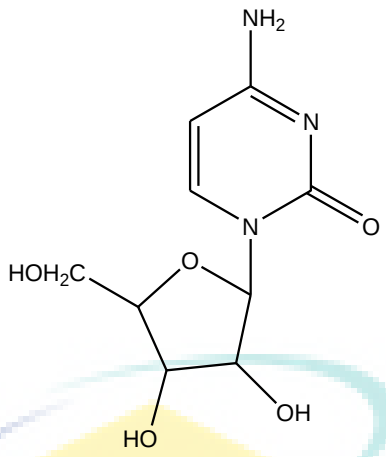

(52)

2.6 BIOLOGICAL ACTIVITIES OF ALKALOIDS

Most alkaloids possess curative and variety of pharmacological activities, thus they are extremely important in therapeutic applications.

2.6.1 Acetylcholinesterase Inhibitory Activity

Alzheimer's disease (AD) is a neurodegenerative disorder of the brain that leads to a progressive decline in cognitive function, incapacitation and ultimately death. Current treatment approaches and major therapeutic strategies for this disease are focused on the cholinergic hypothesis. The cholinergic hypothesis of AD suggests that low levels of acetylcholine (ACh) in specific regions of the brain results in learning and memory dysfunction, and therefore, one of the most promising approaches is the design of new agents for the treatment of AD (Huang et al., 2010).

The most important changes observed in the brain are a decrease in hippocampal and cortical levels of the neurotransmitter acetylcholine and associated enzyme choline transferase. Acetylcholinesterase inhibitors can restore the level of acetylcholine by inhibiting acetylcholinesterase (Lopez et al., 2002).

It is well known that there are two major forms of cholinesterases in mammalian tissues, acetylcholinesterase (AChE, EC 3.1.1.7) and butyrylcholinesterase (BuChE, EC

3.1.1.8). Recent studies indicated that inhibition of brain BuChE may represent an important therapeutic target for AD as AChE activity in certain brain regions is already decreased, while BuChE levels are unchanged or even increased due to AD. This situation implies that the hydrolysis of ACh may occur more easily than that of BuChE. In fact, some evidence suggests that the inhibition of BuChE can raise ACh levels and improve cognition in AD. Consequently, dual AChE/BChE inhibitors may have better activity and show clinical efficacy without remarkable side effects (Huang et al., 2010).

AChE consists of a narrow gorge with two separate ligand binding sites: an acylation site (CAS) at the bottom of the gorge and a peripheral anionic site (PAS) located at the gorge rim (Huang et al., 2010). Figure 2.8 shows a cross-section of enzyme, which is lined by as many as 14 conserved aromatic residues, the rings of which make up ~70% of the gorge surface, with W84 and F330 contributing to the catalytic anionic site (CAS), and Y70, Y121 and W279 to the peripheral anionic site (PAS) (Silman and Sussman, 2008). On the other hand, quaternary ammonium binding locus in aromatic gorge recognizes the quaternary ammonium function of the ligand via electrostatic interactions.The peripheral anionic site is situated near the top of the aromatic gorge. Various classes of hydrophobic ligands, aromatic cations and bisquaternary ammonium ligands can interact with the peripheral anionic locus of enzyme to influence its catalytic activity allosterically. Since all these compounds were found to be noncompetitive or uncompetitive inhibitors of both cholinesterases, it was deduced that these compounds do not bind to the active site of the enzymes. They might, however, bind at the aromatic gorge of AChE/BChE enzymes both in the presence or absence of substrates (Khalid et al., 2004).

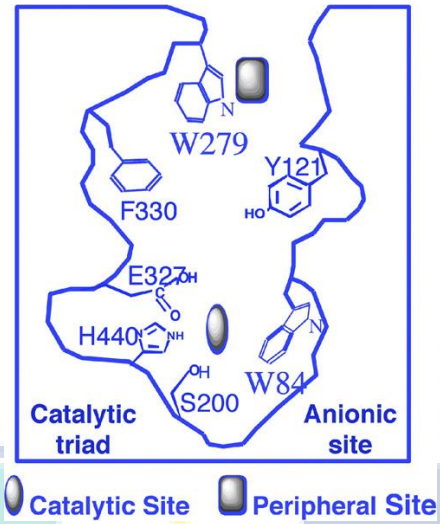

Figure 2.8: Schematic cross-section through the active-site gorge of *Tc*AChE, showing the principal residues involved in the CAS and PAS and the catalytic triad

Source: Silman and Sussman (2008)

Galanthamine (**53**), an amaryllidaceae alkaloid, is a long acting, selective, reversible and competitive acetylcholinesterase (AChE) inhibitor, which produces beneficial effects even after the drug treatment, has been terminated. This product is marketed as a hydrobromide salt under the name Reminyl® for the treatment of Alzheimer's disease. Plants of the genus *Narcissus* which belong to the Amaryllidaceae family are well-known for their alkaloids. Several species were reported to contain of to 0.1% of galanthamine (fresh weight), as found in bulbs of *N. confuses* (Huang et al., 2010).

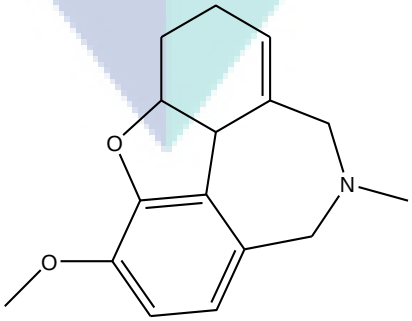

(**53**)

The interest in products for AD treatment, providing desired therapeutic effects and less adverse effects, is based on studies that showed that galanthamine is a less potent alkaloid than physostigmine (**54**) and tacrine (**55**), yet less toxic. A variety of synthetic galanthamine derivatives have been previously described including C-ring derivates, quaternary ammonium derivatives, or other carbamates which have been more active than galanthamine (Pagliosa et al., 2010).

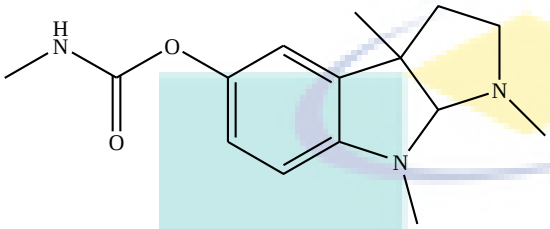

(54)

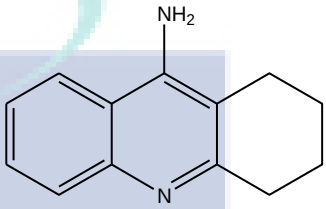

(55)

A series of novel berberine (**37**) derivatives have been designed, synthesized, and biologically evaluated as inhibitors of both acetylcholinesterase (AChE) and butyrylcholinesterase (BuChE). Among these derivatives, berberine linked with 3-methylpyridinium by a 2-carbon spacer (**56**), was found to be a potent inhibitor of AChE, with an IC_{50} value of 0.048 μM and berberine linked with 2-thionaphthol by a 4-carbon spacer (**57**), acted as the most potent inhibitor for BuChE with an IC_{50} value of 0.078 μM. Molecular modelling showed that 9-O substituted berberine derivatives could interact by π–π stacking with the peripheral anionic site PAS of AChE, and the aromatic rings of the non-berberine moiety interacted with the catalytic center of AChE through a cation–π interaction. Biological evaluation showed that the berberine linked with phenol by 4-carbon spacers, exhibited the most potent AChE inhibition (Huang et al., 2010).

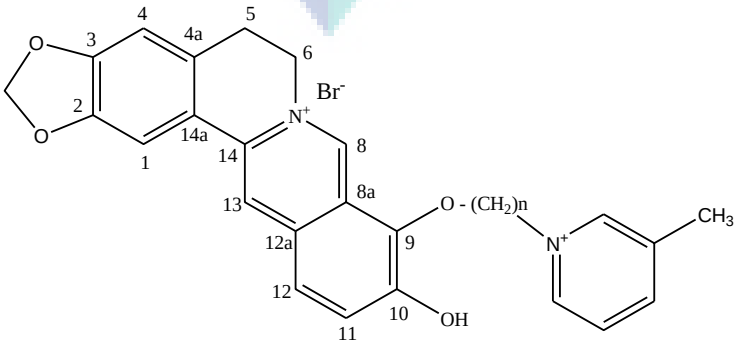

(56)

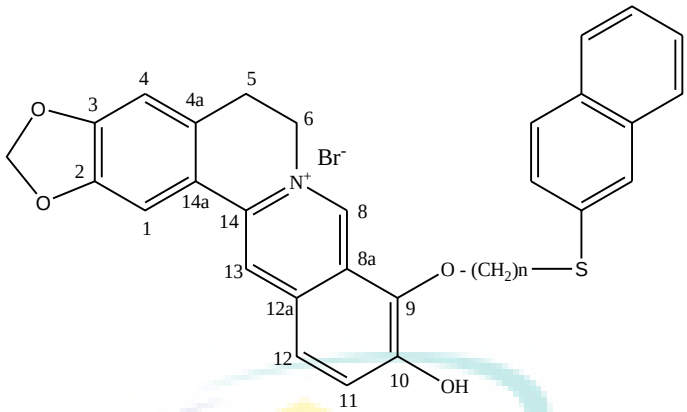

(**57**)

The activities of four isoquinolines alkaloids isolated from *Hippeastrum* species were investigated through AchE assay developed by Ellman et al. (1961). The pretazettine (**58**) and hippeastrine (**59**), alkaloids isolated from *Hippeastrum psittacinum*, did not show anticholinesterase activity by the proposed method. At concentrations 1mM, 500 µM and 100 µM, galanthamine (**53**) presented an AchE inhibition higher than 90%. Montanine (**60**) inhibited, in a dose-dependent manner, more than 50% of the enzyme at 1mM concentration (Pagliosa et al., 2010).

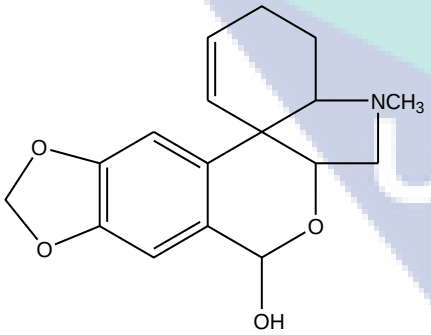

(**58**)

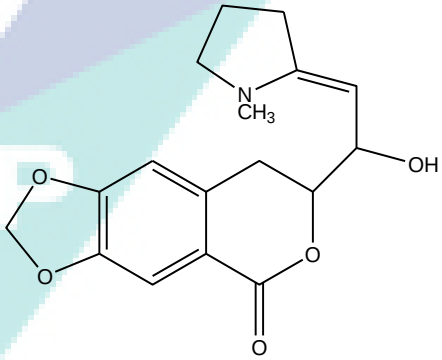

(**59**)

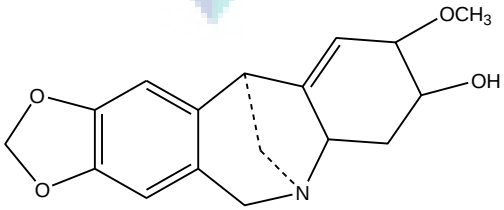

(**60**)

Some alkaloids, such as ungimorine (**61**) isolated from a *Narcissus* cultivar and hamayne (**62**), crinamine (**63**), and haemanthamine (**64**) isolated from two Nigerian *Crinum* species had weaker AChE inhibitory effects (IC_{50} values ranged from 86-50 μM) (Zahid, 2009).

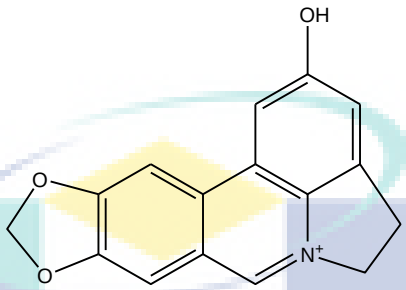

(**61**)

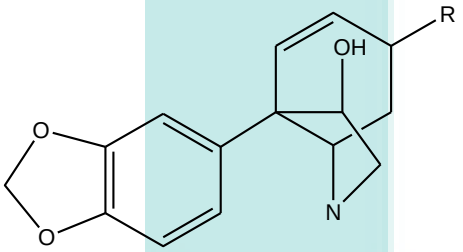

Compound	R_1
(**62**)	β-OH
(**63**)	α-OCH_3
(**64**)	β-OCH_3

2.6.2 Free Radical Scavenging Activity

Assessments of antioxidant properties of natural compounds are very important because of their uses in medicine, food and cosmetics. In living systems various metabolic processes and environmental stresses generate various reactive species. These are free radicals and mainly reactive oxygen species (ROS) (Rackova et al., 2004).

Free radicals, which have one or more unpaired electrons, are produced in normal or pathological cell metabolism, and play important roles in many biochemical processes. Normally, intracellular reactive oxygen species (ROS), including free radicals such as superoxide anion radicals ($O_2^{\bullet-}$) and hydroxyl radicals ($OH^{\bullet}$), non-free radical species (H_2O) and the singlet oxygen ($^1O_2$) have some beneficial effects, such as protection against invading pathogens. The ROS level is precisely controlled by various enzymes. Under pathological conditions, excessive ROS can be induced by various

stimuli, which exceed the anti-oxidative capacity of the involved organ and lead to a variety of physiological disorders such as inflammation, diabetes, genotoxicity and cancer. However, the increase of intracellular ROS level, due to increased production or impaired removal, can also cause cell damage ranging from cytoplasmic swelling to cell death. Consequently, free radical scavenging and removal of excessive ROS are important for restoring normal conditions, which may contribute to the correlation between antioxidant and other activities (Zhao et al., 2006).

DPPH assay is routinely practiced for assessment of free radical scavenging potential of an antioxidant molecule and considered as one of the standard and easy colorimetric methods for the evaluation of antioxidant properties of pure compounds. DPPH is a stable radical in solution and appears as a purple colour absorbing at 515 nm in methanol. This assay is based on the principle that DPPH on accepting hydrogen (H) atom from the scavenger molecule, results in reduction of DPPH to DPPH-H and accompanied by colour changes from purple to yellow with concomitant decrease in absorbance at 515 nm. After about three decades this assay has drawn much attention for the characterisation of antioxidant property (Rackova et al., 2004).

The antioxidant activities of three alkaloids isolated from *Mahonia aquifolium*, berberine (**37**), jatrorrhizine (**39**), and magnoflorine (**40**) were studied with respect to their structure, particularly the presence and the position of OH groups, steric conditions of unpaired electron delocalization and parameters of lipophilicity and hydration energy. The antiradical activities of the compounds tested were evaluated as the reactivities toward free stable DPPH. The antioxidant features of the alkaloids tested were investigated in heterogeneous membrane system of dioleoyl phosphatidylcholine (DOPC) liposomes stressed by peroxidative damage induced by 2,2'-azobis(2-amidinopropane)hydrochloride (AAPH) azoinitiator. Both alkaloids bearing free phenolic groups, jatrorrhizine (**39**) and magnoflorine (**40**) showed better activities in both systems used than berberine (**37**) which did not bear any readily abstractable hydrogen on its skeleton (Rackova et al., 2004).

Free radical scavenging properties of six aporphine, laurotetanine (**65**), boldine (**66**), *N*-methyllaurotetanine (**67**), *N*-ethoxycarbonyllaurotetanine (**68**), norisocorydine

(**69**) , norboldine (**70**), and two benzyltetrahydroisoquinoline alkaloids, reticuline (**71**) and magnocurarine (**72**), isolated from the root of *Lindera angustifolia* had been evaluated. All alkaloids except magnocurarine exhibited remarkable radical scavenging effects in DPPH radical scavenging test, among them norisocorydine showed the highest activity (SC_{50}: 14.1µg/mL). The results illustrated a significant decrease of DPPH radical in the presence of the test samples except magnocurarine. It could be seen that the aporphine alkaloids were better radical scavengers than the benzyltetrahydroisoquinolines. More hydroxyl group attached to the A and D rings of the alkaloids led to higher radical scavenging activities. The compound norisocorydine, which has hydroxyl groups attached to C-11, was the most powerful radical scavenger among the samples.

Most aporphine and benzyltetrahydroisoquinoline alkaloids have multiple phenolic hydroxyls on the benzene ring and are expected to scavenge reactive free radicals at least by generating thermodynamically and kinetically stable phenoxy radicals. But generally, aporphine alkaloids exhibit higher antioxidant activity than the later even without hydroxyl group. The reason may be based on two points: firstly, increased spin delocalization of phenoxy radicals in the plane biphenyl configuration in aporphine led to more stable structure after accepting a radical; secondly, the nonphenolic analogues presumably act through the delocalization of the neighbouring nitrogen lone pair electron, which can stabilize the C-6a radical by further expending electron delocalization beyond the biphenyl nucleus (Zhao et al., 2006).

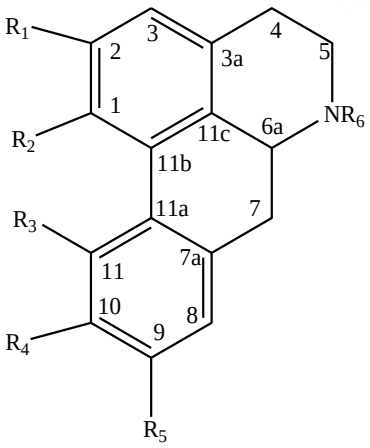

Compound	R_1	R_2	R_3	R_4	R_5	R_6
(**65**)	OCH_3	OCH_3	H	OCH_3	OH	H
(**66**)	OH	OCH_3	H	OCH_3	OH	H
(**67**)	OCH_3	OCH_3	H	OCH_3	OH	CH_3
(**68**)	OCH_3	OCH_3	H	OCH_3	OH	COOEt
(**69**)	OCH_3	OCH_3	OH	OCH_3	H	H
(**70**)	OCH_3	OH	H	OCH_3	OH	H

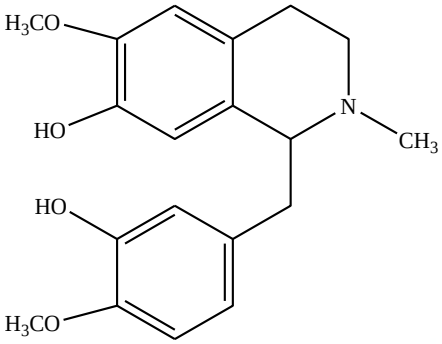

(**71**)

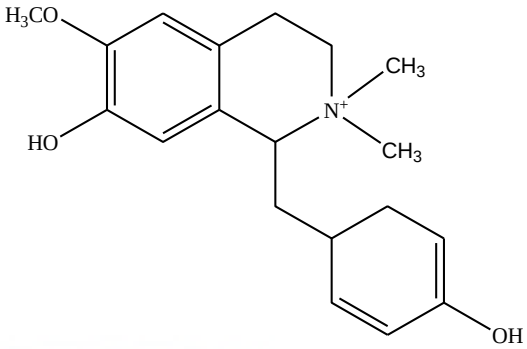

(**72**)

2.6.3 Antimicrobial Activity

The growth thermogenic curves of *Escherichia coli* affected by berberine (**37**), coptisine (**73**) and palmatine (**38**) were determined quantitatively by microcalorimetry. The inhibitory effects of berberine alkaloids on *E. coli* revealed that the sequence of their antimicrobial activity were berberine, coptisine and palmatine. The functional groups methylenedioxy at C2 and C3 on the phenyl ring improved antimicrobial activity more remarkably than methoxyl at C2 and C3 of the phenyl ring. However, the antimicrobial activity does not vary significantly with methylenedioxy or methoxyl at C9 and C10 of the phenyl ring (Yan et al., 2008).

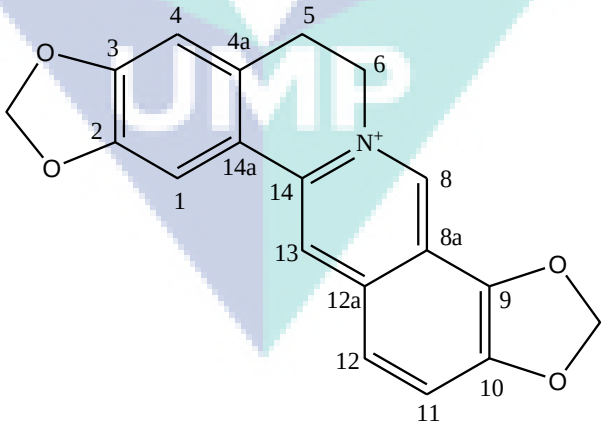

(**73**)

Berberine (**37**) and jatrorrhizine (**39**) from the crude extract of *Mahonia aquifolium* have shown strong activity against twenty clinical isolates of *Propionibacterium acnes* with minimal inhibitory concentration values (Slobodnıkova,

et al., 2004). Berberine (**37**) seems to be more active than jatrorrhizine (**39**) against coagulase-negative Staphylococci.

Two antimicrobial alkaloids, palmatine (**38**) and jatrorrhizine (**39**), were isolated from tubers of traditional Chinese medicinal plant *T. capillipes* using activity-guided isolation method and chromatography. Their antimicrobial activity was determined *in vitro*. The results showed that palmatine (**38**) and jatrorrhizine (**39**) had inhibitory activity against plant pathogens *Colletotrichum gloeosporioides, Fusarium oxysporum f.* sp. *niveum, Mycosphaerella sentina, Pestalotia mangiferae, Cercospora kaki, Gymnosporangium haraeanum, Rhizoctonia solani and Colletotrichum graminicola*, with the EC_{50} values of 0.0348–0.8356 gL^{-1} and 0.0240–0.8649 gL^{-1}, respectively. Palmatine (**38**) and jatrorrhizine (**39**) also exhibited inhibition against animal pathogens *Bacillus cereus, Bacillus megaterium, Bacillus subtilis, Staphyloccocus aureus, Staphylococcus epidermidi, Micrococcus lysodeikticus, Proteus vulgaris, Salmonella typhi and Escherichia coli*, with the MIC values of 0.1–0.8 gL^{-1} and 0.1–0.6 g L^{-1}, respectively. These results suggested that palmatine (**38**) and jatrorrhizine (**39**) showed relatively broad spectrum antimicrobial activity against plant and animal pathogens (Deng et al., 2012).

Experiments with the 8-alkyl and 8-phenyl-substituted berberines and their bromo derivatives showed that the introduction of hydrocarbon groups at position C-8 increased the antimicrobial activities (Iwasa et al., 1998). The 12-bromo derivatives of the 8-alkyl and 8-phenyl-protoberberines showed higher activity against the microorganisms tested than did their non–brominated analogs.

The side carbon chain at position C-13 of quaternary protoberberines was investigated for its potential as fungicide and herbicide activities (Iwasa et al., 2000). Parallel to the QPA, tetrahydroforms with methyl group at position C-13 were tested for *in vitro* and *in vivo* activities. 13-Hexylberberine and 13-hexylpalmatine showed the strong activities towards *Staphylococcus aureus*, being more active than berberine and kanamycin sulfate. Both hexylderivatives possessed antifungal activity (Iwasa and Kamigauchi, 1996).

Two alkaloids, stephanine (**74**) and crebanine (**75**), were isolated from tubers of the traditional Chinese medicinal plant *Stephania dielsiana*, using an activity-directed isolation method, and inhibitory activities stephanine (**74**) and crebanine (**75**) against ten animal pathogenic bacteria were evaluated *in vitro*. The results showed that stephanine (**74**) and crebanine (**75**) exhibited high inhibitory activity towards gram-positive animal pathogenic bacteria, with MIC values of 0.078–0.312 gL^{-1}, but low inhibitory activity against gram-negative animal pathogenic bacteria. Stephanine (**74**) and crebanine (**75**) exhibited high inhibition towards five gram-positive bacteria: *M. lysodeikticus, B. cereus, B. megaterium, B. subtilis and S. aureus*. Stephanine (**74**) and crebanine (**75**) exhibited low inhibitory activity towards gram-negative bacteria: *E. coli, P. vulgaris, S. typhi and S. dysenteriae* (Deng et al., 2011).

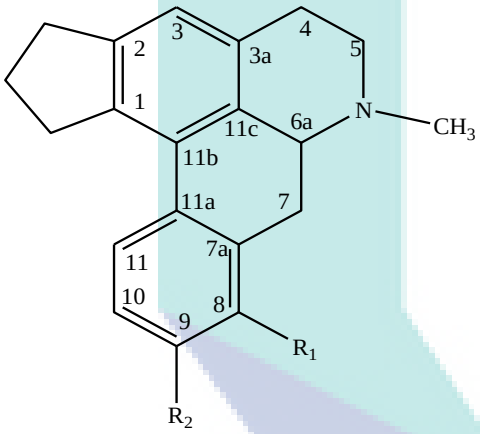

Compound	R_1	R_2
(**74**)	OCH_3	H
(**75**)	OCH_3	OCH_3

2.6.4 Cytotoxic Activity

The most important and most frequently tested property of the quaternary protoberberine alkaloid (QPA) is cytotoxicity. Berberine (**37**) was tested for its potential inhibitory effect against telomerase activity on a human leukemia cell line. It was identified as a moderate inhibitor with 50% inhibition at 35 µM concentration. Results obtained on telomerase of *Plasmodium falciparum* showed that the telomerase is sensitive to inhibition by berberine within 30–300 µM (Sriwilaijareon et al., 2002). A high concentration of berberine (75µg/mL) induced acute cytotoxic activity.

The cytotoxic activity of protoberberine was tested predominantly *in vitro* (Iwasa et al., 2001). Extensive experiments on twenty four quaternary protoberberine alkaloids were evaluated againts thirty eight human cancer cell lines. Six compounds

were cytotoxic and several others exhibited lower levels of cytotoxicity. From a structure–activity point of view, several trends were observed. For berberine (**37**) and palmatine (**38**) derivatives bearing a 13-alkyl side chain, the cytotoxicity increased parallel to the number of CH_2 units in the side chain. 12-Bromo-8-hexylberberine was more cytotoxic than the corresponding 8-phenyl and 8-butyl derivatives, suggesting that the length of the carbon unit at C-8 also influences cytotoxicity. Bromination at C-12 also increased the cytotoxicity level (Iwasa et al., 2000).

2.6.5 Antihyperglyceamic Activity

In the present study, the isoquinoline alkaloid rich fraction (AFTC) derived from the stem of *Tinospora cardifolia*, palmatine (**38**), jatrorrhizine (**39**) and magnoflorine (**40**) were evaluated for insulin-mimicking and insulin-releasing effect *in vitro* and *in vivo* (Patel and Mishra, 2011). Their effect on hepatic gluconeogenesis was examined in rat hepatocytes. Insulin releasing effect was detected *in vitro* using rat pancreatic cell line, RINm5F. Furthermore, effects of AFTC and isolated alkaloids on serum glucose and insulin level were studied in fasting and glucose challenged normal rats. AFTC significantly decreased gluconeogenesis in rat hepatocytes as insulin did and it increased insulin secretion in RINm5F cells similar to tolbutamide. In an acute 30 min test in vitro, AFTC, palmatine (**38**), jatrorrhizine (**39**) and magnoflorine (**40**) stimulated insulin secretion from the RINm5F cell line. Administration of AFTC (50, 100, and 200 mg/kg), palmatine (**38**), jatrorrhizine (**39**) and magnoflorine (**40**) (10, 20 and 40 mg/kg each) orally significantly decreased fasting serum glucose, and suppressed the increase of blood glucose levels after 2 g/kg glucose loading in normal rats. *In vivo* study further justified their insulin secreting potential by raising the serum insulin level in glucose fed rats. These results demonstrate the alkaloid present in *T. cordifolia* contributed to antihyperglycemic activity. AFTC may have hypoglycemic effects via mechanisms of insulin releasing and insulin-mimicking activity and thus improves postprandial hyperglycemia (Patel and Mishra, 2011).

2.6.6 Antimalarial Activity

It has been reported that berberine is potent *in vitro* inhibitor of both nucleic acid and protein synthesis in human malaria protozoa *Plasmodium falciparum* FCR-3. In addition, the inhibitor activity towards telomerase of human malaria *P. falciparum* has been reported (Sriwilaijareon et al., 2002). *In vitro* structure–activity relationship studies for antimalarial activity toward *P. falciparum* have been published (Iwasa et al., 1998). The type of the oxygen substituent on rings A, C, and D and the position of the oxygen functions on ring D influence the activity of the protoberberine alkaloids. Shifting the oxygen function from C-9 and C-10 to C-10 and C-11 resulted in a significant increase in activity.

CHAPTER 3

MATERIALS AND METHODS

3.1 GENERAL

A251 Branson electric sonicator was used for extraction. A Buchi Rotavapor R-II system was used together with an Eyela A-1000 S vacuum pump and Buchi R-II heating bath as unit components for rotary evaporation. Melting points were determined using a Barnstead Electrothermal 9100 melting point apparatus and were uncorrected. Ultraviolet (UV) spectra were recorder on a Genesys 10S UV-VIS spectrophotometer in methanol. Infrared (IR) spectra were recorded on a Perkin Elmer 100 FT-IR spectrophotometer as KBr pellets or thin film. NMR spectra were recorded on BrukerAvance 500 Spectrometer (^{1}H at 500 MHz; ^{13}C at 125 MHz).Chloroform ($CDCl_3$) and methanol (MeOD) were used as solvents. Electron ionization mass spectral (EIMS) were obtained from JEOL JMS-HX-110 mass spectrometer. Gas Gromathoraphy-Mass Spectroscopy (GCMS) was performed on an Agilent Technologies 7890A. The UV light (UVGL-58 Handheld UV Lamp) at 254 and 365 nm was used to visualize TLC plates.

Organic solvents used for extraction and purification of the extracts were hexane, ethyl acetate, chloroform, methanol, acetone and ethanol. Industrial grade solvents were used for extraction processes while analytical grade solvents were employed for chromatography and crystallization. Spraying reagent for TLC used comprising dilute vanillin/sulphuric acid and Dragendorff's reagent. Acetylthiocholine iodide (ATCI), acetylcholinesterase (AChE) from electric eels (type V-S) and 5,5V-dithiobis[2-nitrobenzoic acid] (DTNB), bovine serum albumin fraction V (0.1%), galanthamine, physostigmine were obtained from Sigma-Aldrich, St. Louis. Tris-

hydrochloric acid buffer (50 mM) at pH 8.0 was used to prepare the enzyme solution. Spraying reagent used for detection of enzyme activity was the mixture of 0.25% 1-naphtyl acetate in EtOH and 0.25% aqueous solution Fast Blue B salt. Resazurin, butyrate hydroxyl toluene (BHT) and 1,1-diphenyl-2-picryl-hydrazil (DPPH) were purchased from Sigma Aldrich, St.Lois.

Thin layer chromatography (TLC) was performed on Merck pre-coated silica gel 60 $F_{254+365}$ for normal phase or reverse phase RP-18 pre-coated TLC plate (0.25 mm, aluminium backed). Merck silica gel (70-230 mesh) was used for normal phase column chromatography whereas Merck LiChroprep RP-18 silica gel 40-63 mesh was used for reverse phase column chromatography.

Eight microorganisms were used to determine the antimicrobial activities comprises two *Gram*-positive; *Enterococcus faecalis* (ATCC 14506), *Staphylococcus aureus* (ATCC BAA 1026), four *Gram*-negative; *Klebsiella pneumonia* (ATCC BAA 1144), *Escherichia coli* (ATCC 10536), *Psuedomonas aeurogenosa* (ATCC 1542), *Proteus vulgaris* (ATCC 33420) and two fungi; Candida albicans (ATCC 10231), *Aspergillus niger* (ATCC 16404). All the microbial strains were provided by Microorganism Laboratory, Faculty of Industrial Sciences and Technology, University Malaysia Pahang.

3.2 PLANT MATERIALS

Tinospora crispa stems were collected in Bentong, Pahang and identified by Zainon Abu Samah (FRIM botanist). A voucher specimen is deposit at the Forest Research Institue Malaysia.

3.3 COLUMN CHROMATOGRAPHY

Column chromatography was performed on a glass column using silica gel mesh 70-230 mesh as adsorbent. The size of chromatographic column used depended on the amount (weight) of the sample. The ratio of sample and the absorbent was 1:30-60 by weight. The column was developed with solvents systems, which gave the best

separation and each fraction was monitored by TLC. The organic solvents utilized for column chromatography were of analytical grade. The column was initially eluted with non-polar solvent system, e.g., 100% hexane, and gradually increased polarity, e.g., hexane-ethyl acetate, 100% chloroform and chloroform-methanol with polarity increased by increasing methanol composition.

3.4 THIN LAYER CHROMATOGRAPHY (TLC)

TLC investigation routinely used for chromatographic separations was carried out on Merck pre-coated silica gel 60 $F_{254+365}$ (0.2 mm thickness) supported on aluminium plates. The components were detected by visualization under ultraviolet light at λ 254 and 365 nm and/or sprayed with Dragendorff's reagent/dilute sulphuric acid reagent. If an alkaloid were present, an orange spot will appear after spraying with Dragendorff's reagent. After spraying with vanillin reagent/dilute sulphuric reagent, the TLC plate was heated for 30 s and the colour produced was recorded. The retention factor (R_f) of a compound is a measure of how far it has moved up a plate under certain conditions in relation to the solvent front. It is can be used as a quick way of identification. Differences in R_f are important when considering solvent systems for column chromatography.

3.5 REAGENTS FOR DETECTION OF COMPOUNDS

Vanillin reagent and dilute sulphuric acid reagent were used to detect non alkaloidal compounds. Vanillin reagent was used to identify terpenoids and phenols on TLC plates. It was prepared by dissolving vanillin (1.0 g) in concentrated sulphuric acid (97%, 100 mL). After treatment with both reagents, heating (120°C) was necessary to enhance visualization of TLC spots. Vanillin reagent was prepared by dissolving 1 g of vanillin in 20 ml of concentrated sulphuric acid. Sulphuric acid (6%) reagent was prepared by concentrated sulphuric acid (12 mL) in water (200 mL). Dragendorff's reagent was used to identify alkaloids on the TLC plate. Dragendorff's stock solution A was prepared by dissolving basic bismuth nitrate (0.85 g) in acetic acid (10 mL) and water (40 mL). Stock solution B was prepared by dissolving potassium iodide (8.0 g) in water (20 mL). These stock solutions were mixed together in equal volumes and stored

in a dark coloured bottle. Stock solution (1mL) is mixed with acetic acid (2 mL) and water (10 mL) before use (Stahl, 1969).

3.6 EXTRACTION

Powdered, dried *Tinospora crispa* stems (5.0 kg) were first extracted via percolation with hexane and then filtered (fraction A). The plant material was dried, next extracted with methanol-water (4:1) by sonication for 30 minutes for three cycles and then filtered to give a brown extract (fraction B). The volume of combined extract was reduced to one third by rotary evaporation. The concentrated extract was treated with sulphuric acid drop by drop to pH 2 and then partitioned with chloroform. The chloroform phase was collected and evaporated leaving a brownish gummy residue (fraction C) of nonalkaloidal components. The aqueous phase was basified with ammonium hydroxide, NH_4OH to pH 10 and extracted with chloroform-methanol (3:1) to yield a dark brown gummy residue (fraction D) containing the alkaloidal fraction. The fractionation procedures are summarized in Figure 3.1.

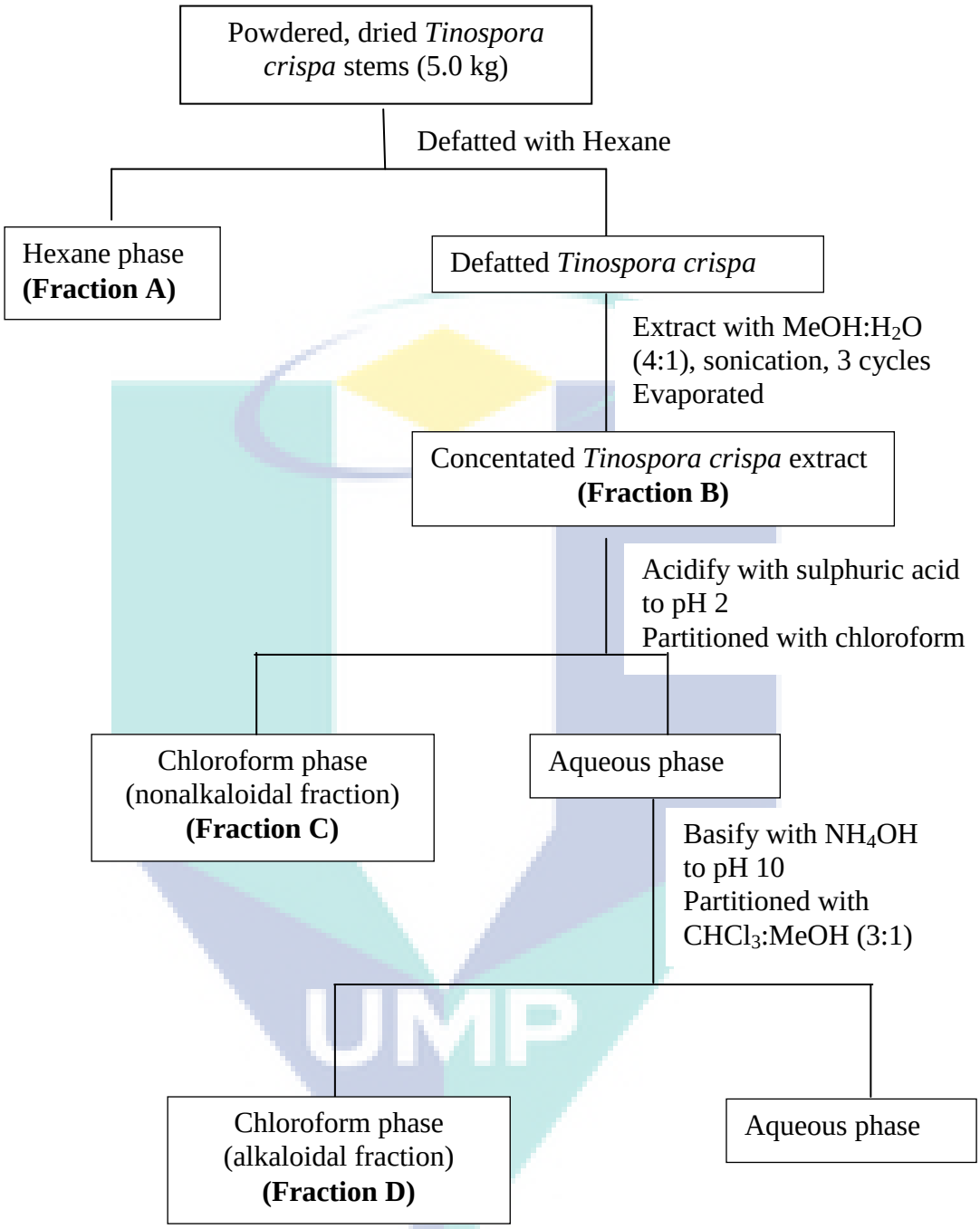

Figure 3.1: Extraction and Fractionation of *Tinospora crispa* stems

3.7 COLUMN CHROMATOGRAPHY OF ALKALOIDAL FRACTION

Fraction D (25.0 g) was chromatographed over a column of silica gel 70-230 mesh, slurry packed in chloroform. Elution was initiated with chloroform and progressed through the solvent series of 10%, 15%, 30%, 50% and 70% of methanol in chloroform, 100% methanol and 10% to 15% of ammonia solutions in methanol and 100 mL fractions were collected. Each fraction was monitored by TLC on silica gel plate with visualization of ultraviolet light and Dragendorff's reagent. Fractions showing similar TLC profiles were pooled to give nine combined fraction as shown in Table 3.1.

Table 3.1: Fractions from the column chromatography of FD

Eluent	Ratio (%)	Fraction	Weight (g)
$CHCl_3$	100	F1	1.40
$CHCl_3$:MeOH	90:10	F2	2.31
$CHCl_3$:MeOH	85:15	F3	3.52
$CHCl_3$:MeOH	70:30	F4	1.88
$CHCl_3$:MeOH	50:50	F5	5.01
$CHCl_3$:MeOH	30:70	F6	2.11
MeOH	100	F7	4.00
MeOH: NH_4OH	90:10	F8	1.52
MeOH: NH_4OH	95:15	F9	3.25

Based on the first column chromatography, six fractions (F1, F2, F3, F5, F8 and F9) were rechromatographed as summarized in Figure 3.2. F4 and F7 were not further purified due to the low concentration of alkaloids.

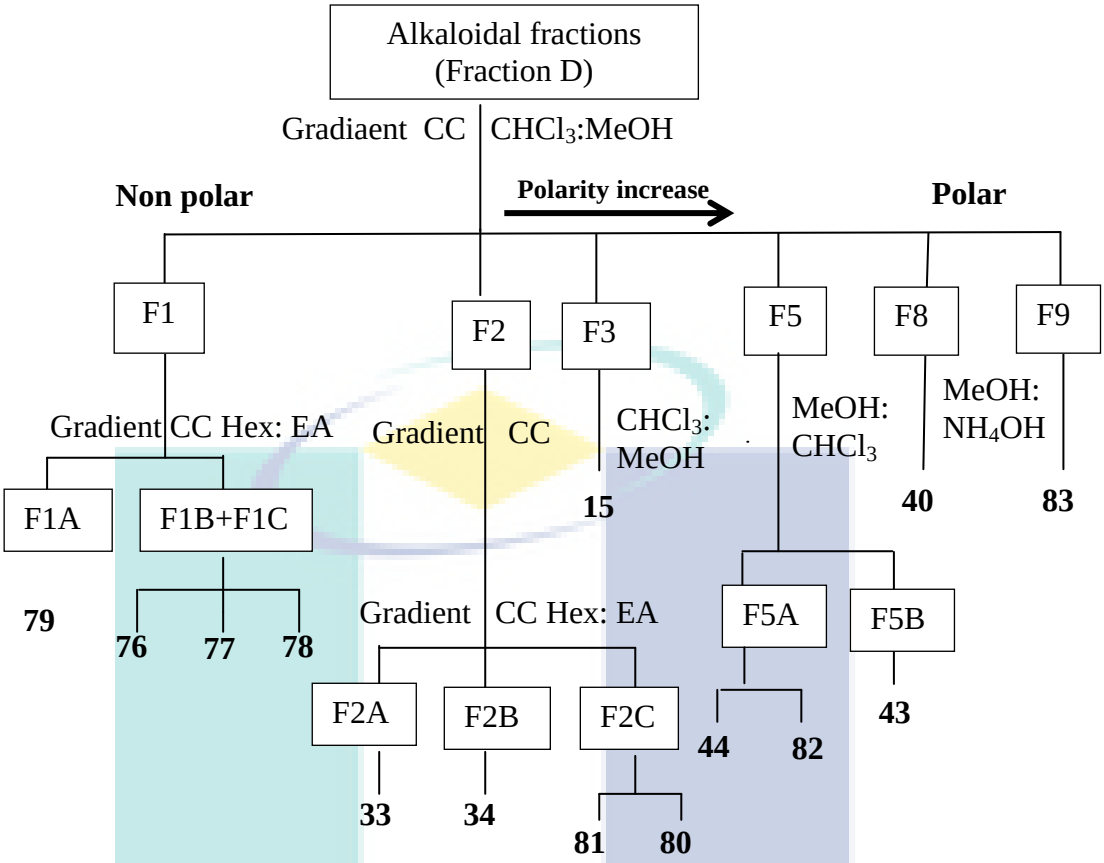

Figure 3.2: Schematic isolation of compounds from alkaloidal fraction from stems of *Tinospora crispa*

3.8 ISOLATION OF COMPOUNDS

3.8.1 Octacosanol (79)

Fraction 1 (1.40 g) was dissolved in chloroform, adsorbed onto silica gel (60 g) and chromatographed over column silica gel using hexane and increasing polarity by adding ethyl acetate gradually to afford 36 fractions. The fractions were monitored by TLC and fractions which show similar TLC profiles were combined to give five new combined fractions labelled F1A-F1E. The combined fraction, F1B (101.0 mg), was further purified by silica gel (30 g) with hexane-ethyl acetate as eluent to afford octacosanol (**79**) (10.0 mg) as a white powder (Figure 3.3).

3.8.2 β-Sitosterol (76)

Combined fraction, F1C (150.0 mg), was chromatographed over SiO_2 (50 g) with hexane-ethyl acetate as eluent. Subfraction seven [R_f 0.65; hexane:ethyl acetate (7:3)] gave white crystalline needles (7.0 mg) after washing with methanol. It was highly soluble in chloroform (Figure 3.3).

3.8.3 Mixture of three sterols (76, 77, 78)

Combined fraction, F1D (98 mg), was purified by SiO_2 using hexane-ethyl acetate (7:3) as eluent and recrystallized from hexane to yield a mixture containing campesterol (**77**), stigmasterol (**78**) and β-sitosterol (**76**) (11.0 mg) as white crystalline needles (Figure 3.3).

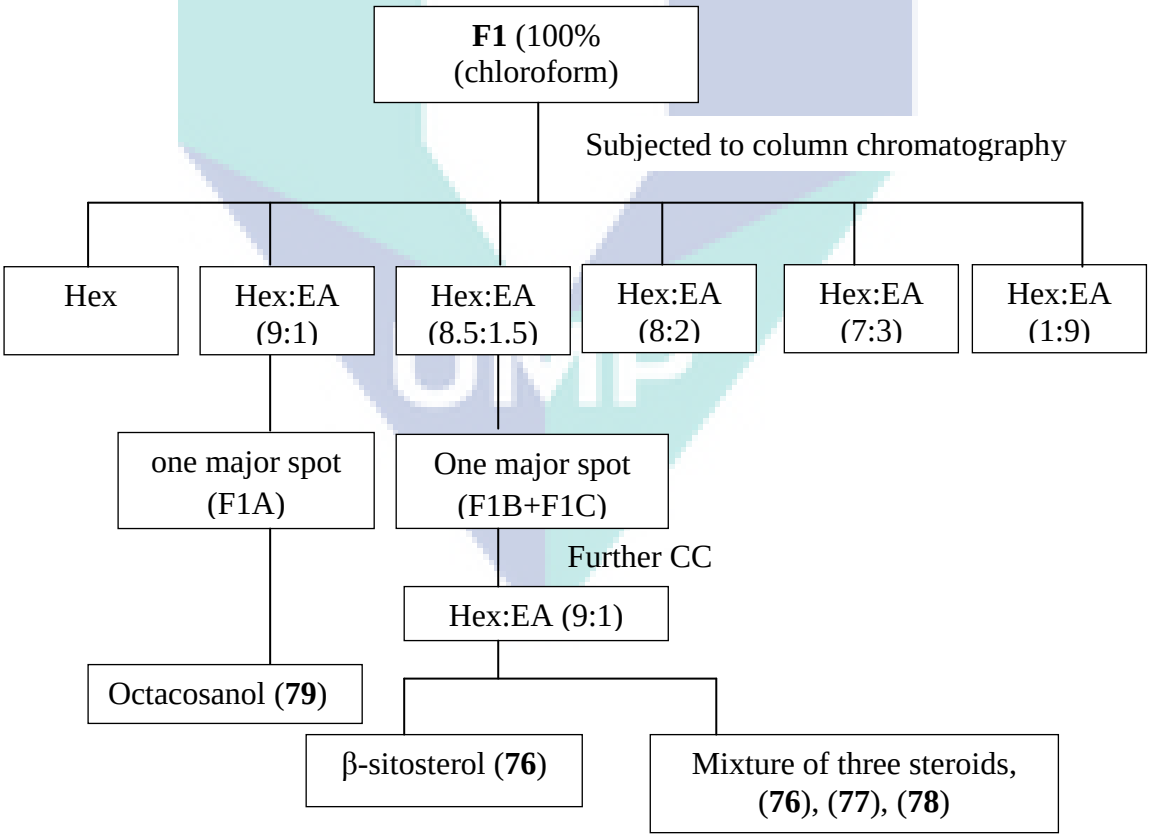

Figure 3.3: Isolation scheme of F1 by column chromatography

3.8.4 *N*-formylannonaine (33)

Combined fraction, F2 (2.31 g), was chromatographed over SiO_2 (100 g) with hexane-ethyl acetate as eluent to give 78 subfractions. Subfractions with similar TLC profiles were combined to give further four new subfractions labelled as F2A–F2C. The combined new subfractions 20-28 labelled F2A was concentrated and further purified with hexane-ethyl acetate as eluent to yield *N*-formylannonaine (**33**) (3.5 mg) [R_f 0.78; hexane:ethyl acetate (6:4)] as white crystals (Figure 3.4).

3.8.5 *N*-formylnornuciferine (34)

Combined fraction, 38-40, from CC of F2 were combined and labelled as F2B (150 mg). This fraction was further purified by using CC packed with SiO_2 (50 g) and eluted with hexane-EtOAc (7:3) to give pale yellow crystals and further purified by recrystallization from chloroform to yield *N*-formylnornuciferine (**34**) (45.0 mg) as a white crystalline needles [R_f 0.61; hexane:ethyl acetate (6:4)] (Figure 3.4).

3.8.6 Lysicamine (80)

Combined fraction, F2C (110 mg), was chromatographed by silica gel column using hexane-ethyl acetate eluent, to yield 30 subfractions. Those with similar TLC profiles were combined and labelled as F2Ca-F2Cc. Subfractions 25-30 labelled as F2Cc (70 mg) was rechromatographed with hexane:EtOAc (9:1) (R_f 0.40) to yield lysicamine (**80**) (8.0 mg; a yellowish powder) (Figure 3.4).

3.8.7 Liriodenine (81)

Subfractions 18-24 from column chromatography of F2Ca and F2Cb were combined and rechromatographed on preparative TLC with hexane:ethyl acetate (8:2) to obtain liriodenine (**81**) (3.5 mg) as a light brown powder with R_f 0.48 (Figure 3.4).

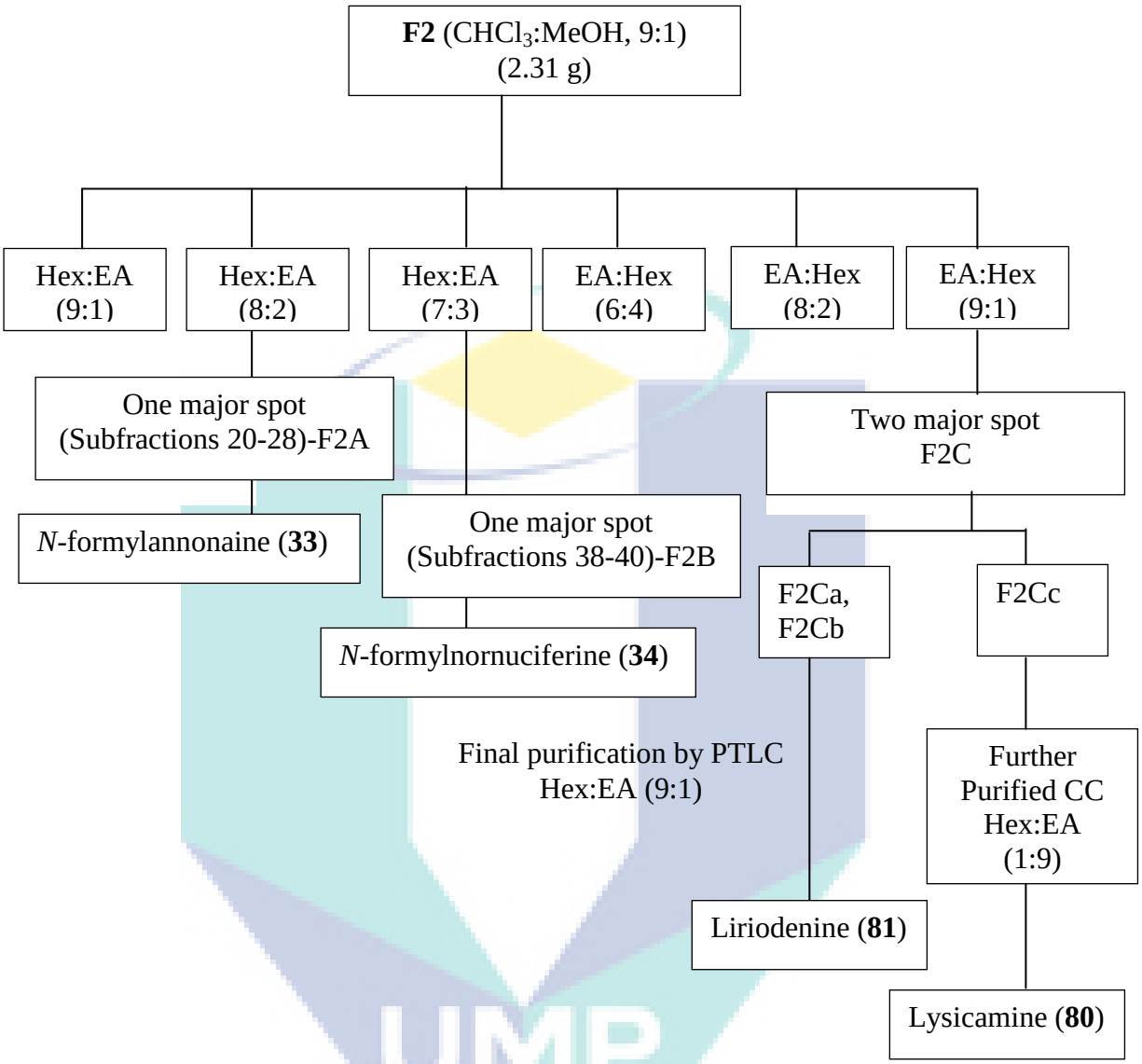

Figure 3.4: Isolation schematics of F2 by column chromatography

3.8.8 *N-trans*-feruloyltyramine (15)

Fraction F3 (3.53 g) was chromatographed over silica gel using 100% chloroform by increasing the polarity of MeOH gradually to obtain 60 fractions. Subfractions 35-42 were combined and washed with chloroform to afford *N-trans*-feruloyltyramine (**15**) as light yellowish solid (40 mg) with R_f 0.60 in hexane:EtOAc (7:3).

3.8.9 Dihydrodiscretamine (44)

Fraction F5 (5.05 g) was chromatographed over silica gel using chloroform-methanol gradient to give 89 subfractions. Subfractions 32-38 labelled F5A (50 mg) were combined as the TLC spots revealed the presence of two spots of alkaloids when tested with Dragendorff's reagent. These two spot were close to each other with R_f values of 0.38 and 0.42 [chloroform:methanol (6:4)]. Fraction F5A was further purified by column chromatography eluted with chloroform, methanol and hexane, (7:3:1), to obtain dihydrodiscretamine (**44**) (5.5 mg) as a gummy orange solid (R_f 0.45) (Figure 3.5).

3.8.10 4,13-dihydroxy-2,8,9-trimethoxydibenzo[a,g]quinolizinium (82)

Subfractions 32-35 from column chromatography of F5A were combined and rechromatographed by preparative TLC using chloroform, methanol and hexane (7:3:1) to obtain 4,13-dihydroxy-2,8,9-trimethoxydibenzo[a,g]quinolizinium (**82**) as a gummy brown solid (4.5 mg; R_f 0.40) (Figure 3.5).

3.8.11 Columbamine (43)

Subfractions 40-52 from column chromatography of F5 were combined as the TLC profiles were similar and labelled as F5B (250 mg). This combined fraction was concentrated and further purified by silica gel column chromatography with chloroform and increasing methanol gradually. At the point of 30% methanol, a gummy yellow solid, columbamine (**43**) (10 mg) was obtained (R_f 0.30) (Figure 3.5).

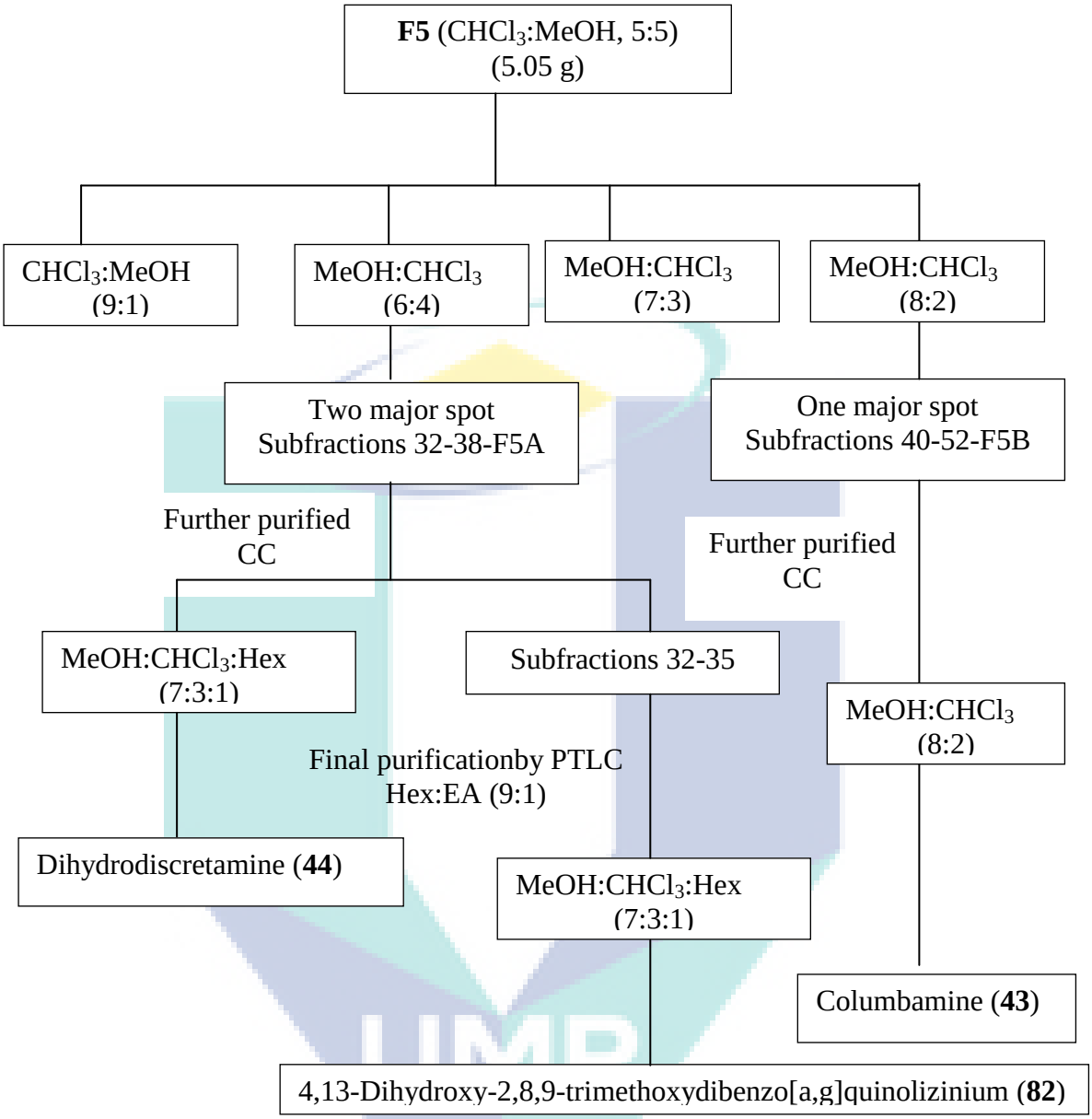

Figure 3.5: Isolation schematics of F5 by column chromatography

3.8.12 Magnoflorine (40)

Fraction F8 was chromatographed over silica gel using chloroform with increasing polarity with methanol gradually. After reaching 50%, a few drops of ammonia solutions were added to the solvent system until the desired band was collected. Magnoflorine (**40**) was isolated as a brown solid (8 mg) [R_f 0.33; MeOH:NH_4OH (9:1)]. A single fluorescence blue spot on the TLC plate was observed under long-wave ultraviolet light.

3.8.13 *N,N*-dimetylhexadecan-1-amine (83)

Fraction F9 (3.25 g) was chromatographed over RP-18 silica gel in methanol and increasing polarity by adding ammonia solutions. The last fraction was evaporated and recrystallized in methanol to afford white crystals of *N,N*-dimetylhexadecan-1-amine **(83)** (100 mg). The compound is UV inactive as it is a pseudo alkaloid. However, it tested positive to Dragendorff's reagent appearing as an orange spot on TLC [R_f, 0.20; MeOH:NH_4OH (8:2)].

3.9 BIOACTIVITY STUDIES

3.9.1 Acetylcholinesterase Inhibitory Activity by Bioautography

The acetylcholinesterase activity by bioautography procedure recently reported by Marston et al. (2002) was employed in this study. Briefly, to make up the enzyme solution, cetylcholinesterase type V-S was dissolved in tris-hydrochloric acid buffer (pH 7.8) and stabilized by the addition of bovine serum albumin fraction V. TLC were spotted with isolated compounds and 1 μg of galanthamine was used as positive control. TLC were developed with three different polarities of the isolated alkaloids, viz., EtOAc:Hex (7:3), MeOH:CHCl3 (7:3) and MeOH:NH_4OH (9:1) and subsequently evaporated. The plates were then sprayed with the AChE enzyme solution (6.6 UmL^{-1}), thoroughly evaporated and incubated at 37°C for 20 min in moist atmosphere. Enzyme activity was detected by spraying the plate with a solution consisting of 0.25% of 1-naphtyl acetate in EtOH (5 mL) plus 0.25% aqueous solution of Fast Blue B salt (20 mL). Potential acetylcholinesterase inhibitors appeared as clear zones on a purple coloured background.

3.9.2 Acetylcholinesterase Activity by Microplate Assay

Acetylcholinesterase activity was evaluated using a 96-well microplate reader (Rhee et al., 2001) based on Ellman's method (Ellman et al., 1961). In this method the enzyme hydrolyzes the substrate acetylthiocholine resulting in the production of thiocholine which reacts with 5,5'-dithio-bis(2-nitrobenzoic acid) (DTNB) to produce

2-nitrobenzoate-5-mercaptothiocholine and 5-thio-2-nitrobenzoate which can be detected at 405 nm. Three buffers were prepared for the assay, Buffer A (50mM Tris-HCl, pH 8), Buffer B (50mM, pH 8, containing 0.1% bovine serum albumin) and Buffer C (50mM Tris-HCl, pH 8, containing 0.1M NaCl and 0.02M $MgCl_2.6H_2O$).

In the 96-well plates, 25 µL of 15 mM acetylthiocholine iodide (ATCI) in water, 125 µL of 3 mM DTNB in buffer C, 50 µL of buffer B, 25 µL of isolated compounds dissolved in MeOH at concentrations ranging from 62.5-1000 µg/mL, were added. Then 25 µL of 0.22 UmL^{-1} of the enzyme acetylcholinesterase were added and the absorbance was read at 405 nm. Physostigmine served as the positive control. All assays were carried out in duplicate in 96-well microplate reader (Tecan Infinite 200 Pro). The percentage inhibition was calculated by following the formula:

$$\% \text{ Inhibition} = [(E - S) / S] \times 100$$

where E is the activity of the enzyme without test compound and S is the activity of enzyme with test compound. The IC_{50} values were calculated by plotting graph of percentage inhibition against extract concentration. The IC_{50} values obtained in unit µg/mL had been converted into µM.

3.9.3 Radical Scavenging Assay with DPPH

The TLC-DPPH assay was performed as described by Takao, et al. (1994). Briefly, after developing and drying, aluminium-backed TLC sheets were sprayed with 1,1-diphenyl-2-picryl-hydrazyl (DPPH) solution (2 mg/mL in MeOH). Active compounds appeared as yellow spots against a purple background.

The compounds showing qualitative positive reaction were selected for quantitative estimation of radical scavenging activity (RAS) according to the method described by Blois (1958). In this method, a microplate reader and 96 well plates were used to carry out the determination of the spectral absorption values. In this method, methanolic DPPH solutions (100 µg/mL, 50 µL) were added to samples of different concentration (20 µL, 200–1000µg/mL). These solutions were gently mixed and

incubated in the dark for 30 min at room temperature. Then, the absorbances of the resulting solutions were measured at 517 nm. Butylated hydroxyl-anisole (BHA) was used as positive control. The antioxidant activity was carried out in duplicate and the reading was averaged. The scavenging activity was measured as a decrease in absorbance of the samples versus DPPH standard solution. The DPPH radical concentration was calculated using the following equation:

$$\text{Scavenging effect (\%)} = (Ao - A_1) / Ao, \times 100\%$$

where Ao is the absorbance of the control reaction and A_1 is the absorbance in the presence of the sample tested. The IC_{50} (concentration providing 50% inhibition) was calculated graphically using a calibration curve in the linear range by plotting the extract concentration versus the corresponding scavenging effect.

3.9.4 Antimicrobial Activity

Eight microorganisms were used to determine the antimicrobial activities of isolated compounds from *T. crispa*. The resazurin reduction method (Karuppusamy and Rajasekaran, 2010) was employed against 6 bacterial strains, two *Gram*-positive; *Enterococcus faecalis* (ATCC 14506), *Staphylococcus aureus* (ATCC BAA 1026), four *Gram*-negative; *Klebsiella pneumonia* (ATCC BAA 1144), *Escherichia coli* (ATCC 10536), *Psuedomonas aeurogenosa* (ATCC 1542), *Proteus vulgaris* (ATCC 33420) and two fungi; *Candida albicans* (ATCC 10231) and *Aspergillus niger* (ATCC 16404). The bacterial strains were cultured overnight at 37°C on nutrient agar (NA). Fungi were cultured in potato dextrose agar (PDA) at 37°C for 48 hours. Each of the selected bacteria was impregnated on nutrient broth (10 mL) in sterilized universal bottle. Potato dextrose broth is used for preparing fungi inoculum. The universal bottle was incubated for 24 hours at 37°C for bacteria and 48 hours for fungi. The microbial suspension should then be compared to the 0.5 McFarland turbidity standards or adjusted to equal the microorganism concentration of 10^6 colony forming unit (CFU/mL) for bacteria and fungi. Tetracycline and Amphotericin B was used as the positive control and solvent was used as the negative control. The 96 well plates were prepared by dispensing microbial inoculum (100 µL) into each well, which was already adjusted to 0.5 of

McFarland's turbidity standard. The compounds (10 µL) were transferred into different wells. The last well contained microbial inoculated and solvent was used as negative control. Plates were sealed and incubated at 37°C for 24 hours for bacteria and at 37°C for 48 hours for fungi. After each incubation period, resazurin solution (5µL) was added into each well, colouring them blue. Plates were incubated at 37°C for an additional 5 hours. Plates were read every hour for colour change from blue to pink and pink to colourless of live microbial strains-containing wells. Compounds which do not possess antimicrobial potential showed fast decolouration of resazurin during preliminary microtitre-plate assay.

A positive result from the screening was further studied by determine the minimum inhibitory concentrations of the isolated compounds. Then, serial two fold dilutions were made in order to obtain a concentration range from 3.9-1000 µg/mL in MeOH. The 96 well plates were prepared by dispensing into each well 125 µL of microbial inoculums which had been adjusted to 0.5 of McFarland's Turbidity Standard. Then 25 µL of serially diluted of isolated compounds were transferred into consecutive wells. The first well contained 125 µL of microbial inoculum which was used as the positive control. The plates were covered with sterile plate sealers. The microtiter plate containing the sample was incubated at 37°C for 24 hours for bacteria and at 37°C for 48 hours for fungi. Microbial growth in each medium was determined by the resazurin reduction method. The MIC then defines the lowest concentration of compounds at which the microorganism does not demonstrate the dye reduction.

CHAPTER 4

RESULTS AND DISCUSSION

4.1 COMPOUNDS ISOLATION

Fractionation and chromatography of the alkaloidal fraction from *Tinospora crispa* (Menispermaceae) resulted also in the isolation of an amine: *N*,*N*-dimetylhexadecan-1-amine (**83**); an acid amide: *N*-*trans*-feruloyltyramine (**15**); three steroids: campesterol (**77**), stigmasterol (**78**) and β-sitosterol (**76**); and a policosanol: octacosanol (**79**). The alkaloids isolated consist of two aporphine alkaloids: *N*-formylannonaine (**33**), *N*-formylnornuciferine (**34**); one quaternary aporphine alkaloid: magnoflorine (**40**); two oxoaporphine alkaloids: lysicamine (**80**) and liriodenine (**81**); and three quaternary protoberberine alkaloids; columbamine (**43**), dihydrodiscretamine (**44**) and 4,13-dihydroxy-2,8,9-trimethoxydibenzo[a,g]quinolizinium (**82**). Compounds that were previously isolated from this plant were *N*-*trans*-feruloyltyramine (**15**), *N*-formylannonaine (**33**), *N*-formylnornuciferine (**34**) and octacosanol (**79**) (Fukuda et al. 1983, 1985, 1986; Pachaly et al., 1992). The rest of the compounds are being reported for the first time for this plant. The isolation of 4,13-dihydroxy-2,8,9-trimethoxydibenzo[a,g]quinolizinium (**82**), with a fully aromatic skeleton and aliphatic amine: *N*,*N*-dimetylhexadecan-1-amine(**83**), are also being isolated for the first time in this plant as well as for the genus *Tinospora*. A possible biosynthesis pathway of a new aromatic protoberberine is being proposed. Compounds were characterized by spectroscopy (UV, IR, NMR and MS) and melting point.

4.1.1 *N-trans*-feruloyltyramine (15)

Compound (**15**) was obtained as to afford a light yellowish powder (40 mg, 0.16 %) as *N-trans*-feruloyltyramine m.p. 89-90 (lit. 91°C) (Fukuda et al., 1983) The IR spectrum (Appendix A1) displayed a broad absorption band in the region 3228-2850 cm^{-1} corresponding to the OH functional group. The carbonyl functional group was observed at 1651 cm^{-1}. N-H stretching appeared at 1511 cm^{-1}, while stretching due to C-O was observed at 1031 cm^{-1}.

The ^{1}H NMR (Appendix A2) spectrum of compound (**15**) exhibited two sets of aromatic signals. The first set at δ 6.73 and δ 7.06, were assigned to H5/H7 and H4/H8, respectively, while the second set appeared at δ 7.13 for H3', δ 7.04 for H9' and δ 6.81 for H9'. Two sets of doublet at δ 6.42 (*J*= 15.7 Hz) and δ 7.45 (*J*=15.7 Hz) were attributed to the *trans*-protons, H2' and H3'. An upfield signal appeared as triplets centred at δ 2.76 (J=7.6 Hz) and δ 3.49, corresponding to the methylene protons, H2 and H1. The sharp singlet at δ 3.92 was assigned to methoxy protons.

The DEPTQ spectra (Appendix A3) confirmed the presence of two methylene carbons at δ 39.63 and δ 32.89; two olefinic carbons at δ 115.83 (C-2') and δ 139.11 (C-3'); and seven aromatic carbons at δ 127.82 (C-4), 115.83 (C-5), 113.36 (C-7), 127.82 (C-8), 106.64 (C-5'), 113.56 (C-8'), 120.30 (C-9'). In addition, six quaternary carbons at 128.41, 154.03, 166.29, 125.38, 146.93, 146.39 and carbonyl carbon at 166.29 have been assigned. Complete assignments of ^{1}H, DEPTQ and HSQC (Appendix A4) of compound (**15**) are summarized in Table 4.1.

Table 4.1: ^{1}H (500 MHz, MeOD), DEPTQ and HSQC of *N-trans*-feruloyltyramine (**15**)

Carbons	**δ_C (ppm)**	**δ_H (ppm)** **Int. Mult. J**
1	39.63	3.49 (1H, t, 7.2)
2	32.89	2.77 (1H, t, 7.6)
3	128.41	-
4	127.82	7.06 (1H, d, 8.5)
5	115.83	6.73 (1H, d, 8.6)
6	154.03	-
7	113.36	6.73 (1H, d, 8.6)
8	127.82	7.06 (1H, d, 8.5)
1’	166.29	-
2’	115.83	6.42 (1H, d, 15.7)
3’	139.11	7.45 (1H, d, 15.7)
4’	125.38	-
5’	106.64	7.13 (1H, d, 1.9)
6’	146.93	-
7’	146.39	-
8’	113.56	6.81 (1H, d, 8.2)
9’	120.30	7.04 (1H, dd, 8.2, 1.9)
6’-OCH3	53.48	3.92 (3H, s)

The mass spectrum (Appendix A5) of compound (**15**) showed $[M]^+$ 313, consistent with the molecular formula $C_{18}H_{19}NO_4$. Figure 4.1 summarize fragmentation patterns of compound (**15**) which shows a prominent peak at m/z 177 corresponding to the radical cation $C_{10}H_{10}O_3$ $[M]^+$ arising from the loss of $C_8H_{10}NO$ from ion $[M]^+$. The peak at m/z 192 corresponds to the $[C_{10}H_{10}NO_3]^+$ arising from the loss of $C_8H_{10}O$.

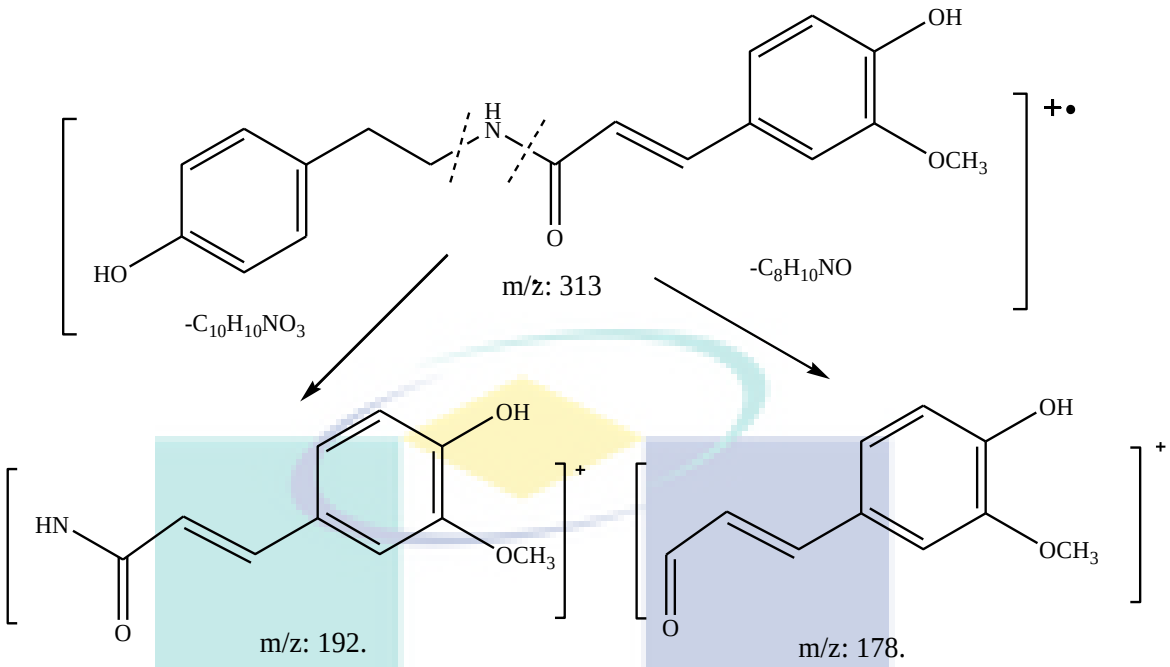

Figure 4.1: Mass fragmentation pattern of *N-trans*-feruloyltyramine (**15**)

Compound (**15**) is established as *N-trans*-feruloyltyramine based on comparison of spectroscopic data of an identical compound isolated from *Synsepalum dulcificum* (Wang et al., 2011).

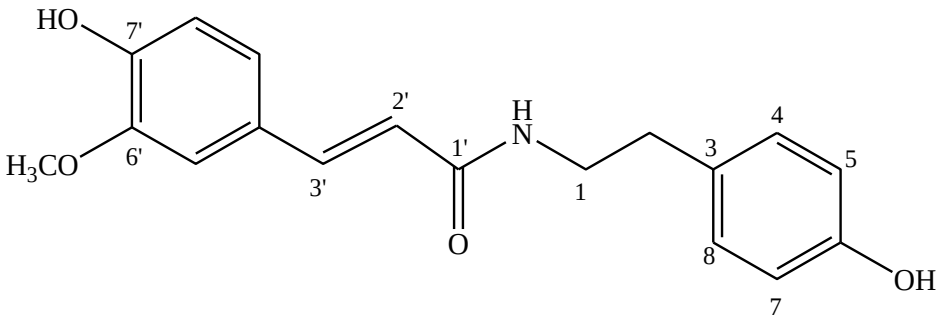

(**15**)

4.1.2 *N*-formylnornuciferine (34)

Compound (**34**) was obtained as white crystalline needles (45.0 mg, 0.18%) with melting point 220-221°C (lit. 222-224°C) (Imphanban, 2009). The IR spectrum (Appendix B1) displayed a carbonyl stretch at 1632.26 cm^{-1} due to amide functionality.

The ^{1}H NMR spectra (Appendix B2) displayed compound (**34**) as being two rotational isomers, viz., *Z*- and *E*- in the ratio of 1.8:1 (*Z*:*E*) due to the planarity of CO-N attached with non-identical functional groups (Pachaly et al., 1992). The respective signals of *E*- and *Z*- differ in their shifts being particularly strong at protons H-6a, H-5 and H-7 due to anisotropy of the carbonyl group (Pachaly et al., 1992). In ^{1}H NMR, *Z*- and *E*- isomers were identified by two sets signal of H6a signals at δ 4.92 and δ 4.43, and H-5 at 3.41/3.82 and 4.43/3.16. Both (**34a**) and (**34b**) displayed two groups of protons at δ 2.75-3.82 and δ 7.26-7.34 which are assigned to methylene protons at H-4, H-5, H7 and aromatic protons H-8 to H-11 in ring D. In addition, two methoxy protons appear as singlets at δ 3.67 and 3.89, each integrated to three protons assigned to one isomer each.

The ^{13}C (Appendix B3) and DEPTQ spectra (Appendix B4) also exhibited two sets of rotational isomers, *E*- and *Z*-. The ^{13}C and DEPTQ for isomer *Z*- indicated the presence of nineteen carbons with an amide carbonyl at 162.18; seven quaternary carbons at δ 145.99 (C-1), 152.48 (C-2), 125.25 (C-3a), 136.14 (C-8a), 131.45 (C-11a), 127.41 (C-11b), 129.53 (C-11c); six methine carbons at δ 111.57 (C-3), 49.42 (C-6a), 127.13-128.63 (C-8, C-9, C-10), 128.43 (C-11); three methylene carbons at δ 30.97 (C-4), 42.06 (C-5), 34.11 (C-7) and two methoxy carbons at δ 55.98 and 60.07.

The ^{13}C and DEPTQ experiments for isomer *E*- indicate the presence of nineteen carbons with an amide carbonyl at 162.98; seven quaternary carbons at δ 145.73 (C-1), 152.61 (C-2), 124.75 (C-3a), 135.46 (C-8a), 131.14 (C-11a), 127.41 (C-11b), 129.52 (C-11c); six methine carbons at δ 111.75 (C-3), 53.48 (C-6a), 127.54-128.19 (C-8, C-9, C10), 128.63 (C-11); three methylene carbons at δ 29.64 (C-4), 36.11 (C-5), 37.95 (C-7) and two methoxy carbons at δ 56.00 and 60.07.

The proton signal singlet at δ 8.44 in the HMQC spectrum (Appendix B6) correlated to carbons at δ 162.18 and δ 8.26 to 161.98 for isomers *Z*- and *E*- confirmed the presence of an *N*-formyl group which is further corroborated by COSY (Appendix B5) and HMBC spectra (Appendix B7). The HMBC crosspeaks from H-3 to C-4, C-3a, C-1, C-2; H-4α to C-3, C-5, C-6a, C-3a, C-11c; H-5 to C-7, C-5, CHO, H-6a to C-11b, C-11c; H-11 to C-8, C-9, C-10, C-11a; CHO to C-5, C-6a; 1-OCH_3 to C-1 and 2-OCH_3 to C-2 are also observed confirming the structure of compound (**34**) as shown in Figure 4.2. The complete assignments of ^{1}H, ^{13}C, COSY and HMQC NMR of compound (**34**) for both isomers are shown in Table 4.2 and Table 4.3.

Table 4.2: ^{1}H (500 MHz, $CDCl_3$), ^{13}C (125 MHz, $CDCl_3$), COSY and HMQC of *Z*- form *N*-formylnornuciferine (**34a**)

Carbons	**δ_C (ppm)**	**δ_H (ppm)** **Int. Mult. J**	**COSY**
1	145.99	-	-
2	152.48	-	-
3	111.47	6.66 (1H, s)	-
3a	125.25	-	-
4a	30.97	2.75 (1H, m)	H4b, H5a
4b		2.91 (1H, m)	H4a
5a	42.06	3.41 (1H, dd, 12.50, 2.75)	H5b, H4a
5b		3.82 (1H, ddd, 12.75,4.60,1.80)	H5a
6a	49.42	4.92 (1H, dd, 14.35, 4.10)	H7a, H7b
7a	34.11	3.15 (1H, m)	H7b, H6a
7b		2.75 (1H, m)	H7a, H6a
8a	136.14	-	-
8,9,10	127.13128.63	7.26-7.34 (3H, overlapped)	H8, H9, H11
11	128.43	8.44 (1H, d, 9.0)	H10
11a	131.45	-	-
11b	127.41	-	-
11c	129.53	-	-
CHO	162.18	8.26 (1H, s)	-
1-OCH_3	55.98	3.67 (3H, s)	-
2-OCH_3	60.07	3.89 (3H, s)	-

Table 4.3: ^{1}H, (500 MHz, $CDCl_3$), ^{13}C (125 MHz, $CDCl_3$), COSY and HMQC of *E*- form *N*–formylnornuciferine (**34b**)

Carbons	**δ_C (ppm)**	**δ_H (ppm)** **Int. Mult. J**	**COSY**
1	145.73	-	-
2	152.61	-	-
3	111.75	6.69 (1H, s)	-
3a	124.75	-	-
4a, 4b	29.64	2.75 (2H, m)	H4a, H4b, H5b
5a	36.11	4.43 (1H, ddd, 12.70, 4.5, 3.65)	H5b
5b		3.16 (1H,m)	H4a, H4b
6a	53.48	4.51 (1H, dd, 14.20, 4.00)	H7b
7a	37.95	3.15 (1H, m)	H7b
7b		2.75 (1H, m)	-
8a	135.46	-	-
8	127.54-128.19	7.26-7.34 (3H, overlapped)	H8, H9, H11
11	128.63	8.41 (1H, d, 9.0)	H10
11a	131.14	-	-
11b	127.41	-	-
11c	129.52	-	-
CHO	161.98	8.26 (1H,s)	-
1-OCH_3	56.00	3.67 (3H,s)	-
2-OCH_3	60.07	3.89 (3H,s)	-

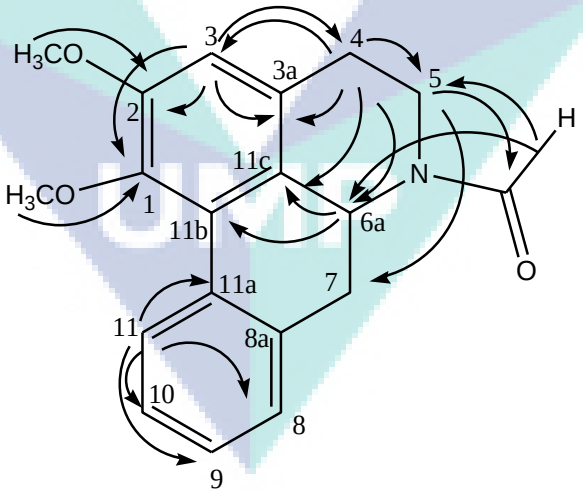

Figure 4.2: HMBC correlation of *N*–formylnornuciferine (**34**)

The EIMS spectrum (Appendix B8) of compound (**34**) exhibits characteristic fragments of an aporphine skeleton possessing a prominent peak at m/z 251 (Figure 4.3). The molecular ion peak at m/z 309 is in agreement with the molecular formula $C_{19}H_{19}NO_3$.

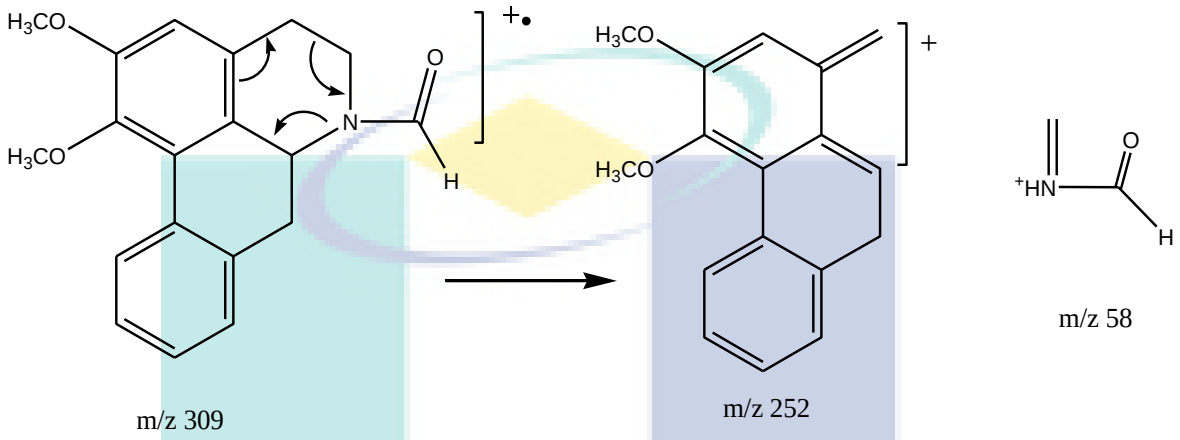

Figure 4.3: Mass fragmentation pattern of compound (**34**)

Based on its spectroscopic data and comparison with literature values (Pachaly et al., 1992; Imphanban 2009), compound (**34**) is identified as *N*-formylnornuciferine.

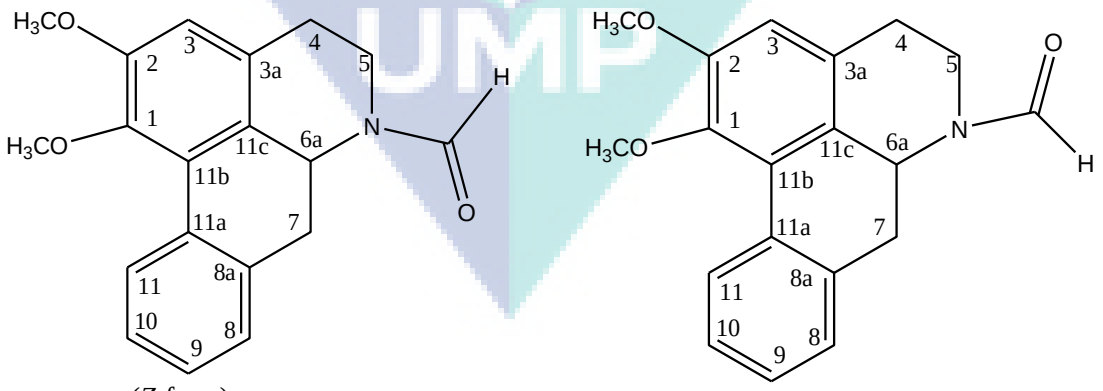

(*Z*-form) (*E*-form)

(**34a**) (**34b**)

4.1.3 *N*-formylannonaine (33)

Compound (**33**) is a white crystal (3.5 mg, 0.014%) with melting point 216-217°C (lit. 218-219°C) (Imphanban, 2009). The infrared spectrum (Appendix C1) displayed absorptions at 1658.44 cm^{-1} due to an amide carbonyl and at 2925cm^{-1} and 2854 cm^{-1} due to C-H (sp^3) stretches.

The ^{1}H (Appendix C2) and COSY spectra (Appendix C5) of compound (**33**) exhibited similar profile to the ^{1}H and COSY NMR spectra of compound (**34**) except the disappearance of two methoxy groups at C-1 and C-2 of compound (**34**). Instead the appearance of doublets at δ 6.14 and δ 6.02 with coupling constant *J*=1.0 and *J*=0.5, respectively, was attributed to the methylenedioxy proton.

The ^{1}H NMR spectra indicated that compound (**33**) exists as *E*- and *Z*- rotational isomers in the ratio of 2.4:1(*Z*:*E*) attributed to *N*-acylated noraporphines (Pachaly et al., 1992). The *Z*- and *E*- isomers were identified by two sets signal of H-6a signals at δ 5.09 and δ 4.66 and H-5 at δ 3.41/3.87 and δ 3.15/4.51, respectively. The signal of *Z* isomer should be observed at higher field than *E* isomer due to shielding arising from carbonyl anisotropy (Figure 4.4) (Imphanban, 2009). Protons falling within the conical area are shielded and those falling outside the conical are deshielded.

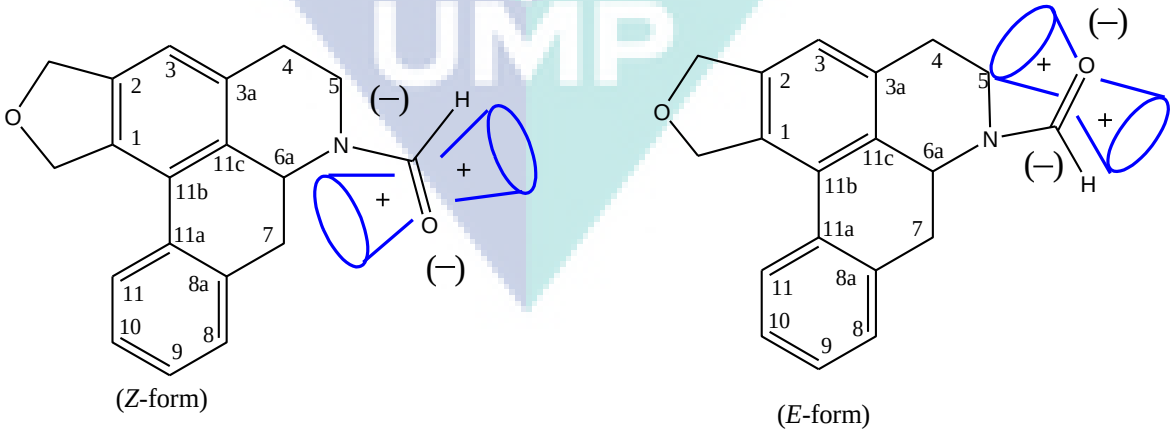

Figure 4.4: Effects of anisotropy in isomer of compound (**33**)

The ^{13}C (Appendix C3) and DEPTQ spectra (Appendix C4) also exhibited two sets of rotational isomers *E*- and *Z*-. The ^{13}C and DEPT for both isomers *Z*- and *E*- of

compound **(33)** indicated the presence of eighteen carbons with an amide carbonyl at δ 162.12, methylenedioxy carbons at δ 101.04, seven quaternary carbons, six methine carbons and three methylene carbons. The complete assignments of ^{1}H, ^{13}C, COSY and HMQC (Appendix C6) NMR data of compounds (**33a**) and (**33b**) are tabulated in Table 4.4 and Table 4.5.

Table 4.4: ^{1}H (500 MHz, $CDCl_3$), DEPTQ, COSY and HMQC of *Z*- form *N*-formylannonaine **(33a)**

Carbons	**δ_C (ppm)**	**δ_H (ppm) Int. Mult. J**	**COSY**
1	143.32	-	-
2	147.12	-	-
3	107.51	6.61 (1H, s)	-
3a	126.61	-	-
4a	31.03	2.87 (1H, m)	H5a
4b		2.97 (1H, m)	H5b
5a	42.19	3.41 (1H, dd, 12.45, 2.80)	H4a, H5b
5b		3.87 (1H, ddd, 12.80, 4.60, 1.80)	H4b, H4a
6a	49.46	5.09 (1H, dd, 14.00, 4.40)	H7a, H7b
7a	33.61	2.87 (1H, m)	H7b
7b		3.27 (1H, m)	-
8a	135.15	-	-
8, 9, 10	127.13-128.03	7.27-7.37 (3H, overlapped)	H8, H9, H11
11	128.89	8.13 (1H, d, 9.0)	H10
11a	130.65	-	-
11b	117.49	-	-
11c	124.71	-	-
CHO	162.12	8.29 (1H, s)	-
OCH_2O	101.01	6.14 (1H, d, 1.0)	-
		6.02 (1H, d , 0.5)	-

The EI-MS spectrum (Appendix C7) of compound (**33**) revealed a molecular ion peak $[M]^+$ at m/z 293, consistent with the molecular formula $C_{18}H_{15}NO_3$. The base peak at m/z 235 exhibited characteristic fragments due to retro Diels Alder cleavage of the aporphine skeleton (Figure 4.5).

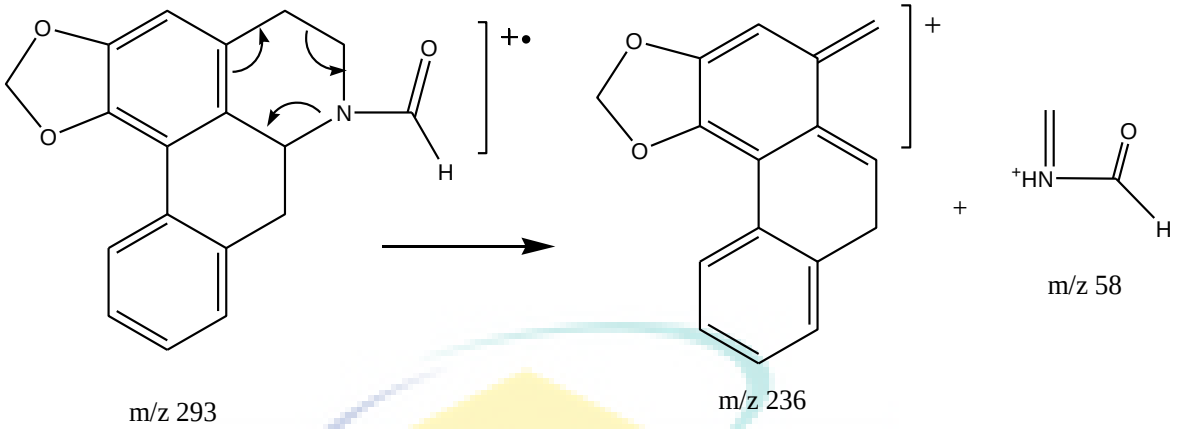

Figure 4.5: Mass fragmentation pattern of compound (**33**)

Table 4.5: ^{1}H (500 MHz, $CDCl_3$), DEPTQ COSY and HMQC of *E*- form *N*-formylannonaine (**33b**)

Carbons	**δ_C (ppm)**	**δ_H (ppm) Int. Mult. J**	**COSY**
1	143.17	-	-
2	147.41	-	-
3	107.05	6.61 (1H, s)	-
3a	126.61	-	-
4a, 4b	29.77	2.87 (2H, m)	H5a, H5b
5a	36.19	3.15 (1H, m)	H4a, H4b
5b		4.51 (1H, ddd, 12.70, 4.45, 1.80)	H4a,H4b, H5b
6a	53.30	4.66 (1H, dd, 14.50, 4.40)	H7a, H7b
7a	37.78	2.87 (1H, m)	-
7b		3.15 (1H, m)	-
8a	134.46	-	-
8, 9, 10	127.13-128.03	7.27-7.37 (3H, overlapped)	H8, H9, H11
11	128.89	8.15 (1H, d, 9.0)	H-10
11a	130.45	-	-
11b	117.05	-	-
11c	124.14	-	-
CHO	162.03	8.42 (1H, s)	-
OCH_2O	101.11	6.14 (1H, d, 1.0)	-
		6.02 (1H, d , 0.5)	-

Hence, the structure of compound (**33**) is established as *N*-formylannonaine, base on its spectrometric data and comparison with the literature value of the compound previously reported from *T. crispa* (Pachaly et al., 1992).

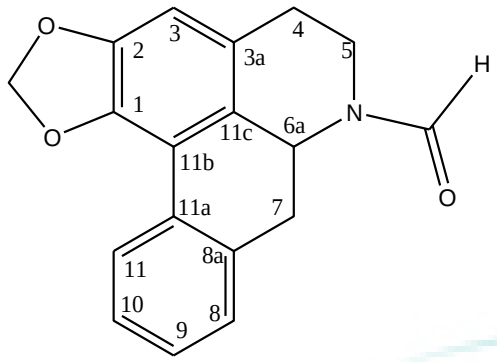

(*Z*-form)

(**33a**)

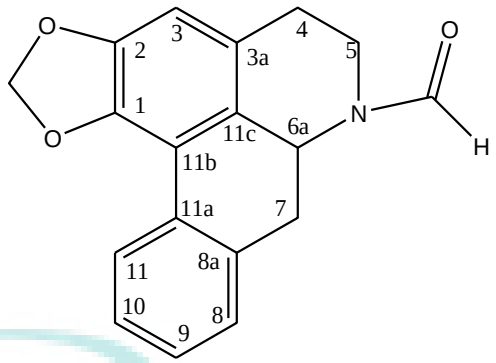

(*E*-form)

(**33b**)

4.1.4 Lysicamine (80)

Compound (**80**) was isolated as a yellow powder (8.0 mg, 0.032%) with melting point 212-213°C (lit. 210-211°C) (Israilov et al., 1980) and formed an orange precipitate in Dragendorff's reagent indicating a positive test for the presence of alkaloid. The IR spectrum (Appendix D1) displayed absorption at 1737 cm^{-1} due to a carbonyl functionality group and at 1094 cm^{-1} for C-O.

The ^{1}H spectrum (Appendix D2) of compound (**80**) comprised a total of seven aromatic protons and two methoxy. The ^{1}H spectrum revealed pyridine protons at δ 8.96 and 7.86 that had a coupling constant *J*=5.2 Hz were assigned to H-5 and H-4 of an oxoaporphine skeleton. Another four signals due to aromatic protons at δ 9.22 (d, *J*=8.0, H-11), 8.63 (*dd*, *J*=8.0, H-8), 7.80 (*dd*, *J*=8.5, 1.5, H-10) and 7.60 (*t*, *J*=8.0 H-9) were assigned as an ABMX system characteristic of 1,2-disubstituted benzene nucleus of ring D. The remaining signals were also assigned to one aromatic proton, resonating as a singlet at δ 7.27 due to H-3 and two sets of three proton singlets for an aromatic methoxyl δ 4.14 (3H, s) and 4.05 (3H, s). The COSY spectrum (Appendix D5) revealed a partial structure from H-4 to H-5, H-8 to H-9, H-9 to H-10 and H-10 to H-11 in the existence of six methine of an aromatic ring.

The ^{13}C-NMR (Appendix D3) of compound (**80**) revealed signals due to eighteen carbon atoms as shown in Table 4.6 which were classified by DEPTQ technique

(Appendix D4) as seven methine, two methoxy and nine quaternary carbons. The signal at δ C182.74 is assigned to a quaternary carbon of a conjugated carbonyl, seven aromatic methines at δ 106.49 (C-3), 123.69 (C-4), 145.08 (C-5), 128.48 (C-8), 128.85 (C-9), 123.95 (C-10), 134.38 (C-11), eight quaternary carbons at δ 152.36 (C-1), 156.94 (C-2), 145.41 (C-3a), 135.62 (C-6a), 132.11 (C-7a), 130.88 (C-11a), 122.26 (C-11b) and 119.09 (C-11c).

The structure of this compound was further characterized by HMQC (Appendix D6) and HMBC (Appendix D7) studies. The presence of a singlet aromatic proton H-3 (δ 7.24) showed correlation with a quaternary carbon at δ 123.69 (C-4), 156.94 (C-2) and 156.94 (C-1) which then defined the position of two methoxy groups at C-2 and C-1, respectively. The signal at δ 7.86 (H-4) correlated with signals at C-3a and C-3. The signal at δ 8.63 (H-8) correlated with signals at C-7a and C-7. The signal at δ 4.14 (2-OCH_3) correlated with the signal at C-2 while the signal at 4.05 (1-OCH_3) correlated to C-1. HMBC correlation of various protons to carbons is shown in Figure 4.6. Based on the assignments, compound (**80**) is elucidated as an oxoaporphine-type alkaloid with two methoxy groups located in the A ring at C-1 and C-2, respectively. A comparison of spectral data summarized in Table 4.6 with published data (Husain et al., 2012) confirms the structure of compound (**80**) to be lysicamine.

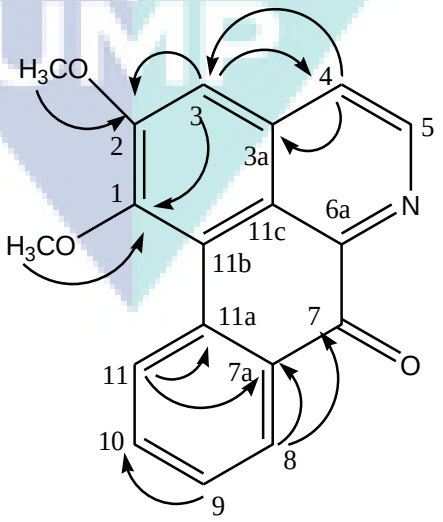

Figure 4.6: HMBC correlations of lysicamine (**80**)

Table 4.6: ^{1}H (500 MHz, $CDCl_3$), DEPTQ, COSY, HMQC and HMBC of lysicamine (**80**)

Carbons	δ_C (ppm)	δ_H (ppm) Int. Mult. J	COSY	HMBC
1	152.36	-	-	-
2	156.94	-	-	-
3	106.49	7.27 (1H, s)	-	C1, C2, C3a
3a	145.41	-	-	-
4	123.69	7.86 (1H, d, 5.20)	H5	C3a, C3
5	145.08	8.96 (1H, d, 5.20)	H4	-
6a	135.62	-	-	-
7	182.79	-	-	-
7a	132.11	-	-	-
8	128.48	8.63 (1H, d, 8.0)	H9	C7a, C7
9	128.85	7.60 (1H, t, 8.0)	H8	-
10	123.95	7.80 (1H, dd, 8.5, 1.5)	H11	C9
11	134.38	9.22 (1H, d, 8.0)	H10	C11a, C7a
11a	130.88	-	-	-
11b	122.26	-	-	-
11c	119.09	-	-	-
1-OCH_3	60.72	4.05 (3H, s)	-	C1
2-OCH_3	56.27	4.14 (3H, s)	-	C2

The EIMS (Appendix D8) fragmentation data could be rationalized as in Figure 4.7. The mass spectrum revealed a molecular ion peak at m/z 291corresponding to $C_{18}H_{13}NO_3$.

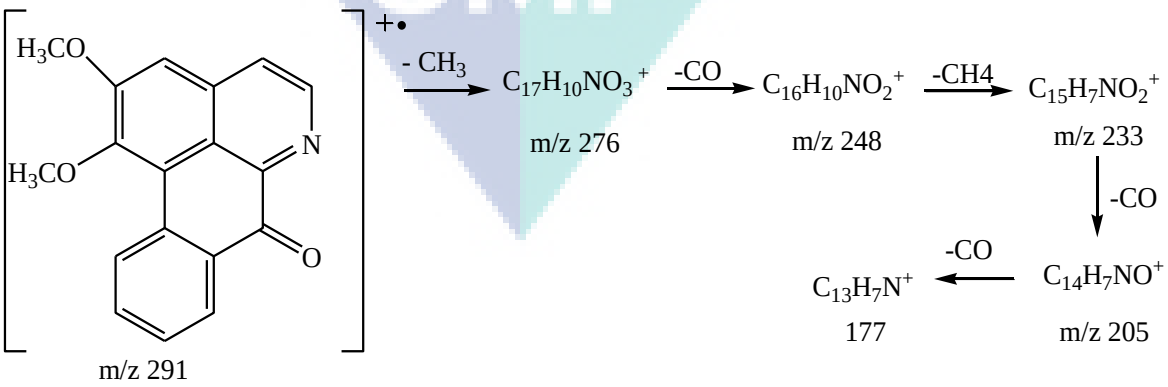

Figure 4.7: Mass fragmentation of lysicamine (**80**)

4.1.5 Liriodenine (81)

Compound (**81**) is a light brown powder (3.5 mg, 0.014 %) with melting point 278-279°C (lit. 280-282°C) (Israilov et al., 1980) and R_f value of 0.48 appearing above compound (**80**) which has an R_f value of 0.40. Compounds (**80**) and (**81**) exhibited intense yellow fluorescent coloration in solution, characteristic of the presence of an oxoaporphine chromophore. Compound (**80**) yielded a UV spectrum (Appendix E1) with λ_{max} at 229, 315 and 368 nm, while compound (**81**) absorbed at 229, 275 and 324 nm (Husain et al., 2012).

The ^{1}H (Appendix E2) and COSY spectra (Appendix E4) of compound (**81**) exhibited similar profile to the ^{1}H and COSY NMR spectra of compound (**80**) except the absence of two methoxy groups at C-1 and C-2 of compound (**80**). Instead the appearance of a singlet at δ 6.65 (2H, s) was attributed to the methylenedioxy proton. In the ^{1}H-NMR spectrum of (**81**), the singlets at δ 7.23 assigned to H-3, a doublet at δ 8.90 (*J*=5.0 Hz) and δ 7.81 (*J*=5.0 Hz) indicated the presence of H-5 and H-4. In the aromatic region, three doublets at δ 8.60 (*J*=8.0 Hz), δ 7.78 (*J*=7.4 Hz) and 8.67 (*J*=8.5 Hz) were assigned to H-8, H-10 and H-11 protons, respectively, while the triplet at δ 7.61 (1H, *t*, *J*=8.0 Hz) was attributed to H-9.

The DEPTQ spectrum (Appendix E3) of (**81**) indicated the presence of one methylenedioxy, seven methine, and nine quaternary carbons including a carbonyl carbon at δ 182. The HMQC (Appendix E5) spectrum clearly proves that the methylenedioxy protons were attached to the carbon at δ 101.84. Meanwhile the quaternary carbon for C-1 and C-2 were at δ 148.03 and δ 151.93. Upon comparison with reported data (Guo et al., 2001), a complete assignment of ^{1}H, DEPTQ, COSY and HMQC NMR data of compound (**81**) are tabulate in Table 4.7.

This was supported by the GCMS spectrum (Appendix E6) which gave rise to a molecular ion peak at m/z 275 attributed to the molecular formula $C_{17}H_9NO_3$ and m/z 247 are due to the loss of CO consistent with an oxoaporphine alkaloid.

Table 4.7: ^{1}H (500 MHz, $CDCl_3$), DEPTQ, COSY and HMQC of liriodenine (**81**)

Carbons	**δ_C (ppm)**	**δ_H (ppm)** **Int. Mult. J**	**COSY**
1	148.03	-	-
2	151.93	-	-
3	103.14	7.23 (1H, s)	-
3a	145.83	-	-
4	124.50	7.81 (1H, d, 5.00)	H5
5	145.32	8.91 (1H, d, 5.00)	H4
6a	135.46	-	-
7	182.46	-	-
7a	130.95	-	-
8	128.08	8.60 (1H, d, 8.00)	H9
9	128.87	7.61 (1H, t, 8.00)	H8
10	134.23	7.78 (1H, m)	-
11	127.72	8.70 (1H, d, 8.50)	-
11a	132.57	-	-
11b	108.74	-	-
11c	122.62	-	-
OCH_2O	101.84	6.39 (2H, s)	-

Compound (**81**) was a sequence arising from same metabolism of compound (**80**) and both are scattered in *Duguetia* species (Perez and Cassels, 2010). This oxoaporphine alkaloid (**81**) is being reported for the first time from *Tinospora* species.

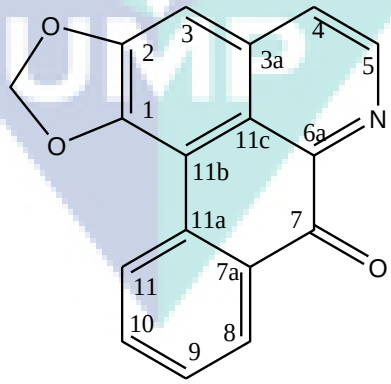

(**81**)

4.1.6 Magnoflorine (40)

Compound (**40**) was isolated as a brown powder (8.0 mg, 0.32 %) with melting point 250-251°C (lit 248°C) (Israilov et al., 1980) and R_f value of 0.44 (MeOH:NH_4OH, 9:1). It appeared as blue fluorescence in long wave UV light. The UV spectrum (Appendix F1) of magnoflorine is characteristic of 1,2,10,11-tetrasubstituted aporphines having the absorption at λ_{max} 221 nm, 274 nm and 310 nm (Slavik et al., 1985).

The ^{1}H NMR spectrum (Appendix F2) demonstrated the presence of two singlets at δ 2.98 and δ 3.36, each integrated to three protons. These were represented as two unequivalent methyl groups attached to the nitrogen atom. The absence of two methoxy signals at high field, δ 3.83 and δ 3.84 indicated the absence of a C-1 and C-10 methoxy functional group. The absence of the low field aromatic proton at δ 6.75-6.62 indicated substitution at position C-11. A total of three aromatic protons were observed as two doublets forming an AB system. The most downfield doublet at δ 6.75 integrated to one proton with an ortho coupling constant (*J*=7.95) and was assigned as H-8. A doublet at δ 6.62 (*J*=7.80) was assigned as H-9. The singlet signal at δ 6.64 was overlapped with doublet protons at δ 6.62 and was assigned as H-3.

The DEPTQ spectra (Appendix F3) of compound (**40**) showed the presence of twenty carbon atoms with nine quaternary carbons, three methylene, four methine, two methoxy δ 55.07, δ 54.70 and two *N*-methyl carbons at δ 42.07 and δ 52.55. Three aromatic carbons at δ 109.67 (C-3), 108.09 (C-8) and 115.61 (C-10) were attributed to four methine carbons while δ 70.41 was assigned to C-6a. Meanwhile the signals for quaternary carbons of the aromatic methoxy were detected at δ 151.43 and δ 150.52. Another five quaternary carbons were assigned δ 119.67 (C-3a), 126.28 (C-8a), 123.54 (C-11a), 123.24 (C-11b) and 120.10 (C-11c) and the last two were assigned as quaternary carbons for aromatic hydroxyl groups at δ 149.31 (C-1) and δ 148.14 (C-11).

In order to confirm the position of methoxy and hydroxyl groups, COSY (Appendix F4) and HMBC (Appendix F6) NMR were used. COSY clearly showed correlation between H-4 to H-5, H-6a to H-7 and H-8 to H-9. The presence of a singlet aromatic proton H-3 (δ 6.64) showed correlation with quaternary carbons at δ 151.43

(C-2) and δ 119.67 (C-3a), which then defined the position of one of the methoxy groups, namely, at C-2 and correlation of one of two *o*-substituted aromatic doublet protons (H-9) at δ 6.62 to quaternary carbons at δ 150.52 (C-10), δ 123.24 (C-11b) and δ 124.54 (C-11a), revealing the position of methoxy group at C-10 and hydroxyl group at C-11. The correlation between methyl protons at δ 2.98 and δ 3.36 to carbons at δ 61.27 (C-5) and δ 70.41 (C-6a), revealed binding of the protons to nitrogen. The complete HMBC correlation of compound (**40**) is shown in Figure 4.8 and upon comparison with data obtained by Patel et al. (2011) full assignment of ^{1}H, DEPTQ, HMQC (Appendix F5), COSY, and HMBC NMR are summarized in Table 4.8.

Table 4.8: ^{1}H (500 MHz, MeOD), DEPTQ, COSY, HMQC and HMBC of magnoflorine (**40**)

Carbons	**δ_C (ppm)**	**δ_H (ppm) Int. Mult. J**	**COSY**	**HMBC**
1	149.31	-	-	-
2	151.43	-	-	-
3	109.37	6.64 (1H, s)	-	C3a, C2
3a	119.67	-	-	-
4a	23.41	3.28 (1H, m)	H4b, H5a	N-CH_3β, C5, C6a
4b		2.88 (1H, dd, 17.50, 4.05)	H4a, H5b	C-5, C6a
5a	61.27	3.59 (1H, m)	H4a	N-CH_3β
5b		3.68 (1H, m)	H4b	-
6a	70.41	4.23 (1H, d, 12.30)	H7a, H7b	C6a, C11b, C11c
7a	30.73	2.75 (1H, t, 12.60)	H7b, H6a	-
7b		3.16 (1H, m)	H6a	C6a, C8a
8a	126.28	-	-	-
8	108.09	6.75 (1H, d, 7.95)	H9	C8a, C8, C11
9	115.61	6.62 (1H, d, 7.80)	H8	C11a, C11b, C10
10	150.52	-	-	-
11	149.14	-	-	
11a	124.54	-	-	-
11b	123.24	-	-	-
11c	120.10	-	-	-
2-OCH_3	55.05	3.84 (3H, s)	-	C1
10-OCH_3	54.63	3.83 (3H, s)	-	C2
N-CH_3α	42.07	2.98 (3H, s)	-	N-CH_3β, C5, C6a
N-CH_3β	52.55	3.36 (3H, s)	-	N-CH_3α, C5, C6a

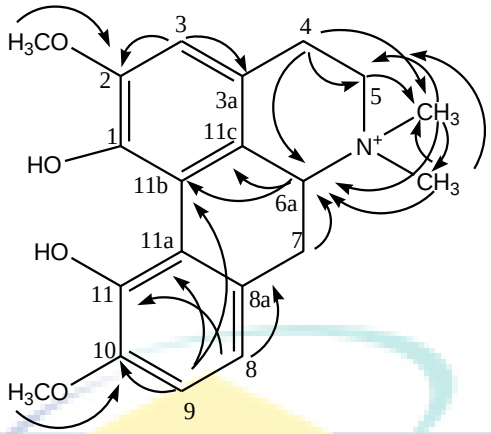

Figure 4.8: HMBC correlations of magnoflorine (**40**)

The EIMS spectrum of compound (**40**) (Appendix F7) showed a small molecular ion peak with m/z 341, corresponding to a molecular formula of $C_{20}H_{24}NO_4$. Elimination of methylene imine unit through the retro Diels-Alder reaction of ring B resulted in peak m/z 284. The mass fragmentation of compound (**40**) is shown in Figure 4.9.

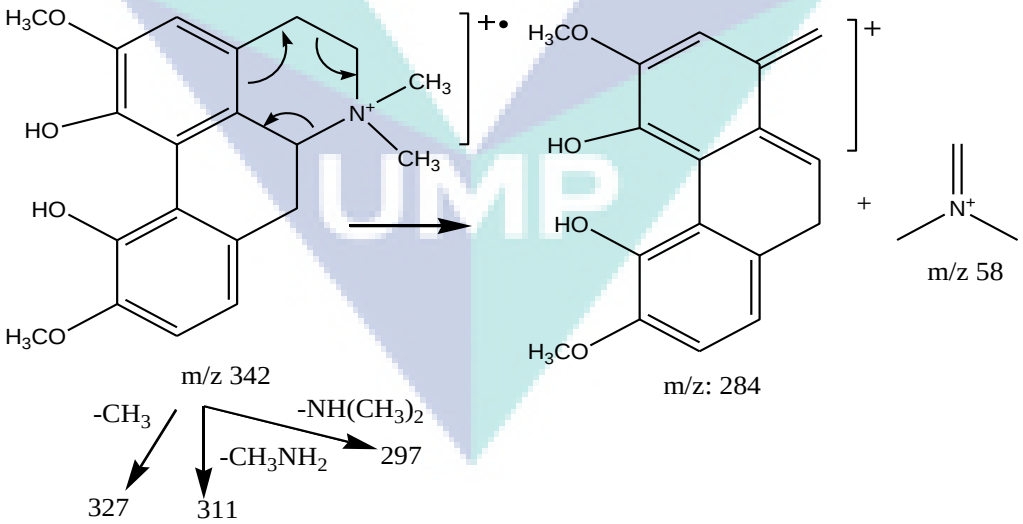

Figure 4.9: Mass fragmentation of magnoflorine **(40)**

4.2.7 Columbamine (43)

Compound (**43**) was isolated as a yellow gummy solid (10 mg, 0.04 %). It showed a strong yellow fluorescence under UV light (254 and 366 nm) and tested positive with Dragendorff's reagent. The UV spectrum (Appendix G1) showed maximal absorptions at 290 and 348 nm indicating a protoberberine chromophore (Shamma et al., 1969). The IR spectrum (Appendix G2) displayed absorption bands at 3459 cm^{-1} for hydroxyl group (broad), 1639 cm^{-1} for C=N and at 1092 cm^{-1} for C-O.

The ^{1}H NMR spectra of compound (**43**) (Appendix G3) revealed two typical signals of the berberine skeleton at δ 9.77 and 8.67, which were assigned to H-8 and H-13. Two coupling methylene groups at 3.29 (2H, t, *J*=6.25) and the downfield shifted signals caused by a quaternary amine at δ 4.85 (2H, t, *J*=6.25) were assigned to H-5 and H-6, respectively. The presence of two aromatic protons at δ 8.14 and 8.03 with coupling constants, *J*=9.15 and *J*=9.10, assigned to H-11 and H-12 indicates the *ortho* substitution of ring D. In addition, the ^{1}H NMR spectra displayed two proton singlets at δ 7.05 and 7.59 in the aromatic region which was assigned to H-4 and H-1.

The DEPTQ spectra (Appendix G4) showed twenty carbon signals with two attributed to methylene carbons at δ 26.41 (C-5) and 56.35 (C-6); six due to methine carbons at δ 111.72 (C-1), 110.68 (C-4), 144.82 (C-8), 126.68 (C-11), 123.14 (C-12), 119.72 (C-13); nine due to quaternary carbons at δ 151.11 (C-3), 150.50 (C-10), 146.67 (C-2), 144.25 (C-9), 138.51 (C-14), 133.87 (C-12a), 127.44 (C-4a), 121.89 (C-8a), 119.22 (C-14a) and three due to methoxy carbons at δ 55.36 (3-OCH_3), 56.35 (10-OCH_3), 61.26 (9-OCH_3).

Complete assignment and aromatic protons were established by COSY (Appendix G5) and HMBC (Appendix G7) experiments. Significant correlations between H5 to H6 and H11 to H12 were observed in the COSY spectrum. The HMBC spectrum showed strong correlations between H-1 at δ 7.59 to C-4a, C-14 and C-2, C-3; H3 at δ 7.05 to C-5, C-14a and C-2; H-8 at δ 9.77 to C-14 and C-12a; H-12 at δ 8.03 to C-12a and C-9; H-11 at δ 8.14 to C-10; and H-13 at δ 8.67 to C-14a, C-13 and C-14

(Figure 4.10). Full assignment of ^{1}H, DEPT, HMQC (Appendix G6), COSY, DEPTQ and HMBC NMR are summarized in Table 4.9.

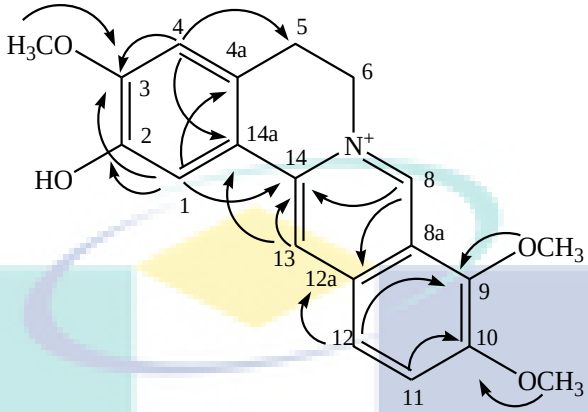

Figure 4.10: HMBC correlations of columbamine **(43)**

Table 4.9: ^{1}H (500 MHz, MeOD), DEPTQ, COSY, HMQC and HMBC of columbamine (**43**)

Carbons	**δ_C (ppm)**	**δ_H (ppm) Int. Mult. J**	**COSY**	**HMBC**
1	111.72	7.59 (1H, s)	-	C4a, C14, C2, C3
2	146.67	-	-	-
3	151.11	-	-	-
4	110.68	7.05 (1H, s)	-	C5, C14a, C3
4a	127.44	-	-	-
5	26.41	3.29 (2H, t, 6.25)	H6	-
6	56.35	4.85 (2H, t, 6.45)	H5	-
8	144.82	9.77 (1H, s)	-	C12a, C14
8a	121.89	-	-	-
9	144.25	-	-	-
10	150.50	-	-	-
11	126.68	8.14 (1H, d, 9.15)	H12	C10
12	123.14	8.03 (1H, d, 9.10)	H11	C12a, C9
12a	133.87	-	-	-
13	119.72	8.67 (1H, s)	-	C14a, C13, C14
14	138.51	-	-	-
14a	119.22	-	-	-
2-OH	-	-	-	-
3-OCH_3	55.36	3.99 (3H, s)	-	C3
10-OCH_3	56.35	4.13 (3H, s)	-	C10
9-OCH_3	61.26	4.23 (3H, s)	-	C9

The GC-MS spectrum (Appendix G8) exhibited an $[M]^+$ 338 peak and the molecular formula of compound (**43**) was deduced as $C_{20}H_{20}NO_4^+$. The spectrum also exhibited characteristic retro Diels Alder fragments of berberine skeleton possessing two methoxy groups in the D ring (m/z 165) as well as a methoxy group in ring A (m/z 178). Further the 1-methoxy, 2-hydroxyl substituents on the AB ring fragmentation formed m/z 149. The mass fragmentation of compound (**43**) is shown in Figure 4.11.

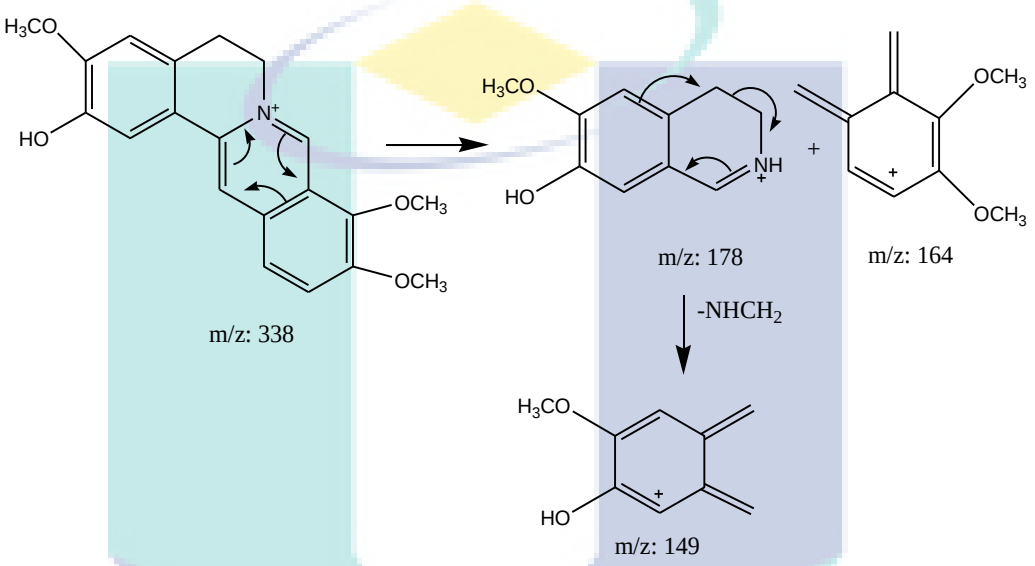

Figure 4.11: Mass fragmentation of columbamine (**43**)

Based on its spectroscopic data and comparison with literature (Thuy et al., 2006) compound (**43**) was concluded as columbamine. Columbamine (**43**) had previously been isolated from the root extract of *T. cappillipes* by Chang et al. (1984) and was the first reported quarternary alkaloid isolated from the stems of *T. crispa*.

4.1.8 Dihydrodiscretamine (44)

Compound (**44**) isolated as an orange gummy solid (5.5 mg, 0.022 %), and tested positive with Dragendorff's reagent. The UV spectrum (Appendix H1) showed maximal absorptions at 293 and 372 nm attributed to a protoberberine chromophore (Shamma et al., 1969). The IR spectrum (Appendix H2) showed absorption bands at 3371 cm^{-1}(broad) due to a hydroxyl group and at 1361 cm^{-1} due to C-N and at 1090 cm^{-1} due to C-O.

The ^{1}H NMR spectra of compound (**44**) (Appendix H3) revealed four aromatic protons, two of which were *para*-oriented, appearing at δ 7.49 and δ 7.05 attributed to H-1 and H-4 of the A ring of the berberine skeleton. The remaining two *ortho*-coupling aromatic protons at δ 7.65 and δ 7.77, each with coupling constant *J*=8.0, could only be bonded to C-11 and C-12. This was confirmed by the HMBC spectrum. ^{1}H NMR also displayed two typical signals of the berberine skeleton at δ 9.39 and δ 8.44, which were assigned to H-8 and H-13. Signals at δ 3.95 and δ 4.07 were attributed to two methoxy protons. Two coupling methylene groups at δ 3.23 (2H, t, *J*=5.25) and the downfield shifted signals caused by quaternary amine at δ 4.85 (2H, t, *J*=5.90) were assigned to H-5 and H-6, respectively.

The ^{13}C NMR (Appendix H4) and DEPTQ (Appendix H5) spectra revealed the presence of nineteen carbon atoms including methine, methoxy, methylene and quaternary carbons. The ^{13}C NMR features were similar to those of columbamine (**43**) except for the different distribution of hydroxyl and methoxy group.

In the COSY spectrum (Appendix H6), correlations were found from δ 3.23 to δ 4.85 indicating the positions of the two methylenes were at C-5 and C-6. The proton at δ 7.65 was correlated to δ 7.77 and assigned to H-11 and H-12. These two aromatic protons could only be bonded to C-11 and C-12, which was confirmed by the HMBC spectrum (Appendix H8). Another aromatic proton signal at δ 9.39 (s, 1H) was determined to be connected at C-8 based on the HMBC correlations with C-8, C-12a and C-14 and the two signals at δ 7.49 (H-1) and δ 7.05 (H-4) should be due to C-1 and C-4 based on the correlation with C-14a, C-14, C-2, C-3 and C-14a, C-3, respectively. The position of methoxy at δ 4.07 was confirmed by a correlation of proton at δ 7.65 (H-11) to C-12a, C-9 and C-10. A full analysis of all C-H long range correlations is shown in Figure 4.12. In order to establish the substitution pattern of the suspected skeleton, the HMQC (Appendix H7) and HMBC spectra of compound (**44**) were recorded and analysed accordingly (Table 4.10).

Table 4.10: ^{1}H (500 MHz, MeOD), DEPTQ, COSY, HMQC and HMBC of dihydrodiscretamine (**44**)

Carbons	**δC (ppm)**	**δH (ppm) Int. Mult. J**	**^{1}H-^{1}H COSY**	**HMBC**
1	111.27	7.49 (1H, s)	-	C4a, C14, C2, C3
2	150.53	-	-	-
3	146.69	-	-	-
4	110.58	7.05 (1H, s)	-	C-14a, C3
4a	126.43	-	-	-
5	26.43	3.23 (2H, t, 5.25)	H6	-
6	55.97	4.85 (2H, t, 5.90)	H5	-
8	141.69	9.39 (1H, s)	-	C-12a, C14, C8
8a	123.07	-	-	-
9	142.13	-	-	-
10	151.02	-	-	-
11	133.98	7.65 (1H, d, 8.00)	H12	C9, C10
12	123.25	7.77 (1H, d, 8.00)	H11	C12
12a	132.22	-	-	-
13	119.62	8.44 (1H, s)	-	C13, C14
14	135.46	-	-	-
14a	119.92	-	-	-
2-OCH_3	55.28	3.95 (3H, s)	-	C2
3-OH	-	-	-	-
9-OCH_3	60.36	4.07 (3H, s)	-	C9
10-OH	-	-	-	-

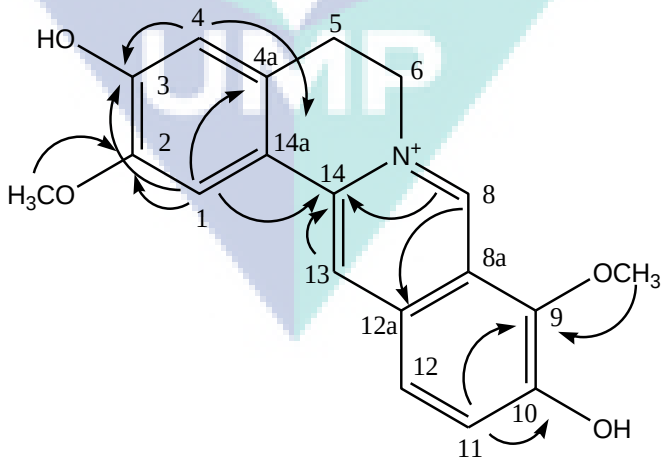

Figure 4.12: HMBC correlations of dihydrodiscretamine (**44**)

The EIMS (Appendix H9) fragmentation pattern of compound (**44**) was diagnostic of berberine and the fragment ions at m/z 178 fixed the distribution of one methoxy and one hydroxyl groups in ring D. Furthermore, the peak at m/z 149 is due to the 2-hydroxy-3-methoxy group in ring D. Based on the fragmentation pattern (Figure 4.13) the molecular formula of compound (**44**) was deduced as $[C_{19}H_{18}NO_4]^+$.

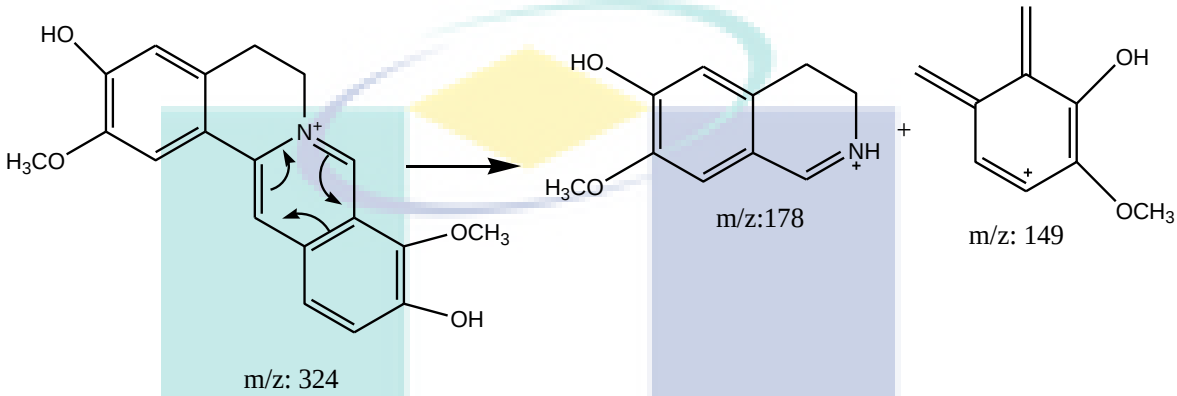

Figure 4.13: Mass fragmentation of dihydrodiscretamine (**44**)

Based on agreement of spectroscopic data, compound (**44**) is established as dihydrodiscretamine. Dihydrodiscretamine (**44**) had previously been isolated from the root extract of *T. cappillipes* by Chang et al. (1984) and was the first reported quarternary alkaloid isolated from the stems of *T. crispa*.

4.1.9 4,13-dihydroxy-2,8,9-trimethoxydibenzo[a,g]quinolizinium (82)

Compound (**82**) was isolate as a brown gummy solid (4.5 mg, 0.018 %) and tested positive with Dragendorff's reagent. The UV spectrum (Appendix I1) showed maximal absorptions at 213 and 291 nm suggesting the presence of a highly conjugated aromatic system. The IR spectrum (Appendix I2) showed absorptions at 3449 cm^{-1} (broad) due to hydroxyl group, 1637 cm^{-1} (strong) due to C=N and at 1091 cm^{-1} due to C-O.

^{1}H NMR (Appendix I3) demonstrated the presence of a fully aromatic skeleton of protoberberine with seven aromatic protons. Two *ortho*-coupling aromatic protons at

δ 6.52 and δ 6.86 (*J*=8.0, 2.0 and *J*=8.0, respectively) could only be bonded to C-11 and C-12. Another aromatic proton at δ 6.56 with *meta* coupling constant *J*=2.0, could be bonded to C-10. The ^{1}H spectrum revealed pyridine protons at δ 7.96 and 7.87 (*J*=6.0 and *J*=6.5, respectively) assigned to H-5 and H-6 of the skeleton. Two broad singlet aromatic protons at δ 7.35 and 7.35 were assigned to H-4 and H-1. COSY NMR spectrum (Appendix I6) revealed the correlation of H5 to H6, H10 to H11 and H11 to H12.

The ^{13}C NMR (Appendix I4) and DEPTQ (Appendix I5) spectrum revealed the presence of twenty carbon atoms including methine at δ 107.69 (C-1), 103.89 (C-3), 121.33 (C-5), 130.32 (C-6) , 114.86 (C-10), 118.52 (C-11) and 111.85 (C-12); methoxy at δ 55.08 (2-OCH_3), 54.94 (9-OCH_3) , 44.17 (8-OCH_3) and ten quaternary carbons at 127.21 (C-4a), 127.19 (C-12a), 132.05 (C-14a), 136.98 (C-14), 147.22 (C-9), 147.55 (C-13), 150.46 (C-8), 162.37 (C-2) and 163.81 (C-4).

In order to confirm the distribution of methoxy and hydroxy groups, HMQC (Appendix I7) and HMBC (Appendix I8) experiments were executed. HMBC revealed two doublet aromatic protons at δ7.97 (H-6) correlated to the carbon at δ 132.05 (C-14a) 150.46 (C-8), 44.17 (8-OCH_3), 121.33 (C-5) and δ 7.88 (H-5) to 127.21 (C-4a), 121.33 (C-3), 130.32 (C-6). Another two singlet aromatic protons at δ 7.35 and δ 7.29 were assigned to H-3 and H-1 based on HMBC correlations to 127.21 (C-4a), 163.81 (C-4), 121.33 (C-5) and 132.05 (C-14a), 150.46 (C-8), 162.37 (C-2), respectively. The aromatic proton at δ 6.85 (H-12) showed a correlation to 127.19 (C-12a) and 147.55 (C-13). The position of 8-methoxy at δ4.20 were confirmed by a correlation to 150.46 (C-8) and 130.32 (C-6) The position of 9-methoxy at δ3.81 was assigned based on correlation of proton at δ6.56 (H-10) to 147.22 (C-9) and 118.52 (C-11) while the position of 2-methoxy was assigned based on correlation of H-1 to the neighbouring carbon 162.37 (C-2), 132.05 (C-14a) and 150.46 (C-8). The position of hydroxyl at δ 4.71 was assigned base on correlation to 150.46 (C-8) and 127.19 (C-12a) (Figure 4.14).

Table 4.11: ^{1}H (500 MHz, MeOD), DEPTQ, COSY, HMQC and HMBC of 4,13-dihydroxy-2,8,9-trimethoxydibenzo[a,g]quinolizinium (**82**)

Carbons	**δC (ppm)**	**δH (ppm) Int. Mult. J**	**^{1}H-^{1}H COSY**	**HMBC**
1	107.69	7.28 (1H, br s)	-	C14a, C2
2	162.37	-	-	-
3	103.89	7.35 (1H, br s)	-	C5, C4a, C4
4	163.81	-	-	-
4a	127.21	-	-	-
5	121.33	7.87 (1H, d, 6.50)	H6	C3, C4a, C6
6	130.32	7.96 (1H, d, 6.00)	H5	C8, C14a, C5, 8-OCH_3
8	150.46		-	-
8a	121.53	-	-	-
9	147.22		-	-
10	114.86	6.56 (1H, d, 2.0)	H11	C11, C9
11	118.52	6.52 (1H, dd, 8.0, 2.0)	H12	C9, C10
12	111.85	6.86 (1H, d, 8.5)	-	C12a, C13
12a	127.19	-	-	-
13	147.55	-	-	-
14	136.98	-	-	-
14a	132.05	-	-	-
2-OCH_3	55.08	4.07 (3H, s)	-	C2
9-OCH_3	54.94	3.81 (3H, s)	-	C9
8-OCH_3	44.17	4.20 (3H, s)	-	C8, C6
13-OH	-	4.71 (1H, s)	-	C12a, C8

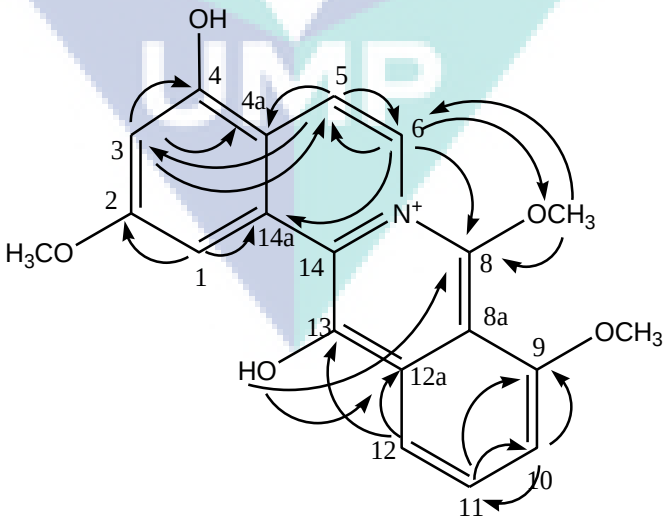

Figure 4.14: HMBC correlation of compound (**82**)

The EIMS spectrum of compound (**82**) (Appendix I9) displayed the $[M]^+$ 352 peak which was consistent with the molecular formula $[C_{20}H_{18}NO_5]^+$. The mass fragmentation of compound (**82**) is shown in Figure 4.15. In the mass spectrum of compound (**82**) the m/z peak 310 has virtually maximum intensity (100%), which indicates high stability of ion $[C_{17}H_{17}NO_5]^+$ with respect to electron impact. Similar fragmentation processes of direct elimination of CH_2 from molecular ion with m/z 352 to m/z 310 were characterized the presence of three methoxy groups in the sample. The ion at m/z 337 was determined as the neutral loss of the radical group radical CH_3• from C9 and the ion at m/z 308 can be produced by loss the carbonyl group formed in C9 of D ring via the molecule rearrangement. The fragmentation patterns of these compounds are similar to those of protoberberine compounds (Le et al., 2013).

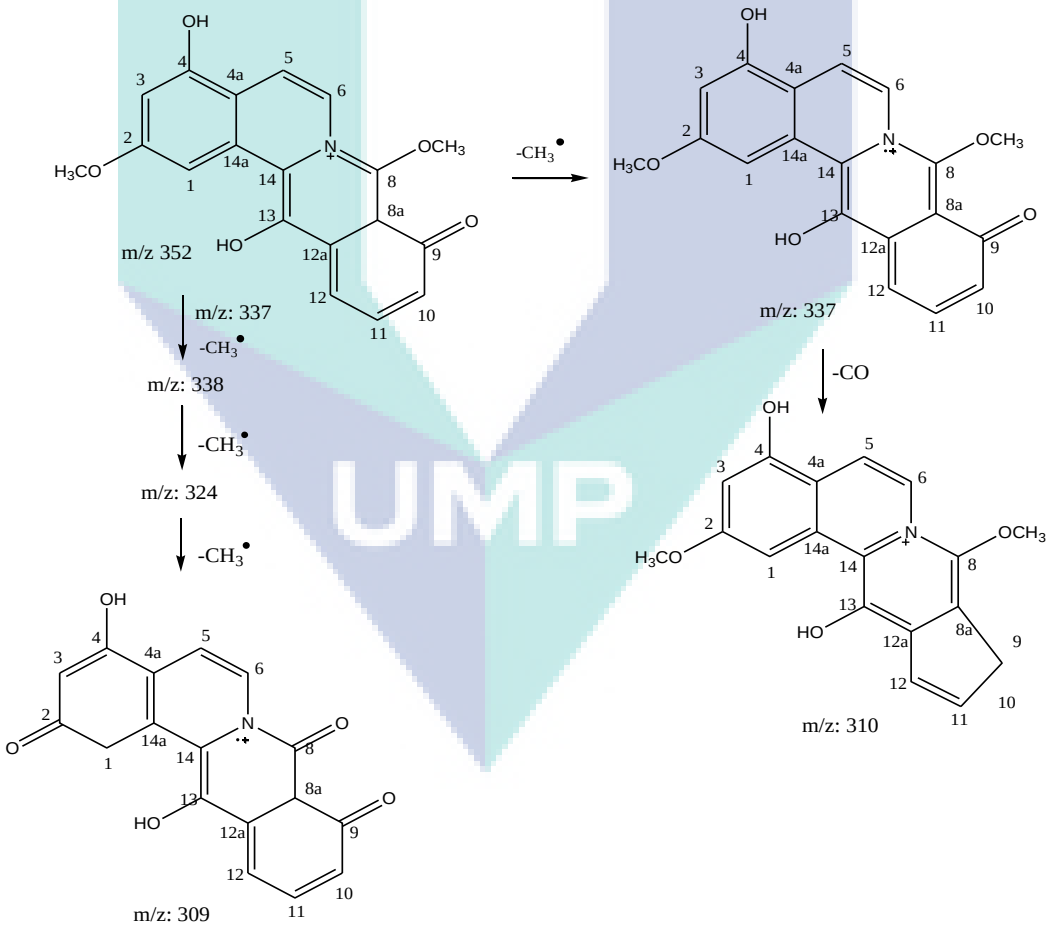

Figure 4.15: Mass fragmentation of 4,13-dihydroxy-2,8,9-trimethoxy dibenzo[a,g]quinolizinium (**82**)

It is interesting to note that the structures of compound (**82**) with a completely aromatic core are rarely found in neutral sources and only two compounds that are reported were deoxythalidastine and dehydroberberrubine (Shamma and Dudock, 1965). Deoxythalidastine is probably an artefact formed by dehydration of the known 5-hydroxyprotoberberine alkaloid, thalidastine (Ikuta and Itokawa, 1982).

In order to understand the formation of the novel compound (**82**), a possible biosynthetic pathway is suggested as illustrated in Figure 4.16. The backbone structure of protoberberine alkaloids is (S)-reticuline. The tetrahydoprotoberberine alkaloid (S)-discretamine results from the oxidative cyclization of (S)-reticuline via a two-step mechanism involving the formation of a methylene iminium ion, followed by nucleophilic attack at the imine carbon by C-2' to yield the C-8 berberine bridge and this reaction is catalyzed by berberine bridge enzyme (BBE). (Hagel and Facchini, 2010). Depending on the type of intramolecular rearrangement that occurs, the hydroxyl and methoxyl groups of (S)-reticuline acquire different positions on the resulting alkaloid (Hagel and Facchini, 2010). The pathway involves the sequence protoberberine to 13-hydroprotoberberine have been defined in several *Corydalis* species (Iwasa et al., 1995). Tetrahydroprotoberberine oxidase is employed in the conversion of tetrahydroprotoberberine to the quaternary form (Amann et al., 1984). The formation of fully aromatize quaternary benzophenanthridine (Iwasa et al., 1993) had been used to predict the pathway of fully aromatize protoberberine. Rearrangement of hydroxyl groups at C-3 to C-4 followed by dehydroxygenase at C-9 and 8-O-methylation were suggested route for the formation of new fully aromatic protoberberine alkaloid, 4,13-dihydroxy-2,8,9-trimethoxydibenzo[a,g]quinolizinium (**82**).

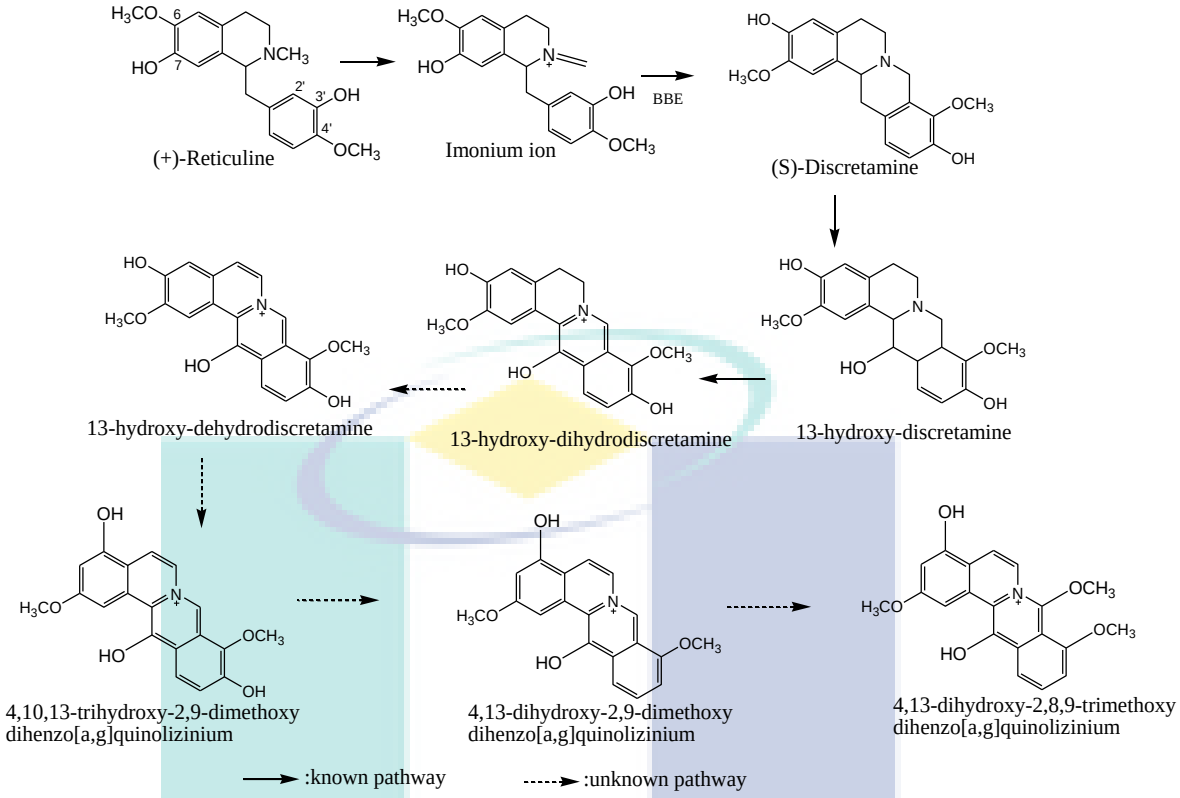

Figure 4.16: Possible biosynthetic pathway of compound (**82**)

4.1.10 *N,N*-Dimetylhexadecan-1-amine (83)

Chromatography and purification of polar fraction over RP18 silica gel afforded *N,N*-dimetylhexadecan-1-amine as white monoclinic crystals (100 mg 0.4 %) with melting point 260-261°C. The IR spectrum (Appendix J1) showed stretches at 2916, 2849 cm^{-1} due to C-H (sp^3) and 1486-1462 cm^{-1} due to CH_2.

The ^{1}H NMR spectrum (Appendix J2) showed triplet signals at 0.89 with a coupling constant of 6.8 Hz assigned to methyl protons at H-16. A sharp singlet at δ 1.25 integrated to 24 protons and was attributed to methylene protons of H3-H15 whereas multiplet signals appearing at δ 1.34 integrated to two protons attributed to H-2. A multiplet centered at 3.55 was attributed to the methylene proton H-1. A singlet at δ 3.39 integrating to six protons was attributed to two methyl groups attached to nitrogen. The assignment of these protons was established by COSY spectrum (Appendix J4) where methyl proton H16 at δ 0.98 correlated to methylene proton H-15

at δ 1.25. The signal at δ 3.55 was cross peaked with the signal at δ 1.34 corresponding to H1 and H2, respectively.

The DEPTQ spectra (Appendix J3) exhibited eighteen carbon atoms which was in agreement with two symmetrical methyl carbons at δ 53.33 (2x N-CH_3), 14.00 (C-1) and fifteen methylene carbons at 66.66 (C-1), 26.16 (C-2) and 29.24-31.28 (C-3-C-15).The EIMS (Appendix J7) exhibited $[M]^+$ peak at m/z 269 corresponding to the molecular formula $C_{18}H_{39}N$ and peak base ion at m/z 58 was due to cleavages of methylene proton at C-1 and C-2 (Figure 4.17). The complete assignment of ^{1}H, DEPT, HMQC (Appendix J5), COSY, DEPTQ and HMBC (Appendix J6) NMR are summarized in Table 4.12. Based on its spectroscopic data, compound (**83**) was suggested as *N*,*N*-dimetylhexadecan-1-amine. This compound (**83**) was isolated for the first time from a natural source.

Table 4.12: ^{1}H (500 MHz, $CDCl_3$), DEPTQ, COSY, HMQC and HMBC of *N*,*N*-dimetylhexadecan-1-amine (**83**)

Carbons	**δ_C (ppm)**	**δ_H (ppm) Int. Mult. J**	**COSY**	**HMBC**
1	66.66	3.55 (2H, m)	H2	C3, C4
2	26.16	1.75 (2H, m)	H1	C3, C2
3	23.09	1.35 (2H, m)	-	C3, C2, C4
3-15	29.24-31.81	1.25 (24H, s)	H16	C3-C13, C15, C16
16	14.00	0.89 (3H, t, *J*=6.8 Hz)	H15	C15, C14
N-CH_3	53.33	3.39 (6H, s)	-	C1

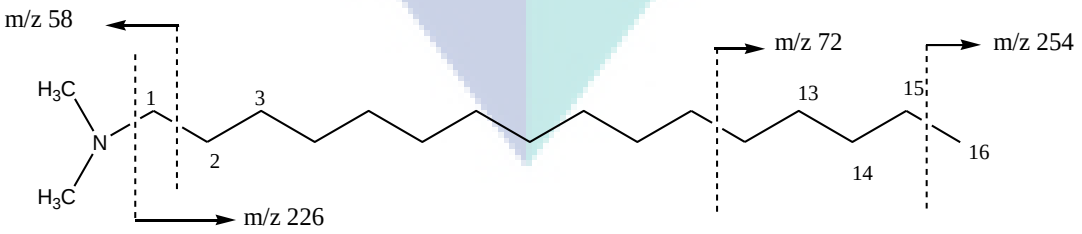

Figure 4.17: Mass fragmentation of *N*,*N*-dimetylhexadecan-1-amine **(83)**

4.1.11 β-Sitosterol (76)

Purification of fraction 1 by column chromatography yielded β-sitosterol (**76**) (7.0 mg, 0.50%) as white crystalline needles with melting point 138-139°C (lit. 140°C) (Khaleque et al., 1970). The IR spectrum (Appendix K1) showed the presence of OH at 3435 cm^{-1}, C-H (sp^3) at 2966$cm^{-1}$and C-O 1052 cm^{-1}.

The ^{1}H NMR spectrum (Appendix K2) displayed two singlets at δ 0.70 and δ 1.03 attributed to two methyl groups at H-18 and H-19, respectively. Signals resonating as doublets at δ 0.85 and 0.87 integrated to three protons were assigned as H-26 and H-27. Doublets resonating at δ 0.95 were assigned to H-21 and triplet signals centered at δ 0.83 were assigned to H-29. In addition, a multiplet at 1.07-2.36 was assigned to methylene protons present in the molecule. A doublet with a coupling constant 5.4 Hz resonating at 5.38 was attributed to an olefinic proton at H-6. The signal at 3.52 was assigned to H-3. Table 4.13 summarizes the ^{1}H spectra and assignments for β-sitosterol (**76**).

Table 4.13: ^{1}H NMR (500 MHz, $CDCl_3$) of β-sitosterol (**76**)

Position	**δH (ppm)** **Int. Mult. J**
3	3.55 (1H, m)
6	5.38 (1H, d, *J*=5.40 Hz)
18	0.70 (3H, s)
19	1.03 (3H, s)
21	0.95 (3H, d, *J*= 6.55 Hz)
26	0.85 (3H, d, *J*=4.40 Hz)
27	0.87 (3H, d, *J*= 1.60 Hz)
29	0.83 (3H, t, *J*=1.45 Hz)
11x CH_2	1.07-2.36 (22H, m)

This data was further supported by mass spectrum (Appendix K3), showing a molecular ion peak at m/z 414 corresponding to the molecular formula $C_{29}H_{50}O$. Based on its physical properties and spectroscopic data, the compound was assigned as β-sitosterol (**76**). This compound had previously been isolated from the leaves of *T. cordifolia* (Khaleque et al., 1970).

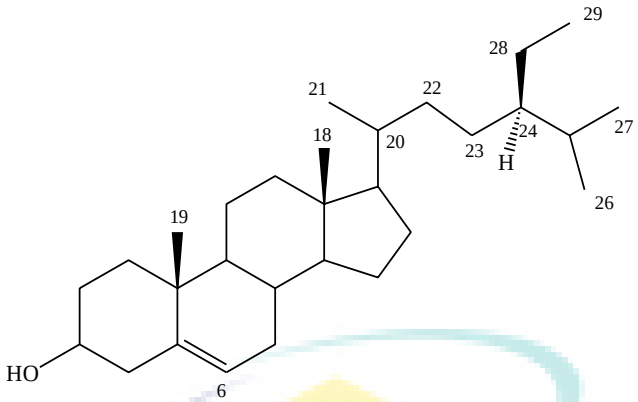

(76)

4.1.12 Octacosanol (79)

Purification of fraction one by CC on silica gel yielded compound (**79**), a white powder (10.0 mg, 0.71%) with melting point 80-81°C (lit 82-83°C) (Pollard et al.,1933) and R_f 0.75 in hexane:ethyl acetate (7:3). The IR spectrum (Appendix L1) showed a broad absorption band due to O-H at 3407cm^{-1} and a C-H (sp^3) stretching band at 2934 cm^{-1} suggesting that compound (**79**) was a long chain alcohol.

The structure was supported by ^{1}H NMR spectrum (Appendix L2) which exhibited a quartet downfield at δ 3.64 due to the presence of hydroxyl group and assigned to methylene proton H-1. The triplet signal (*J*=7.7 Hz) resonating at δ 1.55 was attributed to methylene protons H-2. A singlet at δ 1.25 integrated to 22 methylene protons was assigned to H-3 to H-27. Triplet signals at 0.87 with a coupling constant of 6.5 Hz were assigned to the methyl proton H-28. These data is summarized in Table 4.14.

Table 4.14: ^{1}H NMR (500 MHz, $CDCl_3$) of octacosanol (**79**)

Position	**δ_H (ppm)** **Int. Mult. *J*)**
1	3.64 (2H, q, *J*=6.25 Hz)
2,3	1.57 (4H, t, *J*=7.7 Hz)
28	0.87 (3H, t, *J*=6.5 Hz)
22XCH_2	1.25 (48H, s)

This was supported by a GCMS spectrum (Appendix L3) which gave a molecular ion peak at m/z 410 attributed to the molecular formula $C_{28}H_{58}O$. Octacosanol (**79**) had been previously isolated from leaves of *T. cordifolia* (Khaleque et al., 1970).

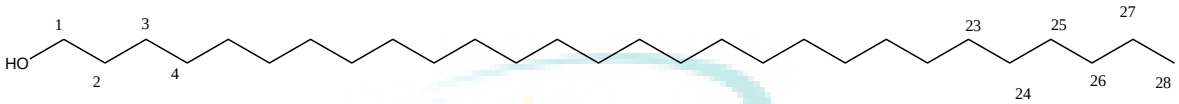

(**79**)

4.1.13 Mixture of three sterols

Purificaton of fraction 1 by column chromatography (silica gel) followed by recrystallization from hexane produced white crystalline needles (11.0 mg, 0.71 %) with melting point 142°C. The TIC of a GC-MS analysis (Appendix M) showed the presence of three peaks each with retention time t_R 28.26, t_R 28.65 and t_R 29.46. The mass spectrum (Appendix 82) of the first component (t_R, 28.26) exhibited a molecular ion peak at m/z 400 consistent with the molecular formula $C_{28}H_{48}O$ and have been identified as campesterol (**77**).

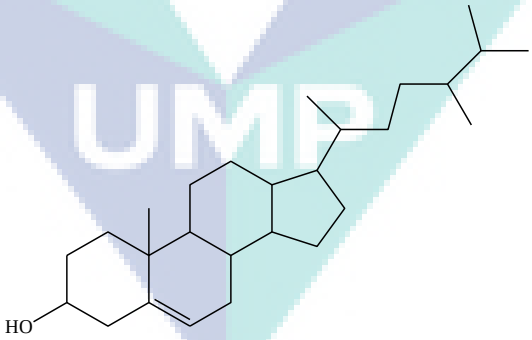

(**77**)

The mass spectrum (Appendix N) of the second component (t_R, 28.65) displayed a molecular ion peak at m/z 412 which was in agreement with the molecular formula, $C_{29}H_{48}O$. Based on NIST data, this compound has been identified as stigmasterol (**78**).

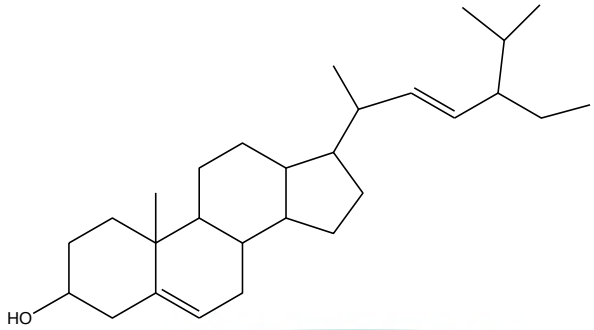

(**78**)

The mass spectrum (Appendix O) of the compound (t_R, 29.46) produced a molecular ion peak at m/z 414, corresponding to molecular formula $C_{29}H_{50}O$, which was identified as β-sitosterol (**76**).

4.2 BIOACTIVITIES

4.2.1 Acetylcholinesterase Inhibitory Activity

AChE inhibitory activity of isolated alkaloids was qualitatively determined using the TLC autograph method (Marston et al., 2002). Active compounds are evident by the white spots on a purple background in Figure 4.18. Four of the isolated alkaloids, namely, *N*-formylnornuciferine (**34**), columbamine (**43**), dihydrodiscretamine (**44**) and 4,13-dihydroxy-2,8,9-trimethoxydibenzo[a,g]quinolizinium (**82**), positively inhibited AChE while *N*-formylannonaine (**33**), lysicamine (**80**), liriodenine (**81**), *N*-transferuloyltyramine (**15**), magnoflorine (**40**) and *N*,*N*-dimetylhexadecan-1-amine (**83**), did not. Galanthamine was used as a positive control, as it is a known AChE inhibitory compound (Heinrich and Teoh, 2004).

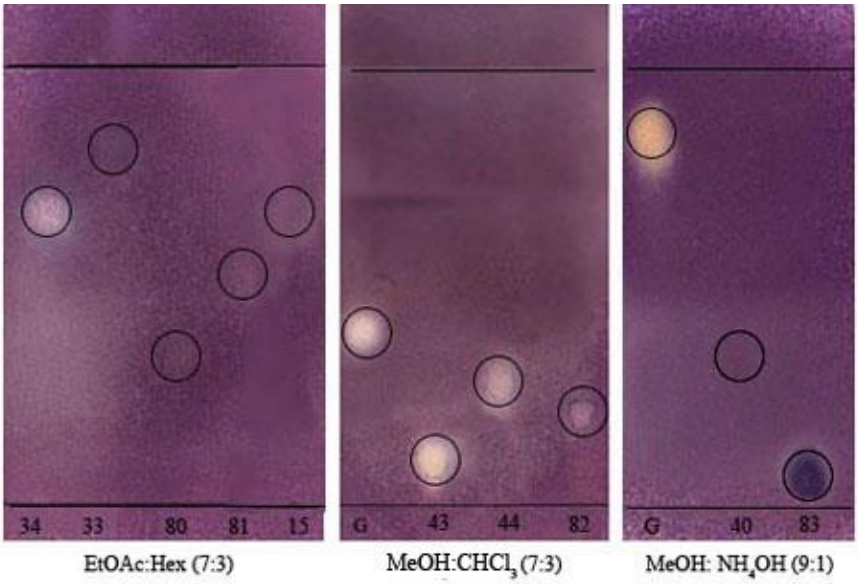

Compound label:

34 - *N*-formylnornuciferine
33 - *N*-formylannonaine
80 - lysicamine
81 - liriodenine
15 - *N*-trans-feruloyltyramine
83 - *N,N*-dimetylhexadecan-1-amine
G - galanthamine
43 - columbamine
44 - dihydrodiscretamine
82 - 4,13-dihydroxy-2,8,9-trimethoxydibenzo[a,g]quinolizinium
40 - magnoflorine

Figure 4.18: Bioautograph showing inhibition of AChE activity by isolated compounds

Thin-layer chromatography-based assays were adopted because this technique can provide fast results on the activity localization of AChE inhibited by complex inhibitors. The separated constituents can be directly detected on the TLC plate qualitatively. A simple and rapid autographic enzyme assay on TLC plates was been developed by Marston et al. (2002) for the screening of possible AChE inhibitors from plant extracts. In this assay, the enzyme reacts with 1-naphthyl acetate to produce 1-naphthol. This in turn undergoes a diazotization reaction with Fast Blue B salt, producing a purple azo dye. When enzyme inhibitors block the formation of 1-naphthol no purple coloration is produced.

Acetylcholinestrase inhibitors (AChEIs) can be divided into two major groups: those which bind to the active site at the bottom of the gorge, and those which bind to the peripheral anionic site (PAS). Alkaloidal inhibitors bind through positively charged nitrogen to the oxyanion area at the bottom of the gorge, especially the Trp84, and a region, separated by a lipophilic area from the positive charge, which can form

hydrogen bonds with the Ser200 residue and others like His44057 (Figure 4.19) (Zahid, 2009). Based on those facts, most of alkaloids may act as acetylcholinestrase inhibitors.

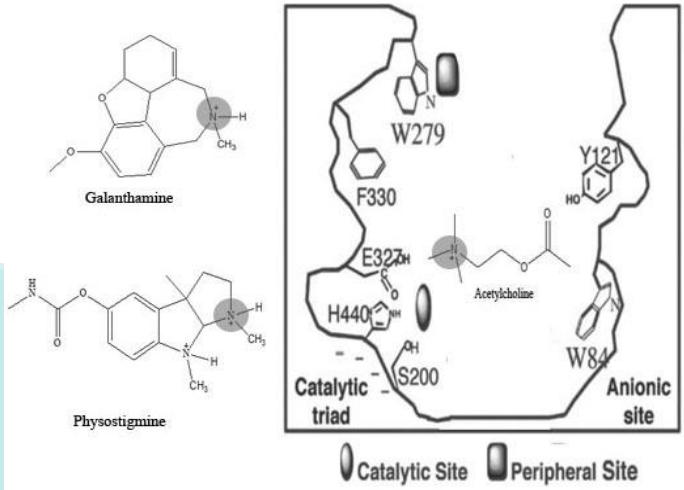

Figure 4.19: Acetylcholinestrase inhibition through the active-site gorge

However, about 15% of investigated compounds identified as hits in the microplate assay were inactive by TLC, and on the other hand, about 2% of investigated compounds active by TLC autograph assay were inactive in the microplate assay. Compounds identified as active inhibitors in the microplate assay but inactive in the TLC bioautograph assay were shown to lose activity during pre-incubation for 20 min at 37◦C with/without AChE. This loss of activity might also occur in the TLC autograph assay during the development of the plate. During the TLC autograph assay possible interactions of either AChE or test compounds with the silica support may occur, resulting in an alteration of the affinity of the enzyme for the compounds (Giovanni et al., 2007). Based on this consideration, the microplate assay was carried out for verification and the results are shown in Table 4.15.

During the microplate assay, hydrolysis of acetylthiocholine was monitored by the formation of yellow 5-thio-2-nitrobenzoate anion as a result of the reaction of DTNB with thiocholine, released by the enzymatic hydrolysis of acetylthiocholine at a wavelength of 406 nm.

Table 4.15: Acetylcholinesterase inhibitory activity by microplate assay of isolated alkaloids and the IC_{50} values

Compound	IC_{50} (µM)
34	564.60 ± 2.08
33	415.26 ± 2.70
40	NA
82	517.64 ± 5.34
44	276.07 ± 1.84
43	48.12 ± 1.34
81	616.44 ± 5.88
80	388.79 ± 9.80
15	NA
Physostigmine	31.40 ± 0.54

The IC_{50} values are the mean ± standard deviations of two independent experiments. The inhibitory effects are represented as compounds concentration (µM) giving 50% inhibition on AChE activity (IC_{50}). Physostigmine was used as a positive control. Compound (**43**) was found to be a competitive inhibitor as the IC_{50} value is close to the IC_{50} value of physostigmine which was the positive control. Three compounds that showed moderately AChE inhibitory activity in microplate assay were compounds (**33**), (**44**) and (**80**). Other compounds with IC_{50} more than 500 µM were considered as weak AChE inhibitors. The efficiency of inhibition of AChe was found to decrease in the order of (**82**)>(**34**)>(**81**).

Structure–activity relationship, predicted from the results presented, suggests that the nitrogen substituents on the skeleton were the most important structural features that determine the inhibitory potency of the alkaloids. Two of the active compounds, (**43**) and (**44**) are quaternary alkaloids. It is generally believed that due to the presence of the rings of the aromatic amino acids in AChE gorges, the cationic ligands moved toward the active sites by diffusion on the surface of the enzyme (Khalid et al., 2004). The diffusion of the quaternary nitrogen-containing compounds to the peripheral site of the aromatic gorge may be facilitated by the positive charge on these compounds (Tang et al., 2009). Although compounds (**82**) and (**40**) are considered as quaternary alkaloids, they exhibited poor inhibition and were inactive due to the presence of a polar hydroxyl group which contributed by slightly decreasing the activity. This suggests that hydrophilicity of this moiety may play an important role during binding.

Based on qualitative and quantitative data, the structure for terminal groups of the side chain also contribute to inhibitory activities. Compounds with aromatic rings showed a better activity compared to those without aromatic rings (**33**), (**34**), (**80**) and (**81**).The lower AChE inhibitory activity of the aporphine and oxoaporphine alkaloids could be due to the lack of ring double bonds. Derivatives lacking ring double bonds demonstrated a decrease in activity, indicating the significance of aromatic planar moiety of compounds in interacting with enzyme-binding sites, while flexibility or floppiness of molecules might be disadvantageous for binding affinity of compounds with the enzyme (Wang et al., 2010).

4.2.2 Radical Scavenging Assay with DPPH

The TLC-DPPH assay was performed as described by (Takao, et al., 1994). Briefly, after developing and drying, aluminium-backed TLC sheets were sprayed with 1,1-diphenyl-2-picryl-hydrazyl (DPPH) solution (2 mg/ml in MeOH). Active compounds appeared as yellow spots against a purple background (Figure 4.20).

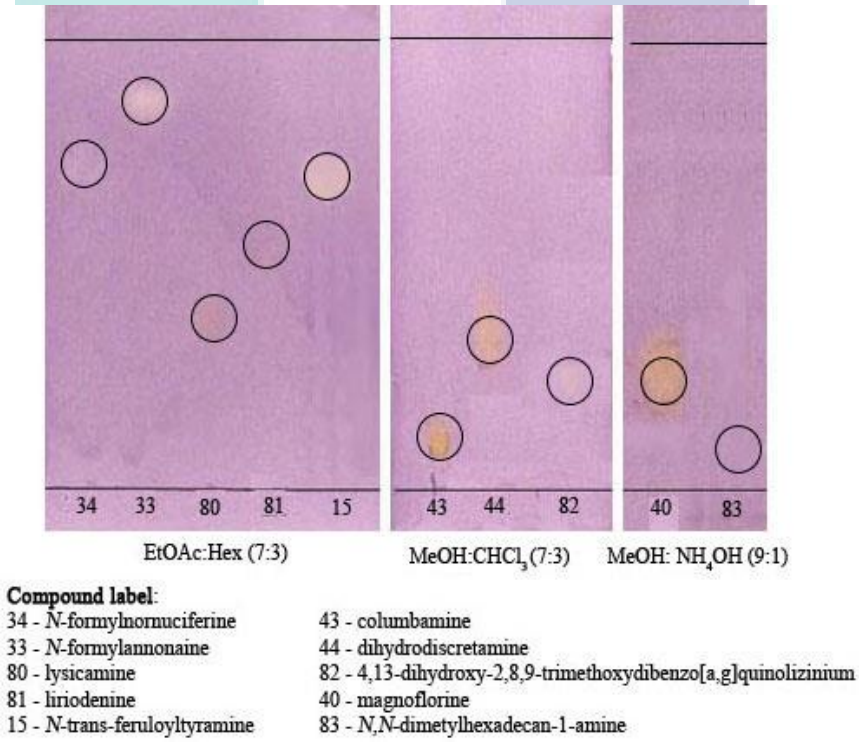

Figure 4.20: TLC-DPPH assay for isolated compounds

N-formylannonaine (**33**), *N*-trans-feruloyltyramine (**15**), columbamine (**43**), dihydrodiscretamine (**44**), 4,13-dihydroxy-2,8,9-trimethoxydibenzo[a,g]quinolizinium (**82**) and magnoflorine (**40**) gave positive reactions toward the DPPH assay while *N*-formylnornuciferine (**34**), lysicamine (**80**), liriodenine (**81**) and *N*,*N*-dimetylhexadecan-1-amine (**83**), did not. Quantitative estimation of radical scavenging activity was based on the method described by Blois (1958). The radical scavenging activity (IC_{50}) of isolated compounds was compared with butylated hydroxyl-anisole (BHA), a synthetic antioxidant. Results of radical scavenging activity of compounds to reduce and decolorized DPPH are shown in Figure 4.21.

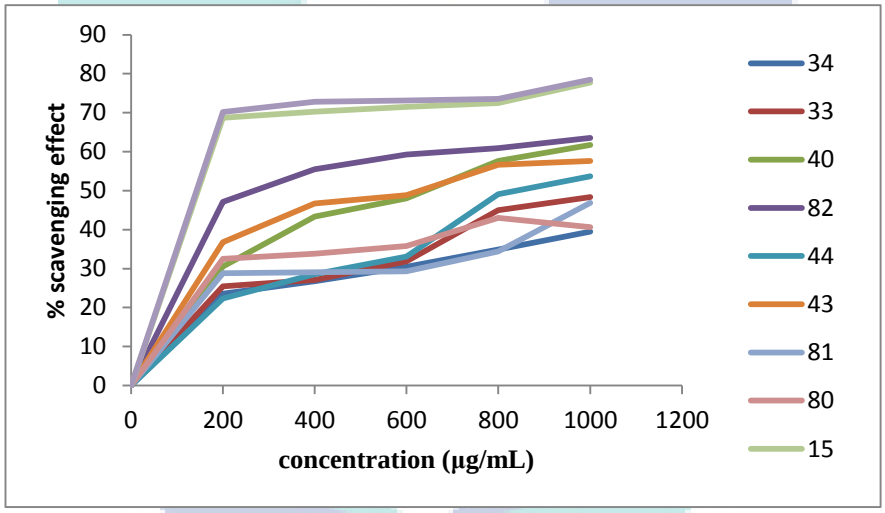

Figure 4.21: Antioxidant activities of isolated compounds based on the ability to reduce and decolorize DPPH

The radical scavenging activities of all the compounds were found to increase with increasing concentration. IC_{50} for DPPH radical scavenging activity is reported in Table 4.16. The IC_{50}values were calculated from linear regression analysis (Appendix P).

Table 4.16: IC_{50} DPPH radical scavenging activity of isolated compounds

Compound	DPPH radical scavenging, IC_{50} (µg/mL)
34	NA
33	NA
40	674.22 ±1.20
82	544.22±1.80
44	873.39±1.57
43	678.10±1.06
81	NA
80	NA
15	323.64±1.53
BHA	302.62±0.64

As shown in Table 4.15, compound (**15**) showed the lowest IC_{50} value and exhibited the strongest antioxidant activity (IC_{50}= 323.64 µg/mL). However, this value was lower than the antioxidant standard, BHA (IC_{50}= 302.62 µg/mL). Moderate radical scavenging activities was shown by all quaternary alkaloids as follows, (**82**)>(**40**)>(**43**)>(**44**) (IC_{50} 500-800 µg/mL). Aporphines (**34**), (**33**) and oxoaporphines (**80**), (**81**) did not demonstrated antioxidant activity. The results were in agreement with the results obtained from the TLC-DPPH assay which show faded yellow colour on a purple background.

The ability of compound (**15**) to act as a strong antioxidant is in agreement with the TLC autograph assays reported by Cavin, et al. (1998). This revealed that *N*-trans feruloyltyramine (**15**) and *N*-cis feruloyltyramine (**16**) isolated from the dichloromethane extract of *T. crispa* exhibited antioxidant and strong radical scavenging properties towards β-carotene and 2,2-diphenyl-1-picrylhydrazyl (DPPH) radicals.

It could also be seen that the protoberberine alkaloids were better radical scavengers than the aporphine and oxoaporphine alkaloids. This is due to the presence of a hydroxyl group within the berberine skeleton compared to the structure of aporphine and oxoaporphine alkaloids which contained only methoxy and methylenedioxy groups. The presence of aromatic O-H groups may be responsible for their antioxidant efficiency, similar to phenolic antioxidants, via chain-breaking

mechanism by donation of phenolic hydrogen. Among the protoberberine alkaloids, compound (**82**) and (**40**) with two hydroxyl groups was the most powerful radical scavenger among the samples. Although compounds (**44**) also have two hydroxyl groups, it's only showed moderate radical scavenging activity. The favorable antioxidant features of the hydroxylated alkaloids are most probably ensured by the combination of reasonably high antiradical reactivity with high lipophilicity, however, the solvation process was found to markedly interfere with these beneficial effects (Rackova at al., 2004).

4.2.3 Antimicrobial Study

The antibacterial screening of isolated compounds were assayed in vitro by microtitre-plate (Drummond et al., 2000) with resazurin reduction method against eight bacterial strains, two *Gram*-positive; *Enterococcus faecalis, Staphylococcus aureus,* four *Gram*-negative *Klebsiella pneumonia, Escherichia coli, Psuedomonas aeurogenosa, Proteus vulgaris* and two fungi, *Candida albican* and *Aspergillus niger.*

Figure 4.22, Figure 4.23 and Figure 4.24 show compounds and their colour retaining properties against each microbial strain in their well. Should colour change occur within a well, metabolic activity of the bacteria is inferred as released CO_2 and O_2 reduce the dye to pink and fluorescent when reduced to resorufin by oxido-reductase activity. Resorufin is further reduced to colorless hydroresorufin. Inhibition of microbial activity by a compound results in the dye colour remaining unchanged in a well (Karuppusamy and Rajasekaran, 2010). The positive control used is tetracycline while the negative controls are culture medium, microbial suspension and solvent used (methanol).

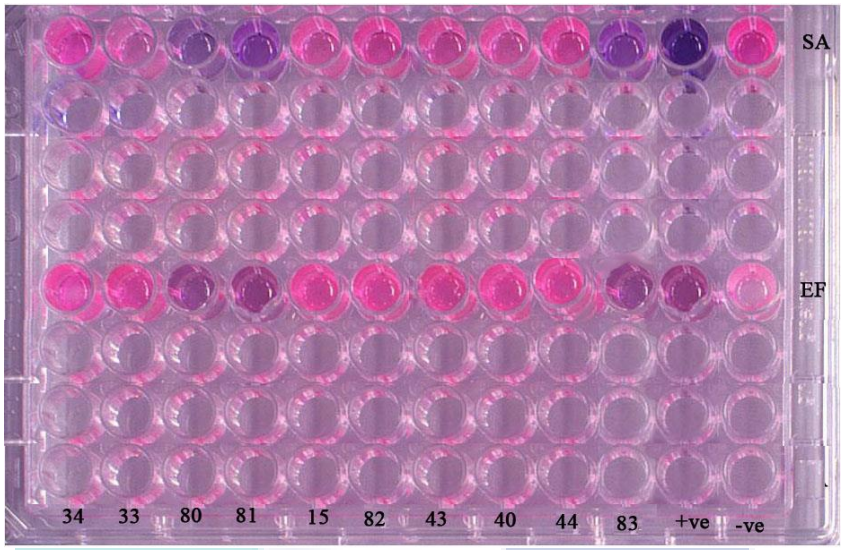

Figure 4.22: Antimicobial activity of isolated compounds against *Gram*-positive; bacteria; *E. faecalis* and *S. aureus*

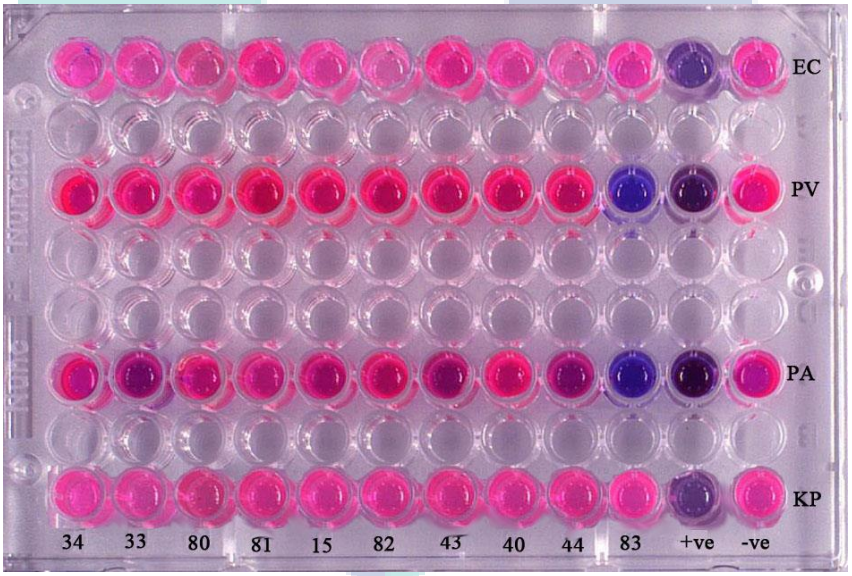

Figure 4.23: Antimicobial activity of isolated compounds against *Gram*-negative bacteria; *E. coli*, *P. vulgaris*, *P. aeurogenosa* and *K. pneumonia*

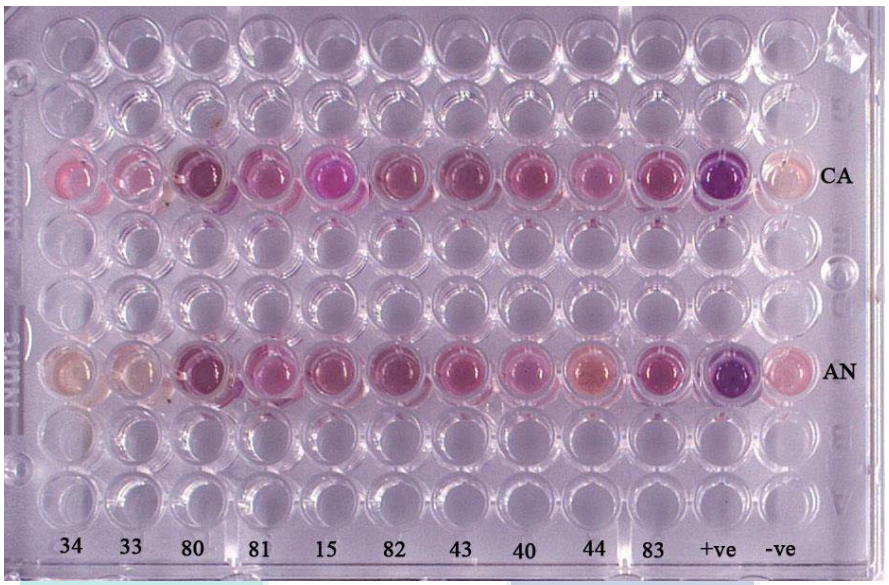

Figure 4.24: Antimicobial activity of isolated compounds against fungi; *C. albican* and *A. niger*

Most of the compounds did not inhibit *Gram*-positive bacteria, *Gram*-negative and fungi except the oxoaporphine alkaloids, lysicamine (**80**) and liriodene (**81**) which inhibited *S. aureus* (+) and *E. faecalis* (+) whereas *N,N*-dimethylhexadecan-1-amine (**83**) inhibited *S. aureus* (+), *E. faecalis (+), P. vulgaris* (-) and *P. aeurogenosa* (-). Liriodenine (**80**) and lysicamine (**81**) are oxoaporphine alkaloids, and have been reported to possess multiple bioactivities. Apparently, the earliest recorded biological activity of lysicamine (**80**) and liriodenine (**81**) were antibacterial (Perez and Cassel, 2010). Liriodenine (**81**) appears to regulate dopamine biosynthesis, inhibit topoisomerease, inhibit platelet aggregation and showed antiproliferative activity (Perez and Cassels, 2010). In this study, the aliphatic amine (**83**) demonstrated the potential as a selective antimicrobial agent.

Based on screening data, the levels of antimicrobial activity against *S. aureus* (+), *E. faecalis* (+), *P. vulgaris* (-) and *P. aeurogenosa* (-) were demonstrated using MIC test, specifically the resazurin reduction method. Resazurin is not able to penetrate viable cells because of membrane potential. However, dead cells lose their membrane integrity and are stained slightly bluish pink.This method is inexpensive and easy to perform compared with conventional agar plate assay. Results were obtained in a short period of time and with very good sensitivity.

Minimal inhibitory concentration is the lowest concentration of the compounds that can inhibit the growth of microorganisms. Table 4.17 shows the MIC data of isolated compounds that can inhibit *Gram*-positive and *Gram*-negative bacteria. The data indicate that *N,N*-dimetylhexadecamine (**83**) exhibited high inhibitory activity against *S. aureus* (+), *E. faecalis* (+) and *P. vulgaris* (-) with MIC value of 3.91µg/mL while low inhibitory against *P. aeurogenosa* (-) with MIC value 62.5 µg/mL; liriodenine (**81**) showed high inhibitory activity against *S. aureus* (+) with MIC value 15.65 µg/mL but low inhibitory activity against *E. faecalis* (+) with MIC value 250 µg/mL. In comparison, lysicamine (**80**) showed the lowest inhibitory activity for both bacteria tested with MIC value 125 µg/mL and 500 µg/mL. Of these oxoaporphine alkaloids, liriodenine (**81**) showed the more significant activity whereas lysicamine (**80**) exhibited weak activity. The structure of compounds (**81**) and (**80**) must be taken into account whereby substituents at C-1 and C-2 are methylenedioxy and methoxy, respectively. This could explain that antimicrobial activity is higher in the presence of 1,2-methylenedioxy for free base to be active (Clark and Hufford, 1992). Although *N,N*-dimetylhexadecan-1-amine (**83**) is an aliphatic amine, the absence of nitrogen atoms contributed to its potential as a competitive antibiotic.

Table 4.17: Antimicrobial activity expressed as minimum inhibitory concentration (MIC) against *Gram*-positive bacteria

Microorganism	**Concentration of compounds (µg/ml)**			
	(80)	**(81)**	**(83)**	**Tetracycline**
Staphylococcus aureus (+)	125.00	15.65	3.91	3.91
Enterococcus faecalis (+)	500.00	250.00	3.91	3.91
Proteus vulgaris (-)	NA	NA	3.91	1.95
Psuedomonas aeurogenosa (-)	NA	NA	62.50	1.95

* positive standard for bacteria is tetracycline

It is reported that *Gram*-positive bacteria should be more susceptible since they possess only an outer peptidoglycan layer which is not an effective barrier. The *Gram*-negative bacteria have an outer phospholipidic membrane that make the cell wall impermeable to lipophilic solutes, while porines constitute a selective membrane that make the cell wall impermeable to lipophilic solutes and a selective barrier to

hydrophilic solutes with an exclusion limit of about 600 Da. Many results have confirmed these observations, thus some plant extracts were found to be more active against *Gram*-positive bacteria than against *Gram*-negative ones (Karou et al., 2006).

Protoberberine alkaloids, berberine, palmatine and jatrorrhizine had been reported to show relatively broad spectrum antimicrobial activities against plant and animal pathogens (Deng et al., 2012). In this finding, none of the protoberberine alkaloids showed inhibition of all the strains tested. Iwasa and Kamigauchi (1996) reported that efficacy of protoberberine alkaloids was related to the ammonium N at position 7 of the aromatic ring in the chemical structure, and the different substituents in rings A and D, increased or decreased the inhibitory activity of protoberberine alkaloids. Karou et al. (2006) have suggested that different alkaloids exert their antimicrobial activity through different mechanisms. In the case of protoberberine alkaloids, the mechanism remains unclear. For example, in the case of indoloquinoline Sawer et al. (2005) demonstrated that the main indoloquinoline alkaloid, cryptolepine, caused cell lysis and morphological changes to *S. aureus*. However, the antimicrobial effects of the alkaloid may be through another mechanism, since the compound is known to be a DNA intercalator and an inhibitor of DNA synthesis through topoisomerase inhibition.

Some of the tested alkaloids only showed a strong activity when tested as a single compound. Although aporphine alkaloids, *N*-formylasimilobine and *N*-formylannonaine (**33**) isolated from *Stephania succifera* had reportedly by Yang et al. (2010) shown significant antimicrobial activity against *S. aureus* but in this findings, aporphine alkaloids (**34**) and (**33**) did not show any significant antimicrobial activity. The difference in the activities may have resulted from the compound being a racemic mixture of *N*-formylnornuciferine (**34**) and *N*-formylannonaine (**33**).

CHAPTER 5

CONCLUSIONS

5.1 PHYTOCHEMICAL INVESTIGATIONS

The present investigation on alkaloidal extracts of *T. crispa* stems has led to the isolation of twelve compounds, viz., *N*-trans-feruloyltyramine (**15**), *N*-formylannonaine (**33**), *N*-formylnornuciferine (**34**), magnoflorine (**40**), lysicamine (**80**), liriodenine (**81**), columbamine (**43**), dihydrodiscretamine (**44**) and 4,13-dihydroxy-2,8,9-trimethoxy dibenzo[a,g]quinolizinium (**82**), *N*,*N*-dimetylhexadecan-1-amine (**83**), octacosanol (**79**) and β-sitosterol (**76**). Four of the compounds are non-alkaloidal due to cross-contamination during fractionation of the crude extract. A total of eight alkaloids isolated in this study and three alkaloids, *N*-formylannonaine (**33**), *N*-formylnornuciferine (**34**) lysicamine (**80**) had previously been reported from *T. crispa* (Bakhari et al., 2005). The alkaloids, magnoflorine (**40**), columbamine (**43**) and dihydrodiscretamine (**44**) had been isolated from other species within genus *Tinospora*. Meanwhile the alkaloids liriodenine (**81**) and 4,13-dihydroxy-2,8,9-trimethoxy dibenzo[a,g]quinolizinium (**82**) are being isolated and reported for *T. crispa* and genus *Tinospora*, for the first time in this thesis.

Distributions of *Tinospora* species in different biogeographical regions would certainly influence the secondary metabolite content of the plants depending on availability of nutrients, climate and ecological conditions influencing the biosynthesis of secondary metabolites. Natural concentrations of certain secondary metabolites such as alkaloids in the plants mostly act as feeding deterrents or are end products of metabolism. One of the outcomes of this investigation suggests that alkaloids are

suitable chemical markers for *T. crispa* as well as genus *Tinospora* given its strong presence within this genus.

5.2 BIOLOGICAL ACTIVITIES

Three types of bioactivity studies, viz., acetylcholinesterase inhibitory, radical scavenging and antimicrobial have been carried out on the isolated compounds containing nitrogen. The acetylcholinesterase inhibitory assay showed that the most active compounds are quaternary protoberberine alkaloids. It is interesting to note that quaternary nitrogens may be necessary for strong AChE inhibitory activity in alkaloids (Tang et al., 2009). The finding is in agreement with a proposal by Marston, et al. (2002) involving use of drug substances of alkaloidal origin as part of the treatment regime for Alzheimer's disease. Results of the present investigation further points to the potential of this plant species as a good source of new AChE inhibitors.

Evaluation of the antiradical scavenging activity revealed the moderately active compounds to be derived from quaternary alkaloids. Most of the isolated compounds showed antioxidant activity whether highest, moderately or weak except the aliphatic amine (**83**). Although oxoaporphine alkaloids and the aliphatic amine were considered inactive for both acetylcholinesterase inhibition and radical scavenging activity; they show positive antimicrobial activity of the *Gram*-positive bacteria, *Staphylococcus aureus* and *Enterococcus faecalis.* Aliphatic amine also exhibited inhibitory activity against *Gram*-negative bacteria, *P. vulgaris* (-) and *P. aeurogenosa* (-).

Compounds which tested positive in the DPPH reaction can be considered as antioxidants and therefore radical scavengers (Dehpour et al., 2009). Antioxidants are molecules which can safely interact with free radicals and terminate the chain reaction before vital molecules are damaged (Kone et al., 2011). According to Gupta and Jain (2010), agents that demonstrate significant antioxidant activity may preserve vital tissue and facilitate wound healing as reduction of bacterial load of a wound may be necessary to facilitate wound healing as well as to reduce local inflammation and tissue destruction (Kone et al., 2011). The antioxidant and antimicrobial properties of different compounds support documented traditional use of *T. crispa* in wound healing and

treatment of rheumatic and diarrhoea (Ahmad and Raji, 1993; Martin et al., 1995). For medicinal purposes, the safety and toxicity of this plant species still need to be addressed.

5.3 RECOMMENDATION

A number of alkaloids from natural sources have been proved efficacious to cure various ailments (Patel and Mishra, 2011). Many scientific reports have been published describing the biological activities of *T. crispa* extracts. The chemical constituents of *T. crispa* extracts have been extensively studied since the 1980s but the pharmacological activities of many of these compounds are yet to be investigated. Studies on structure–activity relationships are vital for understanding the molecular mechanisms of biochemical processes. The later test suggests the involvement of possible central mechanisms in the biological activity of the alkaloids isolated from *T. crispa*.

Results of the present study show that it is reasonable to presume that quaternary protoberberines belong to the biologically active constituents of *T. crispa*. Previous phytochemical studies on the other species of the genus indicate quaternary alkaloids as the major type of alkaloids isolated and these were mostly protoberberines (Hungerford et al., 1998). Protoberberine alkaloids exhibit a great variety of biological and pharmacological activities (Grycova et al., 2007). *T. crispa* is a rich source of quaternary alkaloids including structural analogues of these bases with identical or different biological activities and further investigation may yield more novel compounds with unique biological properties.